Acta Ichthyologica et Piscatoria 51(4), 2021, 339–344 | DOI 10.3897/aiep.51.67056

PENSOFT

ACTA ICHTHYOLOGICA ET PISCATORIA

New record of *Neoclinus lacunicola* (Actinopterygii: Perciformes: Chaenopsidae) from Ulleung Island, Korea revealed by body morphometry and mitochondrial DNA barcoding

Se Hun MYOUNG[1], Laith A. JAWAD[2], Joo Myun PARK[1]

1 *Dokdo Research Center, Korea Institute of Ocean Science and Technology, Uljin 36315, Republic of Korea*

2 *School of Environmental and Animal Sciences, Unitec Institute of Technology, 139 Carrington Road, Mt Albert, Auckland 1025, New Zealand*

http://zoobank.org/5376D968-C0BE-4E04-95C4-4D930E9444F3

Corresponding author: Joo Myun Park (joomyun.park@kiost.ac.kr)

Academic editor: Ronald Fricke ♦ **Received** 7 April 2021 ♦ **Accepted** 30 May 2021 ♦ **Published** 1 October 2021

Citation: Myoung SH, Jawad LA, Park JM (2021) New record of *Neoclinus lacunicola* (Actinopterygii: Perciformes: Chaenopsidae) from Ulleung Island, Korea revealed by body morphometry and mitochondrial DNA barcoding. Acta Ichthyologica et Piscatoria 51(4): 339–344. https://doi.org/10.3897/aiep.51.67056

Abstract

One specimen (38.3 mm SL) of *Neoclinus lacunicola* Fukao, 1980, belonging to the family Chaenopsidae, was first recorded from Ulleung Island, Korea (East Sea, otherwise known as the Sea of Japan) on 5 January 2021. This species was characterized by paired external pores of incomplete lateral line running from the upper margin of the opercle, seven pairs of supraorbital cirri arranged in two rows, occipital region with a pair of cirri, and 13 rays of pectoral fin. This species is morphologically similar to the *Neoclinus toshimaensis* Fukao, 1980, but differs in the number of cirri on the supraorbital (6–7 versus 9–11 cirri). This study documents the first report of *N. lacunicola* in Korean waters and proposes the new Korean name of 'eol-lug-bi-neul-be-do-la-chi' for the species. For the confirmation of the identity of the species, a partial gene sequence of the mt COI (570 bp) of *N. lacunicola* was obtained for the first time.

Keywords

Neoclinus species, tube blenny, new record, rocky shore, East Sea, Sea of Japan

Introduction

The family Chaenopsidae comprises 96 species belonging to 14 genera distributed worldwide, with one genus and eight species occurring in Japanese waters (Aizawa and Doiuchi 2013; Nelson et al. 2016), but only two species representing a single genus have recently been recorded in Korean waters (Kim and Kang 1991; Myoung et al. 2021). The tube blennies (Chaenopsidae) are reef-associated marine fishes, mainly distributed in warm North and South American waters (Nelson et al. 2016). Generally, small-sized, usually elongated and compressed, with a large mouth. The supraorbital and nasal cirri are present or absent (Murase et al. 2015). They exhibit a hiding behavior in crevices between rocky matrices, but occasionally inhabit empty gastropod shells (empty barnacles and empty worm shells) (Stephens and Springer 1971; Fukao 1980; Fukao and Okazaki 1987). Such behavior is advantageous to protect their bodies from potential predators and to care for their spawned eggs within the habitats (Murase and Sunobe 2011; Froese and Pauly 2020).

Neoclinus lacunicola Fukao, 1980 was firstly reported as a new species in 1980 (Fukao 1980) and later, several studies have reported on the taxonomic checklists, phylogeny, and encyclopedic information (Patzner et al. 2009; Aizawa and Doiuchi 2013; Lin and Hastings 2013;

Soniyama et al. 2020). However, there is still a lack of information on its biology and ecology.

To date, one species of tube blennies, i.e., *Neoclinus bryope* (Jordan et Snyder, 1902) has firstly been reported in Korean waters (Kim and Kang 1991) and, more recently, Myoung et al. (2021) documented the first record of *Neoclinus chihiroe* Fukao, 1987 in Dokdo, Korea; consequently, a total of two species have been recorded in Korean waters. This study provides the first record of an additional chaenopsid species (*N. lacunicola*) collected from Ulleung Island, describes its morphological characteristics, and records its mitochondrial DNA cytochrome c oxidase subunit I (mt COI) sequences.

Methods

One specimen of *N. lacunicola* was collected from Tonggumi (37°27′33.50″N, 130°51′28.84″E) in the coastal waters of Ulleung Island, Gyeongsangbuk-do, Korea (East Sea, otherwise known as the Sea of Japan), by a SCUBA diver on 5 January 2021 (Fig. 1). Sampling was conducted at a depth of approximately 22 m, close to the shoreline during the day and the sample was transported to the laboratory immediately after capture in a living condition, using a small fishbowl with seawater. In the laboratory, an image of the specimen was taken, it was euthanized and then meristic counts and body morphometrics were recorded following the method of Hubbs and Lagler (1958). The specimen was measured to the nearest 0.1 mm using digital Vernier calipers and a microscope. The specimen was then preserved in 5% formalin for 24 h and later transferred to 70% ethanol for depositing at the Marine Biodiversity Institute of Korea (MABIK).

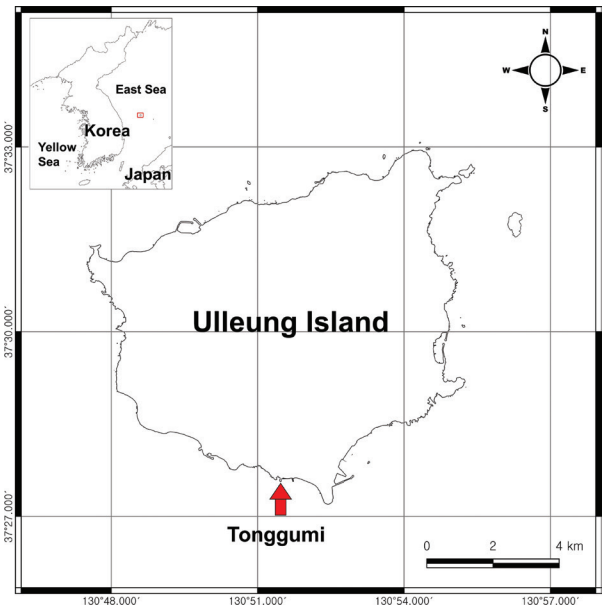

Figure 1. Map showing the sampling area of *Neoclinus lacunicola* from Tonggumi, Ulleung Island, Korea.

To compare molecular data, total genomic DNA was extracted from the muscle tissue using 10% Chelex resin (Bio-Rad, Hercules, CA). A portion of the mitochondrial COI gene was amplified using universal primers (Ward et al. 2005). PCR was performed in a 20 µL reaction tube containing 1 µL genomic DNA, 2 µL 10× PCR buffer, 2 µL 2.5 mM dNTP, 1 µL of each primer, 0.1 µL Ex-Taq DNA polymerase, and 12.9 µL sterile distilled H_2O, using a thermal cycler (MJmini PTC-1148, Bio-Rad USA). The PCR profile consisted of initial denaturation at 95°C for 5 min, followed by 34 cycles of denaturation at 95°C for 1 min, annealing at 50°C, extension at 72°C for 1 min, and a final extension at 72°C for 5 min. PCR products were purified using ExoSAP-IT (United States Biochemical Corporation USA) and sequenced, using an ABI PRISM BigDye Terminator v.3.1 Ready Reaction cycle sequencing kit (Applied Biosystems Inc. USA) on an ABI 3730xl DNA analyzer (Applied Biosystems Inc.). We compared our molecular data with those of the mtDNA COI sequences from other *Neoclinus* species obtained from GenBank (National Center for Biotechnology Information, www.ncbi.nlm.nih.gov). Sequences were aligned using ClustalW (Thompson et al. 1994) in BioEdit, version 7 (Hall 1999). The genetic divergences were calculated using the Kimura 2-parameter (K2P) (Kimura 1980) model with Mega 6 (Tamura et al. 2013). Phylogenetic trees were constructed using the neighbor-joining method (Saitou and Nei 1987) in Mega 6 (Tamura et al. 2013), with confidence assessed, based on 1000 bootstrap replications.

Results

Material examined

MABIK PI00049728, 1 specimen, 38.3 mm SL, Tonggumi, Ulleung Island, Gyeongsangbuk-do, Korea (37°27′33.50″N, 130°51′28.84″E).

Description. The body counts, measurements, and proportions of body parts are shown in Table 1. Body elongated and compressed (Fig. 2). Head short and round. Snout short, but mouth relatively large; posterior tip of upper jaw beyond posterior margin of eyes. Distance of interorbital area narrow. Single nasal cirrus on posterior rim of nostril; cirrus long, thin, and slender with four branches. Seven pairs of supraorbital cirri arranged in double rows with four cirri on outer row and three cirri on inner row and thick and short branches on each cirrus. Occipital region with single pair of cirri; each cirrus short, wide, and monotonous (Fig. 2B). Specimen having single dorsal fin and dorsal fin membrane shallow notched; soft part of ray usually higher than spinous part. Origin of dorsal fin located forward to origin of pelvic fin. Origin of soft part of dorsal fin ray located behind anus. Caudal fin separated from both dorsal and anal fins. End of caudal fin rounded. Entire margin of anal fin serrated; origin of anal fin located in front part of central portion of body. Pectoral fin rounded and located behind pelvic fins.

Head red and body uniformly white with black patterns (Fig. 2). Upper part of head red and white spots scattered under eyes and on chin. Red part of head appearing before fourth spine of dorsal fin and color gradually becoming faded to fourth spine of dorsal fin. Jaw and pelvic fins light yellow. Cirri in nostrils almost transparent. Lower part of supraorbital cirri red, but tip of cirri transparent. Background color of body white, with eight large black bands going down from dorsal to lower middle body and starting points of eight black patterns irregularly appear under the basement of dorsal fin. Black blotch surrounded by red between second and third dorsal spines. Spine and soft rays of dorsal fin having irregular red color and transparent membrane. Upper part of opercular membrane having no black blotch. Overall, pectoral fin is pale red. Basement of pectoral fins with no black dot. Pelvic fins covered in yellow. Anal and caudal fins light red but almost transparent.

Based on an analysis of the mitochondrial cytochrome oxidase subunit I gene (COI) sequence (570 bp), the presently reported specimen was different from other six species of the genus *Neoclinus* with genetic distances of 0.141–0.220 (Fig. 3).

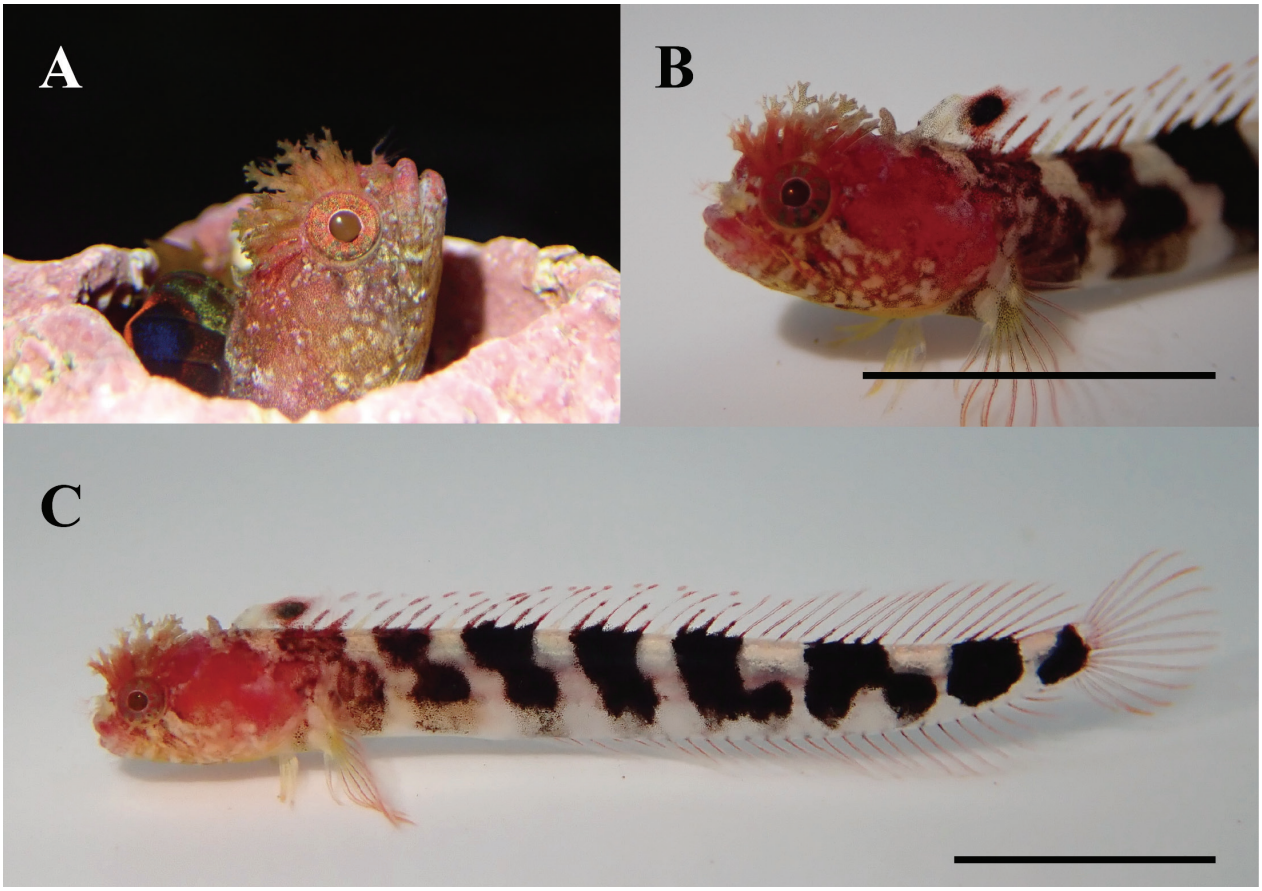

Figure 2. *Neoclinus lacunicola*, living condition, MABIK PI00049728, 38.3 mm SL, Tonggumi, Ulleung Island, Korea. **A.** An underwater photo; **B** and **C.** Images taken in the laboratory. Scale bar: 1 cm.

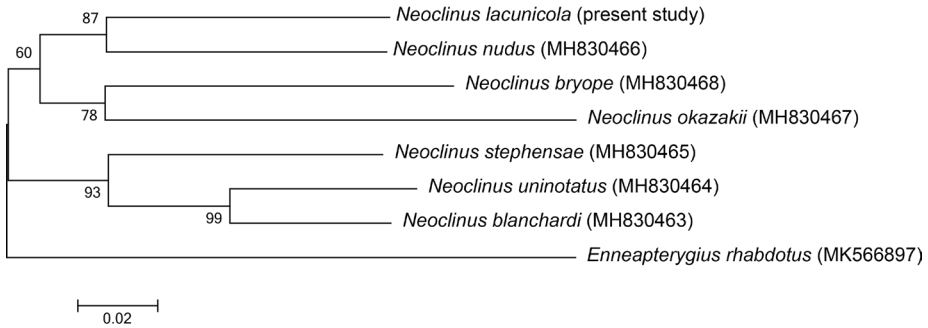

Figure 3. A neighbor-joining tree, based on partial mtDNA COI region using *Neoclinus lacunicola* (MABIK PI00049728) and other species of *Neoclinus*. Numbers at branches indicate bootstrap probabilities in 10 000 bootstrap replications. Scale bar equals 0.02 of Tamura and Nei's distance (1993) with K2 parameter model.

Table 1. Morphometric measurements of the *Neoclinus lacunicola* in comparison with previous records.

Morphological characters	Presently reported specimen	Fukao 1980	Murase et al. 2015	
Sex (number of specimens)	Female (1)	Male (1)	Female (2)	Male (2)
Counts				
Dorsal rays	XXII, 18	XXIII, 19	XXII–XXIII, 17–19	
Anal rays	II, 27	II, 27	II, 27	
Pectoral rays	13	13	12 or 13	
Pelvic rays	I, 3	I, 3	—	
Principal caudal rays	7 + 6 = 13	7 + 6 = 13	7 + 6 = 13	
Measurements				
Standard length [mm]	38.3	48.8	38.9–49.4	38.0–42.8
% of standard length				
Total length	113.8	112.9	113.8–114.7	114.7–115.5
Body depth	12.3	14.5	12.6–13.6	12.9
Head length	20.4	20.5	21.5–24.2	23.1
Head width	13.8	14.1	—	—
Head depth	13.3	—	13.6–15.4	14.5
Orbit diameter	4.3	4.3	5.9–6.9	6.1
Postorbital length	13.1	13.3	—	—
Interorbital width	1.3	—	1.0	0.9
Snout length	4.0	3.9	4.4–4.5	5.1
Upper jaw length	9.9	10.2	10.3–11.1	11.2
Pre-dorsal length	15.9	15.6	15.4–17.5	17.3
Pre-anal length	40.9	41.0	38.7–42.7	40.4
Length of dorsal fin base	82.0	83.8	81.7–87.0	82.9
Length of soft dorsal fin base	34.5	34.8	—	—
Length of anal fin base	53.5	56.1	54.0–56.7	55.4
Anal origin to pelvic insertion	20.1	23.3	—	—
Depth of caudal peduncle	6.1	6.4	5.1–5.4	5.3–5.6
Length of caudal peduncle	5.0	5.7	6.1–6.9	6.3–7.1
Length of 1st dorsal-fin spine	5.5	6.4	5.9	7.0
Longest dorsal spine length	9.0 (13th)	8.4 (13th)	—	—
Longest dorsal soft ray length	11.8 (11th)	10.2 (11th)	—	—
Longest anal ray length	9.1 (24th)	8.2 (24th)	—	—
Length of last dorsal-fin spine	8.1	—	6.5–8.2	7.7
Length of 1st dorsal-fin soft ray	9.7	—	8.7–10.5	9.3
Length of 1st anal-fin spine	5.0	3.9	2.6–4.4	4.0
Length of 1st anal-fin soft ray	7.6	6.4	5.7–6.9	7.9
Longest pectoral ray length	16.4 (9th)	12.5 (9th)	—	—
Longest pelvic ray length	9.4 (2nd)	9.1 (2nd)	—	—

Discussion

In this study, one specimen of chaenopsid fishes has been collected from Ulleung Island with body elongated and compressed, no scales, supraorbital and nasal cirri present (Williams 2003; Nelson et al. 2016). The body morphometrics of the specimen were well matched with the original description of *N. lacunicola* with paired external pores of the incomplete lateral line, seven pairs of supraorbital cirri, occipital region with a pair of cirri, and 13 rays of pectoral fin (Fukao 1980; Aizawa and Doiuchi 2013). There are some differences between the presently reported specimen and that described by Fukao (1980); the differences were mainly the anal origin to pelvic insertion and slightly shorter length of caudal peduncle and longest pectoral ray length. Nonetheless, it is consistent with original descriptions with the main features of no black spot between first and second dorsal spines, occipital region with a pair of cirri, and seven pairs of supraorbital cirri (Fukao 1980; Aizawa and Doiuchi 2013; Murase et al. 2015). The body morphology of *N. lacunicola* is almost similar to *Neoclinus toshimaensis* Fukao, 1980, but distinctly different in the number of supraorbital cirri (6~7 in *N. lacunicola* vs. 9~11 in *N. toshimaensis*) (Fukao 1980; Aizawa 2002; Aizawa and Doiuchi 2013). The findings of two chaenopsids of the genus *Neoclinus*, namely, *N. bryope* and *N. chihiroe* were recently reported from Korean waters (MABIK 2020; Myoung et al. 2021). *Neoclinus lacunicola* is easily distinguished from the other two by lacking the black spot between first and second dorsal spines (without a black spot in *N. lacunicola* vs. with black spot in *N. bryope* and *N. chihiroe*) (Fig. 2B) (Aizawa 2002; Aizawa and Doiuchi 2013). The specimen collected in this survey had a black spot in the membrane of the second and third dorsal spines. This morphological character i.e., the presence or absence of a black spot between first and second dorsal spines, is one of the things that distinguish between males and females of *Neoclinus monogrammus* Murase, Aizawa et Sunobe, 2010 (see Murase et al. 2010) and it cannot be classified as *Neoclinus* species according to the taxonomic key suggested by Aizawa and Doiuchi (2013). For the presently reported specimen, yellow pelvic fins are key to distinguishing it as a female, despite the presence of black spots in the second and third dorsal spines membrane (Murase et al. 2015). Therefore, the presence or absence of the black spot is thought to be more variable in the same species than previously considered. In addition, our specimen

was well distinguished from *Neoclinus nudus* Stephens et Springer, 1971 and *N. bryope* was well separated from other congeners by genetic distances (*d*) of range 0.141 and 0.191 when a comparison of mitochondrial DNA COI sequences is made (Fig. 3). Therefore, this study documents the first record of *N. lacunicola* in Korean waters and suggests the new Korean name of 'eol-lug-bi-neul-be-do-la-chi' for the species.

Chaenopsid fishes, occurring in Korean waters, have previously been known only as two species (*N. bryope* and *N. chihiroe*), but an additional species has now been reported through this study. The ecological characteristics of chaenopsid fishes are known that they do not have large movements and inhabit small caves between rocks or in empty gastropod tubes (Stephens and Springer 1971; Fukao and Okazaki 1987; Fukao 1990). Due to this characteristic, their distribution ranges are expected to be considerably narrow (Hongjamrassilp et al. 2020). However, although the mobile abilities are limited within the habitat ranges, their larvae have potential dispersal possibilities through the oceanographic processes, including currents (Murase et al. 2015). According to Murase et al. (2015), the distribution range of *N. lacunicola* has been extended northwards along with the Tsushima Current and this study confirmed such northern distribution of the species. Although this species has firstly been reported to Korean waters, it is also expected that a number of individuals live in eastern Korean waters as well as Dokdo. In addition, because of the scarcity and the narrow habitat range of the species, there is a need for more ecological information, including their genetic group structure, geographic distribution range, and larval dispersals.

Acknowledgments

We are grateful to Mr. Min-Su Woo and Mr. Jin Young Shin, Korea Institute of Ocean Science and Technology for their assistance with sampling. This research was funded by the Korea Institute of Ocean Science and Technology (grant numbers PE99913, PN90190). This work was also supported by the National Research Foundation of Korea (NRF) grant funded by the Korean government (MSIT) (No. 2020R1F1A1051773).

References

Aizawa M (2002) Chaenopsidae. Pp. 1088, 1089. In: Nakabo T (Ed.) Fishes of Japan with pictorial keys to the species, English edition. Tokai University Press, Tokyo.

Aizawa M, Doiuchi R (2013) Chaenopsidae. Pp. 1292–1294. In: Nakabo T (Ed.) Fishes of Japan with Pictorial Keys to the Species, 3rd ed. Tokai University Press, Hadano, [In Japanese]

Froese R, Pauly D (2020) FishBase. World Wide Web electronic publication. www.fishbase.org, version (12/2020).

Fukao R (1980) Review of Japanese fishes of the genus *Neoclinus* with description of two new species and notes on habitat preference. Publications of the Seto Marine Biological Laboratory 25(1–4): 175–209. https://doi.org/10.5134/175985

Fukao R (1987) Fishes of *Neoclinus bryope* species complex from Shirahama, Japan, with description of two new species. Japanese Journal of Ichthyology 34(3): 291–308. https://doi.org/10.11369/jji1950.34.291

Fukao R (1990) Fishes of *Neoclinus* from Okinawa with notes on the traits of their habitats. Japan. Japanese Journal of Ichthyology 37(2): 116–126. https://doi.org/10.1007/BF02905379

Fukao R, Okazaki T (1987) A study on the divergence of Japanese fishes of the genus *Neoclinus.* Japanese Journal of Ichthyology 34(3): 309–323. https://doi.org/10.11369/jji1950.34.309

Hall TA (1999) BioEdit: A user–friendly biological sequence alignment editor and analysis program for Windows 95/98/NT. Nucleic Acids Symposium Series 41(41): 95–98.

Hongjamrassilp W, Murase A, Miki R, Hastings PA (2020) Journey to the West: Trans-Pacific historical biogeography of fringehead blennies in the genus *Neoclinus* (Teleostei: Blenniiformes). Zoological Studies (Taipei, Taiwan) 59: 9. https://doi.org/10.6620/ZS.2020.59-09

Hubbs CL, Lagler KF (1958) Fishes of the Great Lakes Region. Bulletin of Cranbrook Institution of Science 26: 1–213.

Jordan DS, Snyder JO (1902) A review of the blennoid fishes of Japan. Proceedings of the United States National Museum 25(1293): 441–504. https://doi.org/10.5479/si.00963801.25-1293.441

Kim IS, Kang EJ (1991) Taxonomic revision of the suborders Blennioidei and Zoarcoidei (Pisces, Perciformes) from Korea. Tongmul Hakhoe Chi 34(4): 500–525.

Kimura M (1980) A simple method for estimating evolutionary rate of base substitution through comparative studies of nucleotide sequences. Journal of Molecular Evolution 16(2): 111–120. https://doi.org/10.1007/BF01731581

Lin HC, Hastings PA (2013) Phylogeny and biogeography of a shallow water fish clade (Teleostei: Blenniiformes). BMC Evolutionary Biology 13(1): 1–18. https://doi.org/10.1186/1471-2148-13-210

MABIK (Marine Biodiversity Institute of Korea) (2020) National List of Marine Species. Namu Press, Seocheon.

Murase A, Sunobe T (2011) Interspecific territoriality in males of the tubeblenny *Neoclinus bryope* (Actinopterygii: Chaenopsidae). Journal of Ethology 29(3): 467–472. https://doi.org/10.1007/s10164-011-0276-y

Murase A, Aizawa M, Sunobe T (2010) Two new chaenopsid fishes, *Neoclinus monogrammus* and *Neoclinus nudiceps* (Teleostei: Perciformes: Blennioidei), from Japan. Species Divers 15(2): 57–70. https://doi.org/10.12782/specdiv.15.57

Murase A, Tashiro F, Awata S (2015) The northernmost records of two *Neoclinus* blennies (Teleostei: Chaenopsidae) from the Sea of Japan. Marine Biodiversity Records 8: e124. https://doi.org/10.1017/S1755267215001037

Myoung SH, Min W-G, Woo M-S, Kim Y-B, Shin JY, Park JM (2021) New record of *Neoclinus chihiroe* Fukao, 1987 (Perciformes: Chaenopsidae) in Dokdo, East Sea, Korea. Korean Journal of Ichthyology 33(2): 142–147. https://doi.org/10.35399/ISK.33.2.10

Nelson JS, Grande TC, Wilson VH (2016) Fishes of the world, 5th edn. John Wiley and Sons Inc., New Jersey, NJ, USA. 386 pp. https://doi.org/10.1002/9781119174844

Patzner RA, Gonçalves EJ, Hastings PA, Kapoor BG (2009) (Eds) The biology of blennies. CRC Press, Boca Raton, FL, USA. https://doi.org/10.1201/b10301

Saitou N, Nei M (1987) The neighbor-joining method: A new method for reconstructing phylogenetic trees. Molecular Biology and Evolution 4(4): 406–425. https://doi.org/10.1093/oxfordjournals.molbev.a040454

Soniyama T, Ogimoto K, Hori S, Uchida Y, Kawano M (2020) An annotated checklist of marine fishes of the Sea of Japan off Yamaguchi Prefecture, Japan, with 74 new records. Bulletin of the Kagoshima University Museum 11: 1–152.

Stephens JS, Springer VG (1971) *Neoclinus nudus*, new scaleless clinid fish from Taiwan with a key to *Neoclinus*. Proceedings of the Biological Society of Washington 84 (9): 65–72.

Tamura K, Stecher G, Peterson D, Filipski A, Kumar S (2013) MEGA6: Molecular Evolutionary Genetics Analysis version 6.0. Molecular Biology and Evolution 30: 2725–2729. https://doi.org/10.1093/molbev/mst197

Thompson JD, Higgins DG, Gibson TJ (1994) Clustal W: Improving the sensitivity of progressive multiple sequence alignment through sequence weighting, position-specific gap penalties and weight matrix choice. Nucleic Acids Research 22(22): 4673–4680. https://doi.org/10.1093/nar/22.22.4673

Ward RD, Zemlak TS, Innes BH, Last PR, Hebert PD (2005) DNA barcoding Australia's fish species. Philosophical Transactions of the Royal Society of London. Series B, Biological Sciences 360(1462): 1847–1857. https://doi.org/10.1098/rstb.2005.1716

Williams JT (2003) Chaenopsidae. Tubeblennies. Pp. 1761–1767. In: Carpenter KE (Ed.) FAO species identification guide for fishery purposes. The living marine resources of the Western Central Atlantic. Vol. 3: Bony fishes part 2 (Opistognathidae to Molidae), Sea turtles and marine mammals. FAO, Rome.

Acta Ichthyologica et Piscatoria 51(4), 2021, 345–348 | DOI 10.3897/aiep.51.70917

PENSOFT

ACTA ICHTHYOLOGICA ET PISCATORIA

First record of *Torquigener flavimaculosus* (Actinopterygii: Tetraodontiformes: Tetraodontidae) from Réunion island

Jean GADENNE[1], Patrick DURVILLE[4], Julien WICKEL[2], Eric HOARAU[1], Arnault GAUTHIER[1], Ronald FRICKE[3]

1 *Centre Sécurité Requin, Saint Leu, La Reunion, France*
2 *GIE MAREX, Saint Leu, La Réunion, France*
3 *Staatliches Museum für Naturkunde in Stuttgart, Stuttgart, Germany*
4 *Galaxea, La Saline-les-Bains, La Reunion, France*

http://zoobank.org/F957FA75-4E32-4746-8226-037839ACB2E0

Corresponding author: Jean Gadenne (jean.gadenne@securite-requin.re)

Academic editor: Paraskevi Karachle ♦ **Received** 1 July 2021 ♦ **Accepted** 28 September 2021 ♦ **Published** 2 November 2021

Citation: Gadenne J, Durville P, Wickel J, Hoarau E, Gauthier A, Fricke R (2021) First record of *Torquigener flavimaculosus* (Actinopterygii: Tetraodontiformes: Tetraodontidae) from Réunion island. Acta Ichthyologica et Piscatoria 51(4): 345–348. https://doi.org/10.3897/aiep.51.70917

Abstract

The first record of the yellow-spotted puffer, *Torquigener flavimaculosus* Hardy et Randall, 1983, on Reunion Island is confirmed by numerous video observations and by the capture of a specimen. This tetraodontid fish has been reported from the western Indian Ocean, the Red Sea, and the Mediterranean. In this report, we confirm its presence in Saint-Paul Bay in Réunion and this new observation completes the ichthyological inventory of Réunion Island.

Keywords

Baited Remote Underwater Video System, BRUVS, first observation, Indian Ocean, Mascarenes, pufferfish

Introduction

The most recent inventory of fish species from Réunion includes 984 marine and freshwater species belonging to 164 families (Fricke et al. 2009). This inventory conceals an unequal sampling effort between habitats because the majority of censuses were carried out on the coral reefs of the western side of the island (Pinault et al. 2013). Recent studies have provided a better understanding of the sandy and alluvial zones of the northern half of the island, the volcanic zone of Piton de la Fournaise, in the southeast, and the coastal habitats of an artificial reef or wrecks (Pinault 2013; Pinault et al. 2014). Throughout these studies, many new species were discovered and added to the island's faunistic inventory, and there are likely many more species yet to be observed.

As a part of the shark risk reduction, the missions carried out by the Shark Security Center, underwater cameras were deployed on the west and south-west coast of the island, primarily in sandy and detrital areas. The objective of these cameras was to record the frequentation of these sites by potentially dangerous sharks, as well as obtain a record of fish species living in these areas.

Material and methods

Réunion is a volcanic island in the Mascarene Archipelago, which includes Mauritius and Rodrigues. It is located at 21°06′S and 55°33′E, 690 km east of Madagascar. On the west and south-west coasts, highly urbanized and sheltered from the trade winds, fringing-type coral reefs

develop discontinuously over 25 km (Tessier et al. 2008). The southern and eastern regions, exposed to wind and swell, are sparsely inhabited. They are marked by the volcanic activity of Piton de la Fournaise and are characterized by recent flows and high coastal cliffs. Finally, in the northern region, also very urbanized, stretch pebble shores and alluvial black sand beaches.

As part of the monitoring and surveillance of shark populations in Réunion, Baited Remote Underwater Video Systems (**BRUVS**) were deployed all around the island. While sharks were the target species, an exhaustive list of all observed fish species was compiled.

Additionally, a single, freshly caught specimen of the genus *Torquigener* was brought to the research team for identification. This specimen was used to collect all morphometric information, measuring all characteristics outlined in Sabour et al. (2014) using calipers.

Results

Out of a total of 265 deployments of BRUVS, *Torquigener flavimaculosus* Hardy et Randall, 1983 was observed 22 times at depths ranging from 7 to 50 m (Fig. 1), but the majority of observations were made between 7 and 18 m on volcanic sand substrates. These fish often occurred in small groups ranging from 2 to 11 adult individuals.

Torquigener flavimaculosus is distinguished by the following set of characters which we used to formally identify the species (Fig. 2): the body is elongated. The

Table 1. Morphometric and meristic characters of *Torquigener flavimaculosus* collected from Saint-Paul Bay in Réunion compared with those of Mediterranean specimens reported by other authors.

Character	Presently reported study	Golani 1987	Corsini-Foka et al. 2006	Zenetos et al. 2008
Morphometric				
Number of specimens	1	2	3	1
Total length [mm]	105.0	97.0–98.0	55.0–134.6	133.0
Standard length [mm]	82.0	76.0–77.0	43.1–110.8	110.0
Standard length [%TL]	78.1	78.4–78.6	78.4–82.3	82.7
Head length [mm]	25.0	26.2–27.3	17.1–38.4	25.0
Head length [%SL]	30.5	34.5–35.5	31.1–35.0	22.7
Eye diameter [mm]	8.5	7.2–8.0	4.3–9.6	10.0
Eye diameter [%HL]	34.0	27.5–29.3	25.0–25.1	40.0
Preorbital length [mm]	9.0	—	7.2–11.6	11.0
Preorbital length [%HL]	36.0	—	42.1–43.2	4.0
Postorbital length [mm]	17.0	—	6.4–15.0	21.0
Postorbital length [%HL]	68.0	—	37.4–39.1	84.0
Interorbital space length [mm]	12.0	10.9–11.6	6.5–15.6	—
Interorbital space length [%HL]	48.0	41.6–42.5	38.0–40.6	—
Predorsal fin length [mm]	57.0	54.2–55.4	29.1–76.7	76.0
Predorsal fin length [%SL]	69.5	71.3–71.6	69.0–67.5	69.1
Prepectoral fin length [mm]	27.0	29.7–30.1	18.7–40.9	35.0
Prepectoral fin length [%SL]	32.9	39.1	36.9–43.4	31.8
Preanal fin length [mm]	57	57.6–58.0	31.5–79	83.0
Preanal fin length [%SL]	69.5	75.3–75.8	71.3–73.1	75.5
Caudal peduncle depth [mm]	6.1	5.9	3–8.3	15.0
Caudal peduncle depth [%SL]	7.4	7.8	7–7.5	13.6
Pectoral fin length [mm]	14.0	—	—	25.0
Pectoral fin length [%SL]	17.1	—	—	22.7
Meristics				
Dorsal ray count	9	9	9	—
Pectoral ray count	14	15	14	—
Anal ray count	7	7–8	7	—
Caudal ray count	10	10	10	—

TL = total length, HL = head length; SL = standard length.

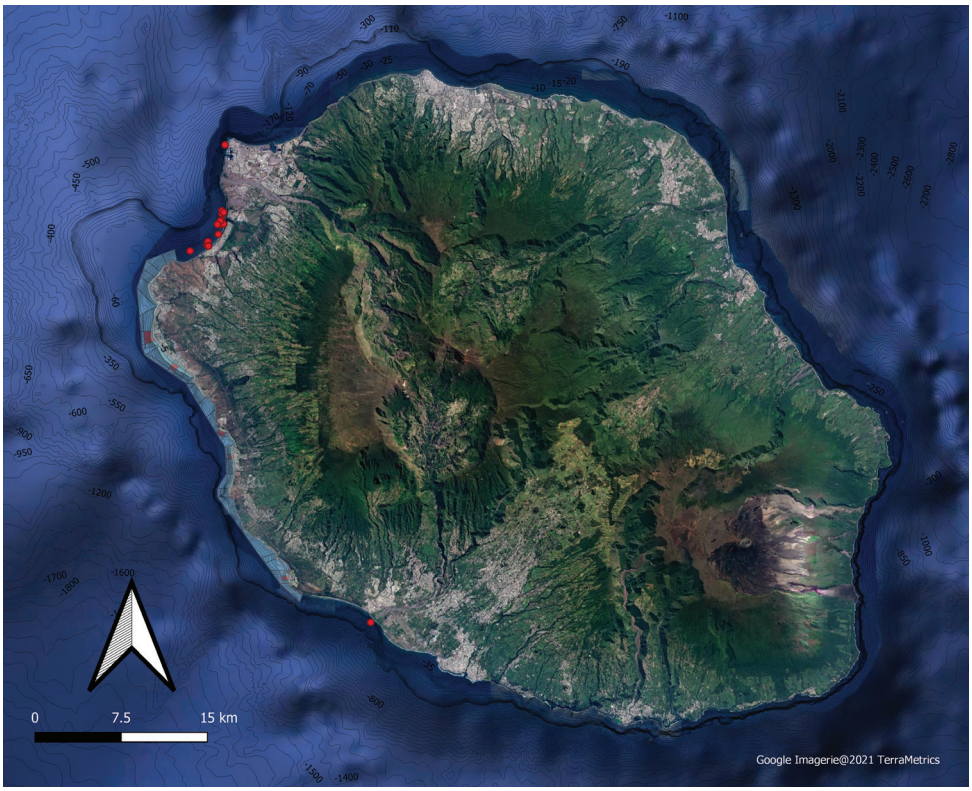

Figure 1. Spots in Saint-Paul Bay, Réunion Island where *Torquigener flavimaculosus* was observed by Baited Remote Underwater Video System (BRUVS) Source: Google Maps.

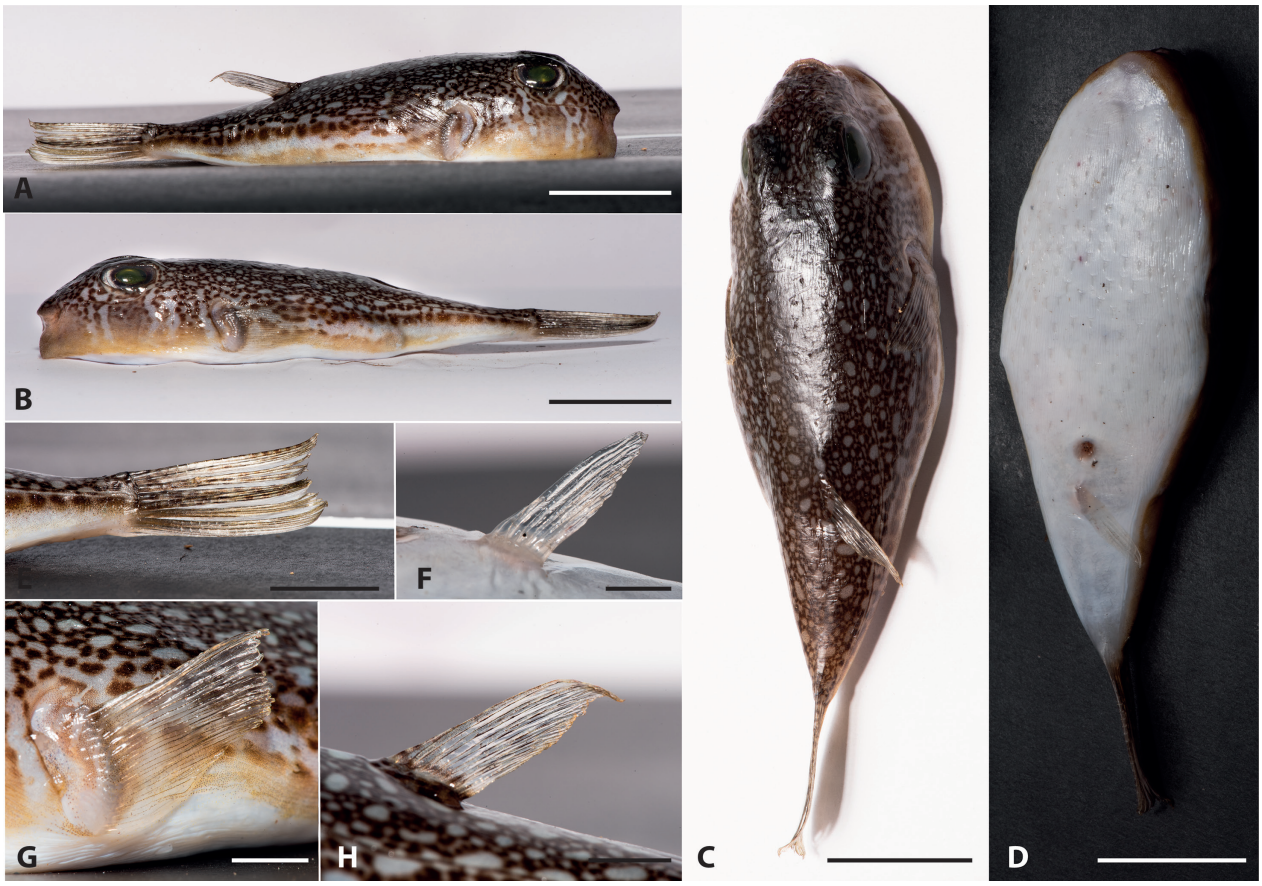

Figure 2. Photo of the *Torquigener flavimaculosus* specimen, collected off Réunion Island; **A** = right side, **B** = left side, **C** = dorsal view, **D** = ventral view, **E** = caudal fin, **F** = anal fin, **G** = pectoral fin, **H** = dorsal fin; scale bars: 2 cm (**A**, **B, C, D**); 1 cm (**E**); 0.5 cm (**F**, **G**, **H**).

eye is surrounded by the dorsal lateral line. The lower margin of the eye is above the level of the corner of the mouth and above the top of the pectoral fin base. The mouth terminal is at the level of the upper end of the pectoral fin. The chin is distinct. The dorsal and anal fins are elongated and pointed. Small spinules are present on the belly, head, sides, and back in a spot that does not reach the dorsal fin. The lower border gill has a cartilaginous spur. The posterior margin of the gills covers small irregularly distributed spines. The dorsal body surface is brown with gray-whitish spots. A median lateral line of yellow-orange spots is distinguished, followed by a pale yellow area, separating the dorsal surface from the white ventral surface. Vertical yellow-brown stripes on the cheek are separated by irregular white stripes. The caudal fin shows brown spots. The dorsal fin is lightly spotted with white. The anal and pectoral fins are transparent. Table 1 summarizes the main morphometric and meristic data of the captured specimen. They are consistent with the description of this species provided by Hardy and Randall (1983) and Golani (1987) for this species which is referenced in the classification as being part of the Class of Actinopterygii, of the Order of Tetraodontiformes, of the Family of Tetraodontidae, of the Genus *Torquigener* Whitley, 1930 and of the species *Torquigener flavimaculosus*.

Discussion and conclusion

The yellowspotted puffer, *Torquigener flavimaculosus*, is found in the western Indian Ocean from the northern Red Sea to Kenya and in the Arabian Gulf and Seychelles (Froese and Pauly 2021). It has also been recorded in the Mediterranean Sea, as a Lessepsian migrant from the Red Sea, by Golani (1987) in Haifa Bay, Israel. Later, the species has also been recorded from Turkish coastal waters, the north-eastern Mediterranean Sea (Bilecenoglu 2003, 2005; Erguden and Gurlek 2010), and from Greek waters (Corsini-Foka et. al. 2006; Zenetos et al. 2008).

By comparing the morphometric and meristic characters of our specimen with other Mediterranean individuals, we do not notice any striking differences in their proportions. The specimen was initially identified visually using body markings and coloration, these matching morphometric measurements help confirm the identification as *Torquigener flavimaculosus*. This is the first sighting of this species in Réunion, where it has been recorded on several occasions, close to the substrate, on a black sandy bottom, between 7 and 50 m of depth. This particular habitat is characterized by an endogenous fauna of mollusks, worms, and echinoderms, which represent abundant food for this invertivorous species (Froese and Pauly 2021). The associated ichthyological fauna

is relatively poor and only a few small pelagic such as *Selar crumenophthalmus* (Bloch, 1793) or *Decapterus macarellus* (Cuvier, 1833) occasionally congregate there (Turquet et al. 1998). The presently reported *T. flavimaculosus* represents a genus with 21 species (Froese and Pauly 2021), none of which have yet been recorded in Réunion. The validation of this species in the area adds to its distribution area and completes the ichthyological inventory of Réunion.

Very little is known about the reproduction of fishes of the genus *Torquigener*. At least one species is known to fabricate intricate nests to attract potential mates (Kawase et al. 2013). Males were observed defending the nest after reproduction but left once the eggs have hatched (Kawase et al. 2013). It is unknown whether the hatchlings stay demersal or whether they become pelagic and part of zooplankton. According to Froese and Pauly (2021), another species, *Torquigener hypselogeneion* (Bleeker, 1852), is present in Seychelles; it would be interesting to know if this species is present in Réunion. Pelagic larval dispersal is known to occur between the Seychelles and Réunion Island, which could have been a way for the species to colonize the coastal waters of Réunion (Crochelet et al. 2016).

References

Bilecenoglu M (2003) Kizildeniz göçmeni balon baligi (*Torquigener flavimaculosus* Hardy & Randall, 1983), Türkiye kiyilarindan ilk gözlemler. Sualti Dunyasi Dergisi 74: 38–39. [In Turkish]

Bilecenoglu M (2005) Observations on the burrowing behaviour of *Torquigener flavimaculosus* Hardy & Randall, 1983 (Osteichthyes: Tetradontidae) along Fethiye Coasts, Turkey. Zoology in the Middle East 35: 29–34. https://doi.org/10.1080/09397140.2005.10638100

Corsini-Foka M, Margie P, Kondilatos G, Economidis PS (2006) *Torquigener flavimaculosus* Hardy and Randall, 1983 (Pisces: Tetraodontidae) off Rhodes island marine areas: A new alien fish in the Hellenic waters. Mediterranean Marine Science 7(2): 73–76. https://doi.org/10.12681/mms.172

Crochelet E, Roberts J, Lagabrielle E, Obura D, Petit M, Chabanet P (2016) A model-based assessment of reef larvae dispersal in the western Indian Ocean reveals regional connectivity patterns—Potential implications for conservation policies. Regional Studies in Marine Science 7: 159–167. https://doi.org/10.1016/j.rsma.2016.06.007

Erguden D, Gurlek M (2010) The presence of Indo-Pacific puffer fish *Torquigener flavimaculosus* Hardy and Randall 1983, in the Iskenderun Bay, the eastern Mediterranean coast of Turkey. CIESM Congress 2010, Venice, article 0505.

Fricke R, Mulochau T, Durville P, Chabanet P, Tessier E, Letourneur Y (2009) Annotated checklist of the fish species (Pisces) of La Réunion, including a Red List of threatened and declining species. Stuttgarter Beitrage zur Naturkunde. Serie A, Biologie 2: 1–168.

Froese R, Pauly D (2021) FishBase. http://www.fishbase.org [version 06/2021]

Golani D (1987) The Red Sea pufferfish, *Torquigener flavimaculosus* Hardy and Randall 1983, a new Suez Canal migrant to the eastern Mediterranean. (Pisces: Tetraodontidae). Senckenbergiana Maritima 19: 339–343.

Hardy GS, Randall JE (1983) Description of a new species of pufferfish (Tetraodontiformes: Tetraodontidae) from the Red Sea and adjacent waters. Israel Journal of Zoology 32(1): 13–20.

Kawase H, Okata Y, Ito K (2013) Role of huge geometric circular structures in the reproduction of a marine pufferfish. Scientific Reports 3(1): 2106. https://doi.org/10.1038/srep02106

Pinault M (2013) Évaluation de la fonctionnalité de récifs artificiels à vocation non extractive, dans un contexte d'habitats naturels fragmentés – côte nord-ouest de l'île de La Réunion. Cybium 37(4): 262.

Pinault M, Chabanet P, Loiseau N, Durville P, Galzin R, Quod JP (2013) Influence des facteurs environnementaux sur la structure des peuplements ichtyologiques de l'île de La Réunion (Sud-Ouest de l'océan Indien). Cybium 37(1–2): 95–109. https://doi.org/10.26028/cybium/2013-371-010

Pinault M, Wickel J, Guyomard D, Fricke R, Quod JP (2014) Premier signalement de *Pseudanthias bicolor* (Serranidae) sur différents habitats artificiels à La Réunion. Cybium 38(4): 255–259. https://doi.org/10.26028/cybium/2014-384-002

Sabour W, Saad A, Jawad L (2014) First record of yellow-spotted puffer *Torquigener flavimaculosus* Hardy & Randall, 1983 (Osteichthys: Tetraodontidae) from Mediterranean Sea coasts of Syria. Thalassia Salentina 36: 29–34.

Tessier E, Bigot L, Cadet C, Cauvin B, Chabanet P, Conand C, Nicet JB, Quod JP (2008) Coral reefs of Réunion Island in 2007: Status report and monitoring network. Revue d'Ecologie – la Terre et la Vie 63: 85–102.

Turquet J, Tessier E, Bosc P, Durville P, Quod JP (1998) Etude sur les récifs artificiels et le recrutement larvaire en zones à habitat limité à la Réunion. Rapport ARVAM/ARDA/CRPEM 58P.

Zenetos A, Vassilopoulou V, Salomidi M, Poursanidis D (2008) Additions to the marine alien fauna of Greek waters (2007 update). Marine Biodiversity Records 1: e91. https://doi.org/10.1017/S1755267207009281

Acta Ichthyologica et Piscatoria 51(4), 2021, 349–356 | DOI 10.3897/aiep.51.63815

PENSOFT

ACTA ICHTHYOLOGICA ET PISCATORIA

The time-area fishing closure impacts on fish stock; Qiantang River before and after a four-month fishing closure

Aiju ZHANG[1], Wei LUO[1], Jun WANG[1], Zhimin ZHOU[1]

1 *Agriculture Ministry Key Laboratory of Healthy Freshwater Aquaculture, Key Laboratory of Freshwater Aquaculture Genetic and Breeding of Zhejiang Province, Zhejiang Research Center of East China Sea Fishery Research Institute, Zhejiang Institute of Freshwater Fisheries, Huzhou, China*

http://zoobank.org/474386D9-60FC-4B5F-B6D5-655AEAFC4822

Corresponding author: Zhimin Zhou (zjhz-zzm@163.com)

Academic editor: Mirosław Przybylski ♦ **Received** 1 February 2021 ♦ **Accepted** 13 September 2021 ♦ **Published** 4 November 2021

Citation: Zhang A, Luo W, Wang J, Zhou Z (2021) The time-area fishing closure impacts on fish stock; Qiantang River before and after a four-month fishing closure. Acta Ichthyologica et Piscatoria 51(4): 349–356. https://doi.org/10.3897/aiep.51.63815

Abstract

Fishing closures, commonly used to manage fisheries' catch, involve temporarily closing a body of water to particular fishing gears to control fishing effort and protect feeding and spawning areas. In recent years in Qiantang River of China, with the socio-economic development, protection of fish stock has become increasingly urgent. The year 2019 was the first year that Qiantang River was included in the unified fishing ban system for the south of Yangtze River basin. Here, fish captures and hydroacoustic surveys were carried out in the research area of Qiantang River in order to present comparative descriptions of the dominant fish species, the temporal changes of fish size, density, biomass, and distribution affected by the four-month fishing closure in 2019. The results showed that *Pseudobrama simoni* (Bleeker, 1864) was the most dominant species both before and after the closure by using the traditional capture method. The mean target strength (TS) of overall fish after closure was –50.28 ± 0.19 dB, which was lower than that before, resulting in a significantly shorter derived mean length (13.42 ± 0.74 cm). The mean fish density and calculated biomass after closure were both significantly higher than that before it. More than 50% of fish species were distributed in the water of 5–20 m depth after the closure, which likely occurred in water deeper than 20 m before. Meanwhile, fewer outliers were found in different depth categories after closure. It is concluded that the four-month closure in 2019 had a positive effect on fish size, density, and biomass, leading to protection of pelagic fishes and a more even distribution of fish.

Keywords

capture, fishing closure, fish resource, hydroacoustics, Qiantang River

Introduction

Given the increased use of modern fishing devices, many marine and freshwater fish resources are intensively exploited, resulting in rapid declines in some fish stock, affecting national economies, local communities' socio-economic well-being, and even their protein saecurity (Tang and Chen 2004; Branch et al. 2011). Subsequently, as a frequently used tool to control fishing effort and protect feeding and spawning areas, time-area fishing closure measure has been taken into account by governments of many countries. The effect of this measure has been assessed on fishing strategies regarding the fishing mode, variations in the population structure of a particular fish, incidental megafauna catches, and social well-being impacts (Britton 2014; Escalle et al. 2016; O'Farrell et al. 2016), but more rarely, on overall fish stock.

With the improvement of instrument performance and the development of computer software, the hydroacoustic method has increasingly become one of the main methods for fishery stock assessments due to its advantage of a rapid, economic and extensive coverage of the water cross-section at distances large enough not to affect fish behavior (Simmonds and MacLennan 2005), and now has been widely used in many bodies of water (Hale et al. 2008; Pavlov et al. 2010; Gerasimov et al. 2019; Guo et al. 2019).

In China, overfishing has also become one of the most serious problems in inland waters, as well as in oceans, and time-area fishing closure measures have been implemented since 2002. However, there has been no published assessment of overall fish stock following a closure in any rivers. Qiantang River is the largest river in Zhejiang province with a basin area of about 55 000 km^2. Except for drinking, it also has functions of power generation, flood control, irrigation, and tourism. The river was historically rich in fish resources, and fish harvests date back several centuries, the highest take was recorded in 1960 with 5318.2 tones. Although harvest strategies incorporating seasonal bans and restricted fishing grounds have been conducted several years before 2019, which were mainly conducted in different tributaries of the river, the effects were not ideal due to inconsistency. The year 2019 was the first year that Qiantang River was included in the unified fishing ban system for the south of Yangtze River basin. Subsequently, all captures except recreational fishing should be banned in the main channel of Qiantang River from 1 March through 30 June every year in the future. So, what happened to fish stock after a four-month fishing closure in 2019?

Here, based on the data obtained from field fish collections and hydroacoustic surveys before and after the implementation of fishing closure in the main channel of Qiantang River, we compared the distribution of species in the research area, identified the dominant species, and evaluated changes in the fish size, density, biomass, and distribution. Our findings will present a description of characteristics of the temporal change effected by the closure and provide a scientific basis for the protection of fish stock in the river.

Materials and methods

Research area

The study area belongs to a section of the main channel of Qiantang River, an important fishing stretch of water for fishermen in Fuyang and Tonglu counties (Fig. 1). This area is located between 29°52.6′N and 30°3.4′N, and 119°45.8′E and 119°59.5′E with a length of 29.9 km from east to west, with an average water depth of 14 m, a water volume of 0.31 km^3, and a maximum water depth of 35 m.

Field collection

Two fish removals were conducted by the hired fishermen in the research area in July 2018 and July 2019. The research area was evenly divided into 4 fish sampling sections, and the fishes were caught by deploying ground bamboo cages and multipanel nylon gillnets with mesh sizes ranging from 1 to 8 cm in each sampling section. All fishes caught were humanely euthanized, counted, and identified. Each specimen was measured to the nearest 0.1 cm (total length, L) and weighed to the nearest 0.01 g (weight, W) simultaneously.

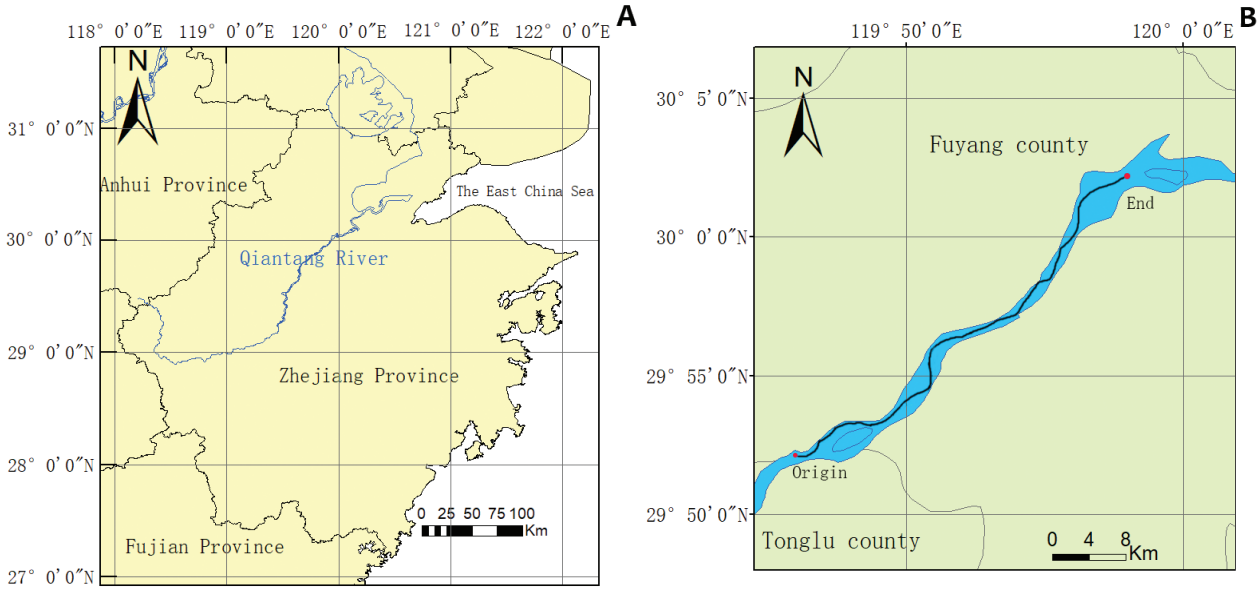

Figure 1. Location and hydroacoustic sampling transects in Qiantang River; (**A**) the location of Qiantang River in Zhejiang, China; (**B**) hydroacoustic sampling transects in Qiantang River.

The dominant species was assessed according to the formula of Pinkas et al. (1971):

$$IRI = (\%N + \%W) \times (\%FO)$$

where $\%N$ is the individual number of a certain species relative to the total number of fishes, $\%W$ is the weight of a certain species relative to the total weight of all fishes, and %FO is the frequency of occurrence of a certain species among the 4 fish sampling sections. According to the evaluation criterion of Zhang et al. (2016), the species is considered to be dominant when its IRI value is above 2000. For the most dominant fish species, the length–weight function,

$$W = aL^b$$

where W is the weight [g], L is the total length [cm], a is the intercept and b is the slope, was fitted with a simple linear regression model using log-transformed data.

Acoustic surveys

Two hydroacoustic surveys were conducted on 17 July 2018 and 19 July 2019 by using a BioSonics split-beam DT-X echosounder (BioSonics, Seattle, WA, USA) with a 201 kHz transducer, an integrated GPS (Garmin 17xHVS, Garmin Ltd., Olathe, KS, USA) and a computer. Surveys were conducted during daylight sunshine, and the daily mean value of water temperature was 26.3°C and 23.5°C, respectively. A fishing boat was hired to help surveys at a speed of 2.0–2.5 m/s in a zig-zag route. During surveys, the transducer face was held 40–50 cm below the water surface. A standard BioSonices 36 mm tungsten carbide sphere was used to calibrate the transducer before each survey (Foote et al. 1987). The degree of coverage (D) was calculated for each survey according to the formula of Aglen (1983). Here, the degree of coverage was 6.14 and 6.36, respectively, which were both higher than 2, indicating the sampling error of density estimates to be less than 10% (Godlewska et al. 2009). The usage method of instruments was consistent with the scheme of Guo et al. (2019).

Acoustic data analysis

The hydroacoustic data were analyzed using BioSonics Visual Analyzer software 4.1 (BioSonics, Seattle, WA, USA), consistent with the scheme of Guo et al. (2019). The fish tracking parameters were set to values in Table 1. Only data between 1.5 m of the transducer and 0.5 m off the bottom were used in order to exclude dead zones. Fish density estimates were calculated by echo integration, defined as the summation of the volume backscattering strength (Sv) divided by the backscattering cross-section (σ_{bs}), derived from the mean echo intensity (target strength, TS) of individual fish. With set appropriate threshold (–60 dB) and manual corrected, data for each transect were cleared of noise (Zhou et al. 2016). The integration interval was set to 1200 pings.

Table 1. Parameter settings for the Bisonics Visual Analyzer.

Parameter	Setting
Echo threshold [dB]	–60
Tracking window [m]	1.79
Min detection range [m]	0
Max detection range [m]	50
Correlation factor	0.9
Pulse width factor	3
Min pulse width	0.75
Max plus width	3
Max ping gap	2

Calculation of fish size and biomass

Based on single echo detections (SED), the TS distributions were examined. The received echo signals were compensated depending on their range (R)[m] by the time-varied gain (TVG). A 40 log(R) TVG was applied to measurements of TS, whereas a 20 log(R) TVG was used to the measurements of Sv used when echo integration. Then, the mean value of TS (based on SED from –60 dB to –30 dB in 2 dB bins) was converted to mean length of tracked fish using the empirical formulas for TS–length relation (Foote 1998); mean length was converted to weight using the calculated length–weight function, $W = aL^b$, for the most dominant fish species; the weight was multiplied by the total density of transects; and the mean weight of the transects was then calculated as the mean biomass.

Statistical data analysis

Statistical analyses were performed using SPSS 16.0 and Excel 2007. Data are presented as mean ± standard error of the mean (SE). Prior to analysis, all data were tested for homogeneity (Levene's test). The nonparametric Kruskal–Wallis H test or one-way ANOVA were used to analyze the effects of fishing closure on mean TS, length, density, and biomass. To compare differences in fish density, water depths were divided into five intervals: 0–5 m, 5–10 m, 10–15 m, 15–20 m, 20–25 m, and >25 m. A two-way ANOVA was also performed to test the effects of water depth and fishing closure on fish densities. All tests were considered significant at a probability level of $P < 0.05$ (95% confidence). Box plot was performed in R 3.6.1 environment (R Development Core Team 2010).

Results

Fish biodiversity resulting from traditional capture method

In total, 47 and 44 fish species were identified before and after fishing closure respectively, both representing

9 orders and 14 families. *Pseudobrama simoni* (Bleeker, 1864) was found to be the most dominant species with the highest IRI values of 2965.31 and 2867.78, respectively, and the estimated length–weight relation (LWR) parameters *a* and *b* of this fish species were 0.0256 and 2.8117, respectively, indicating the LWR equation as:

$$W = 0.0256 \times L^{2.8117}$$
$$(R^2 = 0.957, n = 235).$$

However, subdominant species and common species were found to be changed. Three subdominant species were *Distoechodon tumirostris* Peters, 1881 (IRI = 1581.73), *Carassius auratus* (Linnaeus, 1758) (IRI = 1128.68), and *Squalidus argentatus* (Sauvage et Dabry de Thiersant, 1874) (IRI = 1091.01) before fishing closure, which changed to be *Coilia nasus* Temminck et Schlegel, 1846 (IRI = 1373.68), *Hypophthalmichthys molitrix* (Valenciennes, 1844) (IRI = 1106.22), and *Cyprinus carpio* Linnaeus, 1758 (IRI = 1003.29) after closure. Meanwhile, the first four common species, including *Tachysurus nitidus* (Sauvage et Dabry de Thiersant, 1874) (IRI = 991.73), *Cyprinus carpio* (IRI = 660.82), *Megalobrama terminalis* (Richardson, 1846) (IRI = 515.49), and *Hypophthalmichthys nobilis* (Richardson, 1845) (IRI = 500.08) changed to be *Tachysurus nitidus* (IRI = 953.76), *Carassius auratus* (IRI = 911.04), *Eleotris oxycephala* Temminck et Schlegel, 1845 (IRI = 753.00), and *Megalobrama terminalis* (IRI = 688.85) after closure, two species of which were different.

Fish size distribution

Results of the two hydroacoustic surveys showed a significant difference ($H_{2, 632}$ = 18.797, $P < 0.05$), with the mean TS before fishing closure (–49.17 ± 0.21 dB) greater than that after it (–50.28 ± 0.19). According to the formula, the derived mean lengths before and after closure were 15.26 ± 0.48 cm and 13.42 ± 0.74 cm, respectively, which also showed significant temporal differences (one-way ANOVA, $F_{1, 632}$ = 4.567, $P < 0.05$).

Echoes of more than –58 dB target strength were considered fish. The TS before and after the fishing ban both ranged from –58 dB to –34 dB. To compare differences in fish population sizes, fishes were divided into small-, mid-, and large-sized categories, based on their length (TS conversion). TS distributions varied between two surveys. Before closure, mid-sized fish of TS –50 to –38 dB (≈11−48 cm) accounted for 59.81% of the population, while small-sized fish under –50 dB accounted for 38.51% of all fish (Fig. 2). This was a little different from the results obtained after closure, of which mid-sized fish accounted for 58.86%, while small-sized fish 40.24% (Table 2).

Table 2. Proportional composition of fish populations before and after the fishing closure.

Size class [cm]	Before closure [%]	After closure [%]
Small-size (≈7–11)	38.51	40.24
Med-size (≈11–48)	59.81	58.86
Large-size (>48)	1.68	0.90

Fish density and biomass

Fish density after the fishing closure (3997.4 ± 466.89 fish/ha) was significantly greater than that before it (1716.4 ± 142.47 fish/ha) ($H_{2, 632}$ = 13.086, $P < 0.05$). The mean calculated biomass after closure (3238.1 ± 2543.9 kg/ha) was also significantly higher than that before closure (1282.2 ± 323.37 kg/ha) (one-way ANOVA, $F_{1, 632}$ = 3.673, $P < 0.05$).

Relation between water depth and fish density

More than 50% of fish species were found in the >20 m category before closure. While fish gradually moved towards the upper water layer, leading to the most distributed

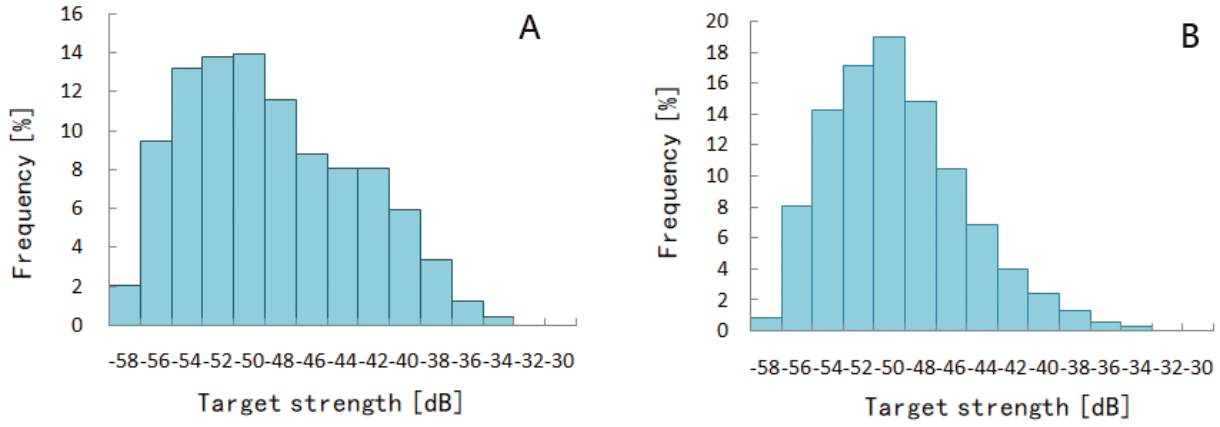

Figure 2. Frequency distribution of fish tracks detected by acoustic target strength (**A**) before and (**B**) after the closure of Qiantang River in Zhejiang, China.

layers of fish being located at 15–20 m, 5–10 m, and 10–15 m depth after closure, accounting for 24.95%, 20.44%, and 18.30% of the total fish in the research area, indicating a wider spread of fish (Table 3). However, the arithmetic means of density was not significantly affected by water depth ($F_{5, 1850} = 1.855$, $P > 0.05$), but affected by the fishing closure ($F_{1, 1850} = 6.571$, $P < 0.05$). As showed in Fig. 3, the medians of all transects in different depth categories after closure were all larger than those before closure, indicating a higher mean fish density after closure. Meanwhile, fewer outliers were found in six different depth categories after closure than before, indicating a more discrete density distribution of the fish before closure.

Table 3. Percentage of fish distributed in different depth categories before and after the fishing closure.

Depth category [m]	Before closure [%]	After closure [%]
0–5	3.19	3.48
5–10	6.79	20.44
10–15	17.36	18.30
15–20	18.69	24.95
20–25	21.55	17.59
>25	32.42	15.25

Discussion

Effects of time-area closure on fish stock

With a time-area closure, an area of water is closed to fishing with particular fishing gears during certain time periods. Originally, a time-area closure is commonly focusing on a single, target species and a single fishery (e.g., parrotfish, shrimp, tropical tuna) (Armsworth et al. 2011; O'Farrell et al. 2016), and now used to manage spatially and temporally acute bycatch problems (Goodyear 1999). The closures have been introduced to manage stocks of fish resources in many countries as well as other concurrent measures, e.g., restricting fishing gear, artificial propagation, and releasing (Torres-Irineo et al. 2011; Escalle et al. 2016). Tang and Chen (2004) confirmed that the timing of harvesting has a strong impact on the persistence of fish population, on the volume of mature fish stock, and on the maximum annual-sustainable yield. O'Farrell et al. (2016) found that the sex ratios of four parrotfish species—*Sparisoma viride* (Bonnaterre, 1788), *Sparisoma aurofrenatum* (Valenciennes, 1840), *Scarus vetula* Bloch et Schneider, 1801, and *Scarus taeniopterus* Lesson, 1829—recovered rapidly in Bermuda following a fishing closure, with male proportions equilibrated at values ranging from 0.36 to 0.54 within 3–4 years, similar to those reported at unfished sites in the region. Nevertheless, the consequences in terms of changes in fishing strategies and effort reallocation may not always be as expected (Hiddink et al. 2006; Torres-Irineo et al. 2011; Escalle et al. 2016). Thus, the optimal management of the time-area regulation, which has a direct relation to sustainable development, should receive much attention, to sustain fisheries at a good level of productivity and meet economic goals.

The necessity of a time-area fishing closure in Qiantang River

In recent years in Qiantang River, with the socio-economic development, protection of fish stock has become increasingly serious. Although modern gears in the river are limited to gillnets, which are three-tiered with mesh sizes varying from 1 to 8 cm, the fishing mode results in indiscriminate harvesting of undersized and non-tar-

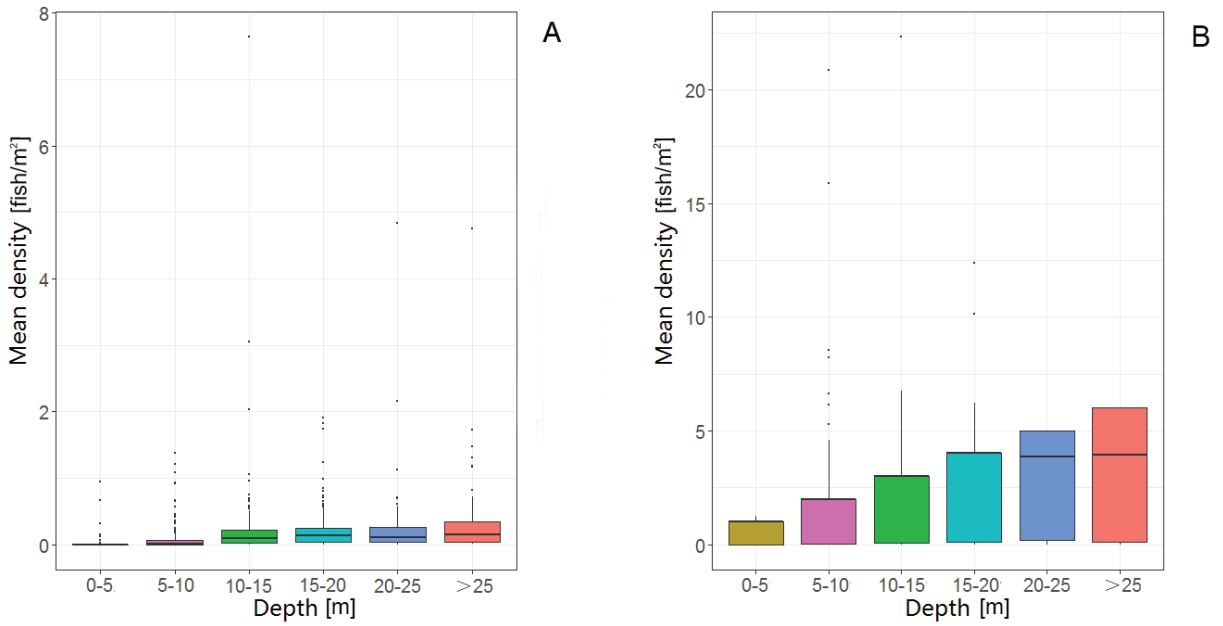

Figure 3. Acoustic mean fish density distribution at different water depth categories of Qiantang River in Zhejiang, China (**A**) before and (**B**) after the closure.

get species. The volume of fish stock in the river has declined, and the fish population structure is known to have changed. According to literature records, 136 fish species could be collected in this river in the late 1970s, receding to 122 species in 2018. Also, it has been found that some native fishes, e.g., *Acipenser sinensis* Gray, 1835, *Psephurus gladius* (Martens, 1862), *Tenualosa reevesii* (Richardson, 1846), and *Protosalanx hyalocranius* (Abbott, 1901), have disappeared and some alien ones, e.g., *Lepomis macrochirus* Rafinesque, 1819 and *Ictalurus punctatus* (Rafinesque, 1818), have become common. Thus, a fishing closure is conducive to the sustainable development of fishery in the river.

Effects of the fishing closure on fish biodiversity

In practice, the general closure period in Qiantang River included in the unified fishing ban system for the south of Yangtze River basin is from 1 March through 31 June, lasting for 4 months. It is confirmed that many economically important fish propagate at this time every year, and the aggregating behavior of breeding fish makes them more vulnerable to capture. Ley et al. (2002) found high diversity and productivity in tropical mangrove-dominated estuaries after closure. Here, the decline of three species after closure may be related to the contingency of fishing. Marks et al. (2015) also confirmed that total catch rates after the closure were significantly higher than before, differences in the size composition of species reflected both the increased survival of older fishes and higher recruitment success. Furthermore, we concluded that the conservation effect would be different for different fish. After a four-month fishing closure, the most dominant species remain unchanged. By contrast, the subdominant and common species changed to some extent. Different from small fishes (*Distoechodon tumirostris*, *Carassius auratus*, and *Squalidus argentatus*) contributing to subdominant species before closure, migratory species (*Coilia nasus*) and releasing species (*Hypophthalmichthys molitrix* and *Cyprinus carpio*) became the subdominant species after closure. Meanwhile, in addition to *Tachysurus nitidus* and *Megalobrama terminalis* remaining unchanged, the other two fishes of the first four common species changed. Thus, it seems that the presently reported fishing ban system could help migratory fish to propagate quickly, rather than being caught when spawning. At the same time, the fishing ban also led to a significant decrease of capture amount for releasing species during the closed period, resulting in a significant increase of abundance in the river.

Effects of the fishing closure on fish size, density, and biomass

It is accepted that such a closure can effectively protect fish spawning and hatching, and is also beneficial for the growth of fish larvae, to promote the natural supplement of fish resources and the self-restoration of the ecological environment in the waters (Tang and Chen 2004). Our results also confirmed this view by using the hydroacoustic method, which showed that the mean fish density and biomass after the closure were both significantly greater than that before it, while the derived mean length after the closure was lower than before. In detail, the mean length of fish decreased after the time-area ban, i.e., the proportions of small-sized fish increased (40.24% vs. 38.51%), while mid-sized (58.86% vs. 59.81%) and large-sized fish (0.90% vs. 1.68%) decreased in July 2019. The mean weight also showed the same trend. Reproduction protection during the closure could somewhat explain the reason. The 2019 fishing closure increased the survival of older fishes and most juvenile fishes, made them supplementary to the total population, increasing fish abundance and the small size composition of fish species.

Effects of the fishing closure on fish distribution

Fishing closure resulted in a change of fish distribution. It is accepted that time-area closures are often preferred for more mobile pelagic species (Hobday and Hartmann 2006; Grantham et al. 2008; Game et al. 2009), maybe due to their easy capture by gillnets with relatively fixed mesh size. In this study, a reduction of these pelagic fish stock, a more discrete size of uncaught fish, and a distribution in deeper water were disclosed before closure. For example, more than 50% of fish were concentrated in >20 m layer. However, after a four-month fishing closure, there was no significant difference in the distribution of water depth, with more than 50% of the fish distributed in 5–20 m layer. Thus, it seems that the fishing closure of 2019 protected the pelagic fish and made fish more evenly distributed.

Conclusion

The reasons for the time-area ban policy are biological, concerned with protecting and restoring fish stock, not only impacting catches of target species, but also non-target species that can be sold, and non-target species that do not have commercial value for fishermen (Chumchuen et al. 2016). Since 2019, a four-month fishing closure from 1 March through 31 June has been adopted in the main channel of Qiantang River of China every year, which has a great positive effect on fish size, density, and biomass, and makes fish more evenly distributed. Future continuous multi-year monitoring combining the traditional capture and hydroacoustic survey methods needs to be carried out, and more additional closure time may be needed except for the critical life stage of important endangered fish species, to realize the sustainable development of fish in the river.

Acknowledgments

The authors are thankful to Dr Aihuan Guo, Zhejiang Institute of Freshwater Fisheries, Huzhou for the assistant analysis of hydroacoustic data. The financial support was provided by Zhejiang Science and Technology Project (No. 2019C02047), Zhejiang, China.

References

Aglen A (1983) Random errors of acoustic fish abundance estimates in relation to the survey grid density applied. FAO Fisheries Report 300: 293–298.

Armsworth PR, Block BA, Eagle J, Roughgarden JE (2011) The role of discounting and dynamics in determining the economic efficiency of time-area closures for managing fishery bycatch. Theoretical Ecology 4(4): 513–526. https://doi.org/10.1007/s12080-010-0093-x

Branch TA, Jensen OP, Ricard D, Yimin YE, Hilborn R (2011) Contrasting global trends in marine fishery status obtained from catches and from stock assessments. Conservation Biology 25(4): 777–786. https://doi.org/10.1111/j.1523-1739.2011.01687.x

Britton E (2014) Ghost boats and human freight: The social wellbeing impacts of the salmon ban on Lough Foyle's Fishing Communities. Pp. 43–164. In: Urquhart J, Acott TG, Symes D, Zhao MH (Eds) Social issues in sustainable fisheries management. Springer, Dordrecht, the Netherlands. https://doi.org/10.1007/978-94-007-7911-2_8

Chumchuen W, Matsuoka T, Anraku K, Premkit W (2016) Size-selective catch by fishing operation technique in tropical tuna purse seine fishery in the western Indian Ocean: Feasibility of free school operation for skippers. Fisheries Science 82(3): 405–416. https://doi.org/10.1007/s12562-016-0976-x

Escalle L, Gaertner D, Chavance P, Alicia DDM, Ariz J, Merigot B (2016) Consequences of fishing moratoria on catch and bycatch: The case of tropical tuna purse-seiners and whale and whale shark associated sets. Biodiversity and Conservation 25(9): 1637–1659. https://doi.org/10.1007/s10531-016-1146-2

Foote KG (1998) Fish target strengths for use in echo integrator surveys. Journal of the Acoustical Society of America 82(3): 981–987. https://doi.org/10.1121/1.395298

Foote KG, Knudsen HP, Vestnes G, MacLennan DN, Simmon ds EJN (1987) Calibration of acoustic instruments for fish density estimation: A practical guide. International Council for the Exploration of the Sea. Cooperative Research Report No. 144; [Internal report published in 2008 by Renegade Press] http://courses.washington.edu/fish538/resources/CRR%20144%20acoustic%20calibration.pdf

Game ET, Grantham HS, Hobday AJ, Pressey RL, Lombard AT, Beckley LE, Gjerde K, Bustamante R, Possingham HP, Richardson AJ (2009) Pelagic protected areas: The missing dimension in ocean conservation. Trends in Ecology and Evolution 24(7): 360–369. https://doi.org/10.1016/j.tree.2009.01.011

Gerasimov YV, Borisenko ES, Bazarov MI, Stolbunov IA (2019) Density and distribution of fish in a river with a pronounced heterogeneity of the environment: Hydroacoustic survey. Inland Water Biology 12(S1): 69–75. https://doi.org/10.1134/S1995082919050079

Godlewska M, Długoszewski B, Doroszczyk L, Jóźwik A (2009) The relationship between sampling intensity and sampling error-empirical results from acoustic surveys in Polish vendace lakes. Fisheries Research 96(1): 17–22. https://doi.org/10.1016/j.fishres.2008.09.014

Goodyear CP (1999) An analysis of the possible utility of time-area closures to minimize billfish bycatch by US pelagic longlines. Fishery Bulletin-National Oceanic and Atmospheric Administration 97(2): 243–255.

Grantham HS, Petersen SL, Possingham HP (2008) Reducing bycatch in the South African pelagic longline fishery: The utility of different approaches to fisheries closures. Endangered Species Research 5(2): 291–299. https://doi.org/10.3354/esr00159

Guo AH, Yuan JL, Chu TJ, Lian QP (2019) Hydroacoustic assessment of fish resources in three reservoirs: The effects of different management strategies on fish density, biomass and size. Fisheries Research 215: 90–96. https://doi.org/10.1016/j.fishres.2019.03.002

Hale RS, Degan DJ, Renwick WH, Vanni MJ, Stein RA (2008) Assessing fish biomass and prey availability in Ohio reservoirs. American Fisheries Society Symposium 62: 517–541.

Hiddink JG, Hutton T, Jennings S, Kaiser MJ (2006) Predicting the effects of area closures and fishing effort restrictions on the production, biomass, and species richness of benthic invertebrate communities. ICES Journal of Marine Science 63(5): 822–830. https://doi.org/10.1016/j.icesjms.2006.02.006

Hobday AJ, Hartmann K (2006) Near real-time spatial management based on habitat predictions for a longline bycatch species. Fisheries Management and Ecology 13(6): 365–380. https://doi.org/10.1111/j.1365-2400.2006.00515.x

Ley JA, Halliday IA, Tobin AJ, Garrett RN, Gribble NA (2002) Ecosystem effects of fishing closures in mangrove estuaries of tropical Australia. Marine Ecology Progress Series 245: 223–238. https://doi.org/10.3354/meps245223

Marks CI, Fields RT, Field JC, Miller RR, Howard D (2015) Changes in size composition and relative abundance of fishes in central California after a decade of spatial fishing closures. California Cooperative Oceanic Fisheries Investigations Reports 56: 1–14. https://doi.org/10.1007/s00338-015-1389-5

O'Farrell S, Luckhurst BE, Box SJ, Mumby PJ (2016) Parrotfish sex ratios recover rapidly in Bermuda following a fishing ban. Coral Reefs 35(2): 421–425. https://doi.org/10.1007/s00338-015-1389-5

Pavlov DS, Mochek AD, Borisenko ES, Degtev AI (2010) Hydroacoustic investigation of taxonomic composition and of vertical distribution of fish in the riverbed depression. Journal of Ichthyology 50(11): 969–976. https://doi.org/10.1134/S0032945210110019

Pinkas L, Oliphant MS, Iverson ILK (1971) Food habits of albacore, bluefin tuna, and bonito in California waters. California Department of Fish and Game Fish Bulletin 152: 1–105.

R Development Core Team (2010) R: a language and environment for statistical computing. R Foundation for Statistical Computing, Vienna, Austria. http://www.R-project.org

Simmonds J, MacLennan D (2005) Fisheries acoustics: theory and practice. Blackwell Science, Oxford, UK. https://doi.org/10.1002/9780470995303

Tang S, Chen L (2004) The effect of seasonal harvesting on stage-structured population models. Journal of Mathematical Biology 48(4): 357–374. https://doi.org/10.1007/s00285-003-0243-5

Torres-Irineo E, Gaertner D, de Molina AD, Ariz J (2011) Effects of time-area closure on tropical tuna purse-seine fleet dynamics

through some fishery indicators. Aquatic Living Resources 24(4): 337–350. https://doi.org/10.1051/alr/2011143

Zhang JL, Bian K, Yan TZ, Gou NN, Shen HB, Zhang JY, Wang KF, Ding QZ (2016) Investigation on status of fish resources in Qinling-Heihe River basin. Freshwater Fisheries 46(1): 103–108.

Zhou L, ZengL, Fu DH, Xu P, Zeng S, Tang QD, Chen QF, Chen LA, Li GF (2016) Fish density increases from the upper to lower parts of the Pearl River Delta, China, and is influenced by tide, chlorophyll-*a*, water transparency, and water depth. Aquatic Ecology 50(1): 59–74. https://doi.org/10.1007/s10452-015-9549-9

Acta Ichthyologica et Piscatoria 51(4), 2021, 357–363 | DOI 10.3897/aiep.51.70223

PENSOFT

ACTA ICHTHYOLOGICA ET PISCATORIA

Effects of synthetic androgen (17α-methyltestosterone) and estrogen (17β-estradiol) on growth and skin coloration in emperor red cichlid, *Aulonocara nyassae* (Actinopterygii: Cichliformes: Cichlidae)

Zafer KARSLI[1]

1 *Sinop University Vocational School 57000, Sinop, Turkey*

http://zoobank.org/BFBFC8E9-F929-4F40-B960-FF05FF5A7877

Corresponding author: Zafer Karslı (zakarsli@sinop.edu.tr)

Academic editor: Sanja Matić-Skoko ♦ **Received** 16 June 2021 ♦ **Accepted** 7 September 2021 ♦ **Published** 8 November 2021

Citation: Karslı Z (2021) Effects of synthetic androgen (17α-methyltestosterone) and estrogen (17β-estradiol) on growth and skin coloration in emperor red cichlid, *Aulonocara nyassae* (Actinopterygii: Cichliformes: Cichlidae). Acta Ichthyologica et Piscatoria 51(4): 357–363. https://doi.org/10.3897/aiep.51.70223

Abstract

In recent years, the use of anabolic steroids in the coloration and growth of fishes, especially ornamental ones, has attracted great interest. In the ornamental fish industry, it is economically advantageous to produce some species with high commercial value and higher demand, depending on size, color, and sex. Therefore, the most commonly used steroids in this study—i.e., 17α-MT and 17β-Es (E_2)—were added to the diet of emperor red cichlid, *Aulonocara nyassae* Regan, 1922, which has not been previously hormone-treated and has high economic value amongst ornamental fishes. A 60-day study was conducted in a closed system, where the juveniles of the emperor red cichlid were acclimatized with the control/basal diet for 15 days. After which, 15 fish with a similar shade of color and about 5 months old were weighed individually (0.71 ± 0.01 g). All fish were placed into aquaria (30 L) in five different groups, in triplicate. Five different groups consisted of control (without hormone), 50 mg · kg^{-1} 17α-MT, 100 mg · kg^{-1} 17α-MT, 50 mg · kg^{-1} E_2, and 100 mg · kg^{-1} E_2. The fish were fed a diet twice a day (10:00 h, 17:00 h) for 60 days till satiation. During the entire trial period, a 12 h light–12 h dark photoperiod was maintained. Water temperature was measured daily and recorded. Growth parameters of experimental fish were calculated. The color measurement of fish skin (L^*, a^*, b^* values) from around the dorsal section was performed using a colorimeter (Konica Minolta CR 400). Significant differences were determined in the following parameters: weight gain (WG), specific growth rate (SGR), feed conversion rate (FCR), survival rate (SR), condition factor (CF), and sex reversal. The fish group fed with 17α-MT displayed brighter coloration as compared to other groups. Color analysis (instrumental) in terms of L^*, a^*, and b^*, values showed that the group fed with 17α-MT displayed brighter coloration compared to other groups ($P < 0.05$). In terms of sex reversal, the fish in the 17α-MT groups exhibited 100% masculinization, whereas in E_2 supplemented fish groups (50 and 100 mg · kg^{-1}), the feminization rates were 88.88% and 93.33%, respectively. In conclusion, both hormones were found to have positive and negative effects for this fish species, but the 17α-MT hormone was found to be more effective in reversing skin pigmentation, growth, and sexing, which is the main driver in the ornamental fish trade.

Keywords

coloration, growth performance, ornamental aquaculture, sex reversal

Introduction

In the recent past, the production of ornamental fish feed was mostly dependent on bycatch and other aquatic organisms being used as live feeds. However, due to the increasing pressure on natural resources, organized industrial sites have been established for the breeding and marketing of ornamental fishes. Nowadays, feed and aquarium equipment used in ornamental fish farming have emerged as an industry that appeals to the global market. In developed and developing countries, the ornamental fish-farming sector has developed with major commercial importance within the aquaculture industry (Sales and Janssens 2003; Hekimoğlu 2006; Dominguez and Botella 2014).

Nutrition is one of the most important elements for the sustainability of fish farming. In addition to carbohydrates, proteins, and fats in the structure of the feed used in nutrition, minerals, vitamins, and anabolic steroids are also used as additives.

Anabolic steroids contain androgen (male sex hormone) and estrogen (female sex hormone), which are commonly used as growth supplements in feed. Steroid hormones can be used in feed without any biological loss since they are resistant to catabolism by digestive enzymes. Thus, fish can be supplemented with hormones without incurring any handling stress compared to other invasive methods like injection, etc. Moreover, administering hormones to multiple fish individuals is a simple procedure (Hoşsu et al. 2003).

The wide use of growth promoters in animal husbandry using the anabolic sex steroids has attracted their application in the aquaculture industry to shorten the production cycle and lower the production cost (Gannam and Lovell 1991).

Anabolic agents (or anabolics) have been defined as substances that enhance the protein synthesis of livestock by positively affecting the nitrogen balance. Therefore, anabolic hormones enable lean meat production and rapid weight gain of fish and livestock with less feed by expediting muscle development. Most of these are steroidal male and female sex hormones (both natural and synthetic) and non-steroidal substances with anabolic effects. Furthermore, growth hormones, somatomedins, insulin, and thyroid gland hormones have also been documented to affect the growth rate positively (Mercure et al. 2001; Karabulut 2008).

Sex reversal by hormone treatment and its application in certain expensive aquarium fish, especially for which market value depends on the sex, have drawn the attention of many ornamental fish farmers and this situation has demanded the requirement of more studies on this subject. Studies related to color enhancement in ornamental fish farming have gained momentum in recent years and particularly the use of anabolic steroids is of great interest. Apart from sex reversal, steroids are also used for enhancing the growth or color of fish for visual appeal.

Cichlids, being one of the most visually appealing fishes in the industry, are amongst the aquarium fish, for which market value depends on sex. The emperor red cichlid, *Aulonocara nyassae* Regan, 1922, attracts attention, especially due to its color in shades of red. The colors of the males are much brighter red with a noticeable difference compared to the females and their dorsal and anal fins are more pointed. Females also usually have grey and dark tones. In this study, the emperor red cichlid was used due to its importance in the aquarium industry and there is a lack of information on the effect of sex steroids on the growth and coloration of this species.

Materials and methods

Experimental design. A 60-day study was conducted in a closed system, where the juveniles of emperor red cichlid (*A. nyassae*) were acclimatized with the control/basal diet for 15 days. After which, 15 fish with a similar shade of color and about 5 months old (unsexed) were weighed individually (0.71 ± 0.01 g) and placed into each aquarium (30 L) in five different groups, in triplicate. Five different groups consisted of control (without hormone), 50 mg · kg^{-1} 17α-MT, 100 mg · kg^{-1} 17α-MT, 50 mg · kg^{-1} 17β-Es (E_2), and 100 mg · kg^{-1} 17β-Es (E_2). The basal feed had the approximate composition of 46.5% crude protein, 8.2% crude fat, 3.3% crude fiber, 5.0% moisture, and 5.3% crude ash. The fish were fed twice a day (10:00 h, 17:00 h) for 60 days a diet till satiation. Experimental fish were weighed at the beginning of the experiment and the last day of the experiment (on the 60th day). Waste materials were siphoned out every day and replacement water was added. In each experimental treatment group, fish were acclimatized to aquarium and feeding conditions for a week. The temperature of the aquarium unit was set to have a water temperature of 24 ± 1°C throughout the experiment by a room air conditioner. Aquaria were aerated using an air stone.

Hormones were added to the commercial diet and the proximate composition of the feed is provided in Table 1. The control/basal feed was without hormone

Table 1. Proximate composition of the experimental diets used for feeding emperor red cichlid, *Aulonocara nyassae*.

Chemical composition	Diet group				
	Control	50 mg 17α-MT	100 mg 17α-MT	50 mg E_2	100 mg E_2
Crude protein [%]	46.5	46.5	46.5	46.5	46.5
Crude lipid [%]	8.2	8.2	8.2	8.2	8.2
Crude fiber [%]	3.3	3.3	3.3	3.3	3.3
Moisture [%]	5.0	5.0	5.0	5.0	5.0
Ash [%]	5.3	5.3	5.3	5.3	5.3
NFE	31.7	31.7	31.7	31.7	31.7
17α-Methyltestosterone [mg · kg^{-1}]	—	50	100	—	—
17β-Estradiol [mg · kg^{-1}]	—	—	—	50	100
Proximate analysis					
GE, [kj · g^{-1}]	19.69	19.69	19.69	19.69	19.69

NFE = Nitrogen Free Extract = 100 – (moisture + crude protein + crude lipid + ash + crude fiber); GE = Gross energy = (crude protein × 23.6) + (crude lipid × 39.5) + (% carbohydrates × 17.3) (Koshio et al. 1993); Vitamin A 30000 IU · kg^{-1}, Vitamin D_3 1500 IU · kg^{-1}, Vit. E (D, L-α-tocoferol asetat) 60 mg · kg^{-1}, Vit. B_1 30 mg · kg^{-1}, Vit. B_2 90 mg · kg^{-1}, Vit. C preparation (L-ascorbic monophosphate) 550 mg · kg^{-1}.

supplementation. The test diets were prepared with supplementation of 17α-MT (50 and 100 mg · kg^{-1}) and E_2 (50 and 100 mg · kg^{-1}) following the methods of Degani (1985) and Santandreu and Diaz (1994). The feed was then stored in tightly sealed plastic bags and placed in a freezer at –20°C. The control diet was sprayed with a steroid-free 95% ethyl alcohol solution, processed in the same way as the treated feed, and stored until the day of use.

During the entire trial period, a 12 h light–12 h dark photoperiod was maintained. Water temperature was measured daily and recorded as 26 ± 1°C, while pH, dissolved oxygen, and NH_4^+ values were evaluated weekly and maintained at 6.5–8.5, > 5 mg · L^{-1} and 2–5 mg · L^{-1}, respectively.

Color measurements. The color measurement of fish skin (L^*, a^*, b^* values) (Hunt 1977; CIE 1986; Nickell and Bromage 1998; Berns 2000) from around the dorsal section was performed using a colorimeter (Konica Minolta CR 400) at the beginning (0th day), 30th day, and the end (60th day) of the experiment. The values of the earlier mentioned variables can be explained as follows: L^*= lightness (also referred to as luminance); the lightness or darkness of a color. It ranges from 0 (pure black) to 100 (diffuse white), a^*= red to green; (+) positive: redness, (–) negative: greenness, b^*= yellow to blue (+) positive: yellowness, (–) negative: blueness. Chroma (C^*) (calculated with a^* and b^* values) indicates the intensity and lightness (clarity) of the colors.

The hue ($H°_{ab}$), also calculated with a^* and b^* values, is an angle value representing the shade of redness, yellowness, greenness, and blueness of the skin color. Hue degree indicates red as it approaches 0°, yellow as it approaches 90°, green as it approaches 180°, and blue as it approaches 270°.

ΔE is the color difference value and was calculated with L^*, a^*, and b^* measurements obtained at the beginning and the end of the trial (Hunt 1977; CIE 1986; Nickell and Bromage 1998; Berns 2000).

$$C^* = (a^{*2} + b^{*2})^{0.5}$$

$$H°_{ab} = 180 + \tan^{-1}(b^* \cdot a^{*-1}) \text{ for } a^* < 0$$

$$H°_{ab} = \tan^{-1}(b^* \cdot a^{*-1}) \text{ for } a^* > 0$$

$$\Delta E = [(L_t - L_0)^2 + (a_t - a_0)^2 + (b_t - b_0)^2]^{0.5}$$

Where L_t is lightness at the end of the experiment, L_0 is lightness in the initial of the experiment; a_t is red to green degree at the end of the experiment, a_0 is red to green degree in the initial of the experiment; b_t is yellow to blue degree at the end of the experiment, b_0 is yellow to blue degree in the initial of the experiment.

Growth parameters. Growth parameters of experimental fish were calculated with the following equations:

The specific growth rate (SGR) [%· day^{-1}], the weight gain (W_G) [%], the survival rate (S) [%], the Feed Conversion Ratio (FCR), and Fulton's condition factor (K) were calculated using the respective formulas:

$$SGR = 100 [\ln W_F - \ln W_0] \cdot t^{-1}$$

$$W_G = 100 (W_F - W_0) \cdot W_0^{-1}$$

$$S = 100 (N_F - N_0)$$

$$FCR = W_F \cdot W_G^{-1}$$

$$K = 100(W_W \cdot L_T^{-3})$$

where W_0 and W_F are the initial and final body weight and t is the time (feeding period) in days; N_t is the number of fish at the end of experiment and N_0 is the number of fish at the beginning of the experiment); W_F is the weight [g] of the food given and L_T is the total length [cm] of the fish.

Sex parameters. In the experiment, the sex reversal of the fish was determined by looking at the primary and secondary sex characteristics.

Statistical analyses. Statistical analyses were conducted with "Minitab Release 17 for Windows" software. Data were subjected to one-way analyses of variance (ANOVA), followed by the Tukey test at a significance level of 5% (0.05).

Ethical note. This research was approved by the Ethics Committee of Sinop University with Reference No. MYO-1901-16-22. All the procedures applied in this study took into account the importance of preventing or at least minimizing, any kind of animal discomfort or suffering.

Results

At the end of the 60-day feeding period, it was observed that the fish group fed a higher dose of 17α-MT (100 mg · kg^{-1}) had a significantly positive effect ($P < 0.05$) in terms of weight increase, weight gain, FCR, and SGR. Growth parameters in the group fed 17α-MT (50 mg · kg^{-1}) were also better compared to the group without 17α-MT. However, no change was observed in the fish groups fed E_2. The highest survival rate was observed in the control group (93.33 ± 2.45%) followed by 50 mg · kg^{-1} 17α-MT treated group (86.67 ± 7.35%) ($P < 0.05$). The survival rates of the remaining fish groups (50–100 mg · kg^{-1} E_2 and 100 mg · kg^{-1} 17α-MT) were low.

In terms of sex reversal, the fish in 17α-MT groups exhibited 100% masculinization, whereas in E_2 supplemented fish groups (50 and 100 mg · kg^{-1}), the feminization rates were 88.88% and 93.33%, respectively (Table 2). No intersex fish were found at the end of the experiment.

Color analysis (instrumental) in terms of L^*, a^*, and b^* values showed that the group fed 17α-MT displayed brighter coloration compared to other groups ($P < 0.05$). In terms of Hue ($H°_{ab}$) values, the skin color of fish in 17α-MT supplemented groups showed more intense

Table 2. Growth performance, feed conversion ratio (FCR), survival, conditions and sex ratio of experimental feeds fed for 60 days to emperor red cichlid, *Aulonocara nyassae*.

Parameter	Control	50 mg 17α-MT	100 mg 17α-MT	50 mg E_2	100 mg E_2
Initial weight [g]	0.71 ± 0.01^{a}	0.71 ± 0.02^{a}	0.71 ± 0.01^{a}	0.71 ± 0.01^{a}	0.71 ± 0.02^{a}
Final weight [g]	1.54 ± 0.13^{c}	1.92 ± 0.17^{b}	2.23 ± 0.19^{a}	1.62 ± 0.14^{c}	1.59 ± 0.11^{c}
Weight increase [g]	0.83 ± 0.09^{c}	1.21 ± 0.13^{b}	1.52 ± 0.11^{a}	0.91 ± 0.12^{c}	0.88 ± 0.07^{c}
Weight gain [g]	116.90 ± 13.4^{c}	170.42 ± 12.09^{b}	214.08 ± 18.4^{a}	128.17 ± 15.07^{c}	123.94 ± 14.3^{c}
SGR	1.29 ± 0.18^{c}	1.66 ± 0.19^{b}	1.91 ± 0.26^{a}	1.37 ± 0.16^{c}	1.34 ± 0.15^{c}
FCR	3.23 ± 0.71^{a}	2.32 ± 0.43^{c}	2.19 ± 0.31^{c}	2.93 ± 0.66^{b}	3.01 ± 0.53^{b}
K	1.11 ± 0.12^{b}	1.23 ± 0.15^{a}	1.09 ± 0.08^{b}	1.24 ± 0.13^{a}	1.27 ± 0.07^{a}
Survival rate [%]	93.33 ± 2.45^{a}	86.67 ± 7.35^{a}	73.33 ± 9.24^{b}	68.8 ± 11.21^{bc}	62.20 ± 12.4^{c}
Males [%]	28.89^{b}	100^{a}	100^{a}	11.11^{c}	6.67^{c}
Female [%]	71.11^{b}	0^{c}	0^{c}	88.88^{a}	93.33^{a}

Values (mean ± standard error of data for triplicate groups) with different superscripts in the same row are significantly different (one-way ANOVA and Tukey multiple-range test, $P < 0.05$). SGR = specific growth rate, FCR = feed conversion ratio, *K* = condition factor.

Table 3. Color parameters measured in fish skin of juvenile emperor red cichlid (*Aulonocara nyassae*) during the experimental period.

			Group		
Color parameters and periods	**Control**	**50 mg 17α-MT**	**100 mg 17α-MT**	**50 mg E_2**	**100 mg E_2**
L*					
Beginning of experiments	41.57 ± 0.11	41.57 ± 0.11	41.57 ± 0.11	41.57 ± 0.11	41.57 ± 0.11
30th day	40.62 ± 0.13	37.60 ± 0.09	29.13 ± 0.05	47.65 ± 0.12	47.28 ± 0.08
60th day	40.15 ± 0.07^{b}	26.11 ± 0.18^{c}	17.22 ± 0.24^{d}	54.34 ± 0.32^{a}	53.16 ± 0.29^{a}
a*					
Beginning of experiments	-2.11 ± 0.04	-2.11 ± 0.04	-2.11 ± 0.04	-2.11 ± 0.04	-2.11 ± 0.04
30th day	-1.57 ± 0.08	7.89 ± 0.11	8.23 ± 0.09	-1.67 ± 0.14	-1.44 ± 0.17
60th day	2.06 ± 0.03^{b}	8.17 ± 0.21^{a}	9.86 ± 0.15^{a}	-1.28 ± 0.04^{c}	-1.53 ± 0.06^{c}
b*					
Beginning of experiments	4.82 ± 0.09	4.82 ± 0.09	4.82 ± 0.09	4.82 ± 0.09	4.82 ± 0.09
30th day	15.21 ± 0.24	9.74 ± 0.15	8.48 ± 0.05	4.89 ± 0.12	4.14 ± 0.16
60th day	9.78 ± 0.06^{a}	5.12 ± 0.13^{b}	4.09 ± 0.09^{b}	5.36 ± 0.14^{b}	5.29 ± 0.19^{b}
H°_{ab}					
Beginning of experiments	113.64 ± 0.14	113.64 ± 0.14	113.64 ± 0.14	113.64 ± 0.14	113.64 ± 0.14
30th day	95.89 ± 0.19	50.99 ± 0.11	45.86 ± 0.23	108.86 ± 1.36	109.79 ± 1.44
60th day	78.11 ± 0.27^{b}	32.07 ± 0.48^{c}	22.53 ± 0.32^{c}	103.43 ± 2.14^{a}	106.13 ± 1.56^{a}
C*					
Beginning of experiments	5.26 ± 0.08	5.26 ± 0.08	5.26 ± 0.08	5.26 ± 0.08	5.26 ± 0.08
30th day	15.29 ± 0.45	12.53 ± 0.37	11.82 ± 0.33	5.17 ± 0.12	4.38 ± 0.15
60th day	9.99 ± 0.02^{a}	9.64 ± 0.24^{a}	10.67 ± 0.21^{a}	5.51 ± 0.01^{b}	5.51 ± 0.03^{b}
ΔE					
0th–60th day	6.63 ± 0.35^{d}	18.57 ± 0.44^{b}	27.14 ± 0.41^{a}	12.81 ± 0.23^{c}	11.61 ± 0.29^{c}

Values (mean ± standard error of data for triplicate groups) with different superscripts in the same row are significantly different (one-way ANOVA and Tukey multiple-range test, $P < 0.05$); L^*= Lightness (also referred to as luminance); the lightness or darkness of a color; a^*= red to green; (+) positive: redness, (–) negative: greenness, b^*= yellow to blue (+) positive: yellowness, (–) negative: blueness; ΔE is the color difference value and was calculated with L^*, a^*, and b^* measurements obtained at the beginning and the end of the trial; Chroma (C^*) (calculated with a^* and b^* values) indicates the intensity and lightness (clarity) of the colors; Hue (H°_{ab}), also calculated with a^* and b^* values, is an angle value representing the shade of redness, yellowness, greenness, and blueness of the skin color.

shades of red, while the skin colors of fish in E_2 supplemented groups were observed to be shades of grey-brown closer to the shade of yellow color. The maximal change in color difference (ΔE) was observed in fish groups supplemented with 50–100 mg · kg^{-1} 17α-MT (Table 3).

Discussion

In the ornamental fish industry, it is economically advantageous to produce certain species that have high commercial value and more demand depending on size, color, and sex. Therefore, in this study, the most commonly used steroids (namely, 17α-MT, and E_2) were supplemented to the feed of emperor red cichlid.

Fish groups fed 17α-MT hormone had a better growth rate. These results are in agreement with the studies on *Labidochromis caeruleus* (see Karsli et al. 2018), *Oreochromis andersonii* (see As et al. 2012), *O. niloticus* (see Greisy and Gamal 2012; Ajiboye et al. 2015), and *Trichogaster lalius* (see Biswas et al. 2014). However, other studies reported that the hormone treatment negatively affected growth and development in a dose-dependent manner in zebra cichlids (George and Pandian 1996), *Betta splendens* (see Kirankumar and Pandian 2002), and *O. niloticus* (see Sreenivasa and Prabhadevi 2018).

In the presently reported study, fish groups fed E_2 had no significant changes in growth parameters, which is in agreement with the results studied on *Amatitlania nigrofasciata* (see George and Pandian 1996) and *Centropomus undecimalis* (see Carvalho et al. 2014). Similarly, studies on *Xiphophorus helleri* by Lim et al. (1992) and Tamaru et al. (2009) stated that the hormones did not have any adverse effect on the growth.

Apart from beneficial effects, the most pronounced negative effect of hormone supplementation is on the sur-

vival rate, which, in turn, is dose-dependent, as well as species and sex specific. In this study, the survival rate was found to be high in the control group and the fish group supplemented with the low dose (50 mg · kg^{-1}) of 17α-MT. On the other hand, the survival rate was low in all fish groups supplemented with E_2 and the fish group treated with a high 17α-MT ratio. It has been reported that the high concentration of 17α-MT and E_2 hormones lower the survival rate of swordtail (Tamaru et al. 2009) and zebra cichlid (George and Pandian 1996). Moreover, in the study of Komen et al. (1989) on *Cyprinus carpio*, the survival rate of fish treated with 25, 75, 125 mg · kg^{-1} E_2 hormone varied between 51 and 69%, while the fish groups treated with 50 and 100 mg · kg^{-1} 17α-MT hormone had survival rates of 28% and 39%, respectively. In several studies involving the use of 17α-MT, the survival rate was negatively correlated in a dose-dependent manner as evident in *Trichogaster lalius* (see Katare et al. 2018), *O. niloticus* (see Das et al. 2010), and *Poecilia sphenops* (see George and Pandian 1998). Basavaraju et al. (2008) supplemented *C. carpio* fry and adults with 17α-MT and determined that compared to the control, the survival rate of the fry was lower, while that of the adults was higher.

When the sex ratios were examined, it was determined that the masculinization rate was 100% in fish groups with 17α-MT hormone. The groups supplemented with E_2 had a positive impact on feminization compared to the control group, although it was not as effective as the 17α-MT in masculinization. George and Pandian (1996) supplemented the zebra cichlid with 17α-MT and E_2 and observed the highest male (55%) and female (100%) rates in groups fed 200–300 mg · kg^{-1} hormone additives. Katare et al. (2018) determined that the 17α-MT supplementation at 50–100 mg kg^{-1} was insufficient for the masculinization of *T. lalius*. Furthermore, in a study carried out on swordtail, it was reported that the female rate in the control group was 74.5% and the optimum dosage for feminization (97%) was 400 mg · kg^{-1} Es (Tamaru et al. 2009). The optimum 17α-MT supplementation rate for masculinization was reported to be 60 mg · kg^{-1} in *O. niloticus* (see Das et al. 2010; Greisy and Gamal 2012), *O. andersoni* (see As et al. 2012), and *Poecilia reticulata* (see Chakraborty et al. 2012). Moreover, Phelps and Okoko (2011) observed the highest male rate (99.3%) in 30 mg · kg^{-1} MT supplemented fish group in *O. niloticus* and Kipouros et al. (2011) obtained 100% males in groups supplemented with 2, 3, and 4 mg · kg^{-1} 17α-MT. On the contrary, 17α-MT supplementation did not cause any significant difference in rosy barb and dwarf gourami (Ramee et al. 2020), as well as in *C. carpio* (see Basavaraju et al. 2008). The findings of the presently reported study suggest that hormone supplementation positively impacts the production of all male fish, thereby fetching a higher market value and increased profitability. This will result in further improvement of the ornamental fish market with the help of mono-sex fish production.

The visual appeal and color of aquarium fish are important criteria for their marketability. In the presently reported study, enhancement in coloration of fish caused by hormone treatment was statistically demonstrated with the applied method and supported by the results of analyses. According to color analyses conducted at the beginning of the study, hue ($H°_{ab}$) values indicated shades of grey-brown as the fish were at the early developmental stage. The color differences amongst groups were apparent according to the analyses carried out on day 30. At the end of the study, the desired coloration was determined in 17α-MT-supplemented fish groups and there were differences between these groups over control. However, no such significant improvement in coloration was seen in the groups supplemented with E_2. As male individuals of emperor red cichlid appear as bright red, the primary reason for enhanced coloration in fish groups supplemented with 17α-MT hormone may be attributed to efficient masculinization in these groups, as it caused production of 100% male population.

Dananjaya et al. (2020) supplemented *Carassius auratus* with various doses (0, 50, 100, 200, and 250 mg · kg^{-1}) of annatto (*Bixa orellana*) and determined that, according to L^*, a^*, and $H°_{ab}$ values, the efficacy of annatto increased in a dose-dependent manner. Ninwichian et al. (2020) administered three different natural sources of carotenoids (*Phaffia rhodozyma*, *Paracoccus* sp., *Haematococcus pluvialis*) to *C. carpio* and determined that the fish supplemented with natural carotenoid sources displayed a higher red color in terms of a^* and $H°_{ab}$ values. Moreover, Gouveia et al. (2003) used various synthetic and natural astaxanthin, *Chlorella vulgaris*, *Arthrospira maxima* (Spirulina), and *Haematococcus pluvialis* coloration supplements in Kawari and Showa fish, varieties of *C. carpio* and observed significant effects on the shade of red (a^* and $H°_{ab}$) according to colorimetric analyses. Larsson et al. (2002) administered 17α-MT hormone to *P. reticulata* and reported that an intense coloration was observed after the 17th day and the difference was statistically significant. Similarly, it has been reported that the 17α-MT hormone increased pigmentation which has a positive impact on coloration in *B. splendens* and *Xiphophorus hellerii* (see Jessy and Warghese 1987). When the physical color analysis results of the Karsli et al. (2018) study on electric yellow cichlid were evaluated, it was determined that the best coloration was obtained in 17α-MT groups, similar to this study. In contrast to these studies, it was reported that 17α-MT supplementation for 28 days did not affect coloration in *Xiphophorus hellerii* (see Koshio et al. 1993; Yanong et al. 2006).

Conclusion

In the presently reported study, the juveniles of emperor red cichlid (*A. nyassae*) which were supplemented with 100 mg · kg^{-1} 17α-MT displayed the highest growth and weight gain. On the other hand, group E_2 was found to be effective in sex reversal, similar to group 17α-MT. When the results of growth, coloration, sex reversal, and survival rate pa-

rameters are analyzed in this study, they were found to be important in the ease of marketing in the ornamental fish trade. Especially, skin coloration is the leading factor that determines the market value of ornamental fish. The discoloration and faded color in aquarium fish cause adverse effects on marketing. Aquarium fish cannot synthesize color pigments sufficiently in the culture environment and thus supplementation of synthetic or natural color through feed should be provided. When the results of growth, coloration, sex reversal, and particularly survival rate are evaluated, the most effective hormone dose for emperor red cichlid fish was determined to be 17α-MT at 50 mg · kg^{-1}.

Acknowledgment

The author is grateful to Assist. sDr Dilek Şahin and Assist. Dr Meryem Öz for contributing to this research.

References

Ajiboye OO, Qari R, Yakubu AF, Adams TE (2015) Growth performance of Nile tilapia, *Oreochromis niloticus* L. reared in glass aquaria tanks under different treatments and durations. International Journal of Biology and Biotechnology 12(2): 203–209.

As K, Kang'ombe J, Kassam D, Katongo C (2012) Growth, reproduction and sex ratios in *Oreochromis andersonii* (Castelnau, 1861) fed with varying levels of 17α-methyltestosterone. Journal of Aquaculture Research and Development 3(08): 155. https://doi.org/10.4172/2155-9546.1000155

Basavaraju Y, Mohan Kumar HM, Pradeep Kumar S, Umesha D, Srivastava PP, Penman DJ, Mair GC (2008) Production of genetically female common carp, *Cyprinus carpio*, through sex reversal and progeny testing. Asian Fisheries Science 21: 355–368.

Berns RS (2000) Billmeyer and Saltzman's principles of color technology. Wiley, NewYork, USA.

Biswas A, Behera S, Das P, Meena DK, Behera BK (2014) Effect of methyl testosterone (17α-MT) on the phenotype, bioindices and gonads of adult male dwarf gourami (*Colisa lalia*). Emirates Journal of Food and Agriculture 26(5): 459–464. https://doi.org/10.9755/ejfa.v26i5.16365

Carvalho CVA, Passini P, Costa WMC, Vieira BN, Cerqueira VR (2014) Effect of estradiol-17β on the sex ratio, growth and survival of juvenile common snook (*Centropomus undecimalis*). Acta Scientiarum. Animal Sciences 36(3): 239–245. https://doi.org/10.4025/actascianimsci.v36i3.22839

Chakraborty SB, Molnár T, Hancz C (2012) Effects of methyltestosterone, tamoxifen, genistein and *Basella alba* extract on masculinization of guppy (*Poecilia reticulata*). Journal of Applied Pharmaceutical Science 2(12): 48–52. https://doi.org/10.7324/JAPS.2012.21209

CIE (1986) The commonly used data on color matching functions is available at the CIE. International Commission on Illumination (CIE) Publication No. 15.2.

Dananjaya SHS, Manjula P, Dissanayake AS, Edussuriya M, Radampola K, Park BK, De Zoysa M (2020) Growth performance and color enhancement of goldfish, *Carassius auratus*, fed diets containing natural dyes extracted from annatto (*Bixa orellana*) seeds. Journal of Applied Aquaculture 32(1): 53–69. https://doi.org/10.1080/10454438.2019.1629371

Das NG, Mamun FA, Barua P, Siddique AAM, Chowdhury SN (2010) Survivality of mono-sex tilapia (*Oreochromis niloticus*) fry using 17α-methyltestosterone in a commercial hatchery of chittagong, Bangladesh. Journal of Aquaculture Feed Science and Nutrition 2(2–4): 16–24. https://doi.org/10.3923/joafsnu.2010.16.24

Degani G (1985) The influence of 17α- methyltestosterone on body composition of eels (*Anguilla anguilla* L.). Aquaculture 50(1–2): 23–30. https://doi.org/10.1016/0044-8486(85)90149-8

Domínguez LM, Botella AS (2014) An overview of marine ornamental fish breeding as a potential support to the aquarium trade and to the conservation of natural fish populations. International Journal of Sustainable Development and Planning 9(4): 608–632. https://doi.org/10.2495/SDP-V9-N4-608-632

Gannam AL, Lovell RT (1991) Growth and bone development in channel catfish (*Ictalurus punctatus*) fed 17 α-methyltestosterone in production ponds. Journal of the World Aquaculture Society 22(2): 95–100. https://doi.org/10.1111/j.1749-7345.1991.tb00721.x

George T, Pandian TJ (1996) Hormonal induction of sex reversal and progeny testing in the zebra cichlid *Cichlasoma nigrofasciatum.* Journal of Experimental Zoology 275(5): 374–382. https://doi.org/10.1002/(SICI)1097-010X(19960801)275:5%3C374::AID-JEZ6%3E3.0.CO;2-M

George T, Pandian TJ (1998) Dietary administration of androgens induces sterility in the female-heterogametic black molly, *Poecilia sphenops* (Cuvier & Valenciennes, 1846). Aquaculture Research 29: 167–175. https://doi.org/10.1046/j.1365-2109.1998.00951.x

Gouveia L, Rema P, Pereira O, Empis J (2003) Colouring ornamental fish (*Cyprinus carpio* and *Carassius auratus*) with microalgal biomass. Aquaculture Nutrition 9(2): 123–129. https://doi.org/10.1046/j.1365-2095.2003.00233.x

Greisy ZA, Gamal AE (2012) Monosex production of tilapia, *Oreochromis niloticus* using different doses of 17a-methyltestosterone with respect to the degree of sex stability after one year of treatment. Egyptian Journal of Aquatic Research 38(1): 59–66. https://doi.org/10.1016/j.ejar.2012.08.005

Hekimoğlu MA (2006) The current state of the aquarium industry in Turkey and globally. Ege University Journal of Fisheries and Aquatic Sciences 23(1/2): 237–241.

Hoşsu B, Korkut AY, Fırat A (2003) Balık Besleme ve Yem Teknolojisi I (Balık Besleme Fizyolojisi ve Biyokimyası). 3. Baskı. [Fish nutrition and feed technology I (Fish nutrition physiology and biochemistry). 3rd edition.] Ege Üniversitesi Su Ürünleri Fakültesi Yayınları No. 50, Bornova, İzmir, Turkey, 276 pp.

Hunt RWG (1977) The specification of colour appearance. I. concepts and terms. Color Research and Application 2(2): 55–68. https://doi.org/10.1002/col.5080020202

Jessy D, Warghese TJ (1987) Hormonal sex control in *Betta splendens* Regan and *Xiphophorus helleri* Heckel. Pp. 123–124. In: Joseph

MM (Ed.) The First Indian Fisheries Forum Proceeding, December 4–8, 1987, Mangalore, Karnataka, India.

Karabulut HA (2008) The effects of anabolic agents and medications, and evaluation of their residue in terms of fish farming. Ege University Journal of Fisheries and Aquatic Sciences 25(1): 83–87.

Karsli Z, Şahin D, Öz M, Aral MO (2018) The effect of hormone (17α-methyltestosterone, 17β-estradiol) usage on development, sex inversion and pigmentation of electric yellow cichlid (*Labidochromis caeruleus* Fryer, 1956). Applied Ecology and Environmental Research 16(6): 8093–8103. https://doi.org/10.15666/aeer/1606_80938103

Katare MB, Lakra W, Chadha N, Pai M, Basavaraja N, Gupta S, Kumar M (2018) Dietary effects of 17α-methyltestosterone on masculinization in dwarf gourami *Trichogaster lalius.* Journal of Entomology and Zoology Studies 6: 2996–3001.

Kipouros K, Paschos I, Gouva E, Ergolavou A, Perdikaris C (2011) Masculinization of the ornamental Siamese fighting fish with oral hormonal administration. ScienceAsia 37(3): 277–280. https://doi.org/10.2306/scienceasia1513-1874.2011.37.277

Kirankumar S, Pandian TJ (2002) Effect on growth and reproduction of hormone immersed and masculinized fighting fish, *Betta splendens.* Journal of Experimental Zoology 293(6): 606–616. https://doi.org/10.1002/jez.10181

Komen J, Lodder PAJ, Huskens F, Richter CJJ, Huisman EA (1989) Effects of oral administration of 17α -methyltestosterone and 17β -estradiol on gonodal development in common carp (*Cyprinus carpio* L.). Aquaculture 78(3–4): 349–363. https://doi.org/10.1016/0044-8486(89)90111-7

Koshio S, Teshima S, Kanazawa A, Watase T (1993) The effect of dietary protein content on growth, digestion efficiency and nitrogen excretion of juvenile kuruma prawns, *Penaeus japonicus.* Aquaculture 192(1–2): 233–247. https://doi.org/10.1016/0044-8486(93)90344-X

Larsson DGJ, Kinnberg K, Sturve J, Stephensen E, Skön M, Förlin L (2002) Studies of masculinization, detoxification and oxidative stress responses in guppies (*Poecilia reticulata*) exposed to effluent from a pulp mill. Ecotoxicology and Environmental Safety 52(1): 13–20. https://doi.org/10.1006/eesa.2001.2139

Lim BH, Phang VPE, Reddy PK (1992) The effect of short-term treatment of 17α -methyltestosterone and 17β -estradiol on growth and sex ratio in the red variety of swordtail, *Xiphophorus helleri.* Journal of Aquaculture in the Tropics 7: 267–274.

Mercure F, Holloway AC, Tocher DR, Sheridan MA, Kraak GVD, Leatherland JF (2001) Influence of plasma lipid changes in response to 17β estradiol stimulation on plasma growth hormone, somatostatin, and thyroid hormone levels in immature rainbow trout. Journal of Fish Biology 59: 605–615. https://doi.org/10.1111/j.1095-8649.2001.tb02365.x

Nickell DC, Bromage NR (1998) The effect of dietary lipid level on variation of flesh pigmentation in rainbow trout (*Oncorhynchus mykiss*). Aquaculture 161(1–4): 237–251. https://doi.org/10.1016/S0044-8486(97)00273-1

Ninwichian P, Chookird D, Phuwan N (2020) Effects of dietary supplementation with natural carotenoid sources on growth performance and skin coloration of fancy carp, *Cyprinus carpio* L. Iranian Journal of Fisheries Science 19(1): 167–181.

Phelps RP, Okoko M (2011) A non-paradoxical dose response to 17α -methyltestosterone by Nile tilapia *Oreochromis niloticus* (L.): Effects on the sex ratio, growth and gonadal development. Aquatic Resources 42(4): 549–558. https://doi.org/10.1111/j.1365-2109.2010.02650.x

Ramee SW, Lipscomb TN, Dimaggio MA (2020) Effects of 17α-methyltestosterone feeding and immersion on masculinization of rosy barbs *Pethia conchonius* and dwarf gouramis *Trichogaster lalius.* Journal of the World Aquaculture Society 51(6): 1341–1353. https://doi.org/10.1111/jwas.12703

Sales J, Janssens GPJ (2003) Nutrient requirements of ornamental fish. Aquatic Living Resources 16(6): 533–540. https://doi.org/10.1016/j.aquliv.2003.06.001

Santandreu JA, Diaz NF (1994) Effects of 17 α-methyltestosterone on growth and nitrogen excretion in masu salmon (*Oncorhynchus masou).* Aquaculture 124(1–4): 321–333. https://doi.org/10.1016/0044-8486(94)90405-7

Sreenivasa V, Prabhadevi L (2018) Optimization of hormone induced all male production of *Oreochromis niloticus* under laboratory condition at ambo, Ethiopia. Acta Scientific Agriculture 2(4): 16–21.

Tamaru CS, Yamasaki LS, Hopkins KM, Malecha S, Vincent D (2009) Feminization of commercial swordtails, *Xiphophorus helleri*, by dietary administration of 17β Estradiol. Journal of the World Aquatic Society.

Yanong RPE, Hill JE, Daniels CJ, Watson CA (2006) Efficacy of 17α -Methyltestosterone for expression of male secondary sexual characteristics in the green swordtail. North American Journal of Aquaculture 68(3): 224–229. https://doi.org/10.1577/A05-061.1

Acta Ichthyologica et Piscatoria 51(4), 2021, 365–370 | DOI 10.3897/aiep.52.73207

PENSOFT

ACTA ICHTHYOLOGICA ET PISCATORIA

A southward range extension of a wreckfish, *Stereolepis doederleini* (Actinopterygii: Acropomatiformes: Polyprionidae), to tropical water off eastern Taiwan

Hsuan-Ching HO[1,2], Chi-Ngai TANG[3], Chiu-Min CHENG[4]

1 *National Museum of Marine Biology and Aquarium, Pingtung, Taiwan*
2 *Australian Museum, Sydney, Australia*
3 *Institute of Oceanography, National Taiwan Ocean University, Taipei, Taiwan*
4 *Department and Graduate Institute of Aquaculture, National Kaohsiung University of Science and Technology, Taiwan*

http://zoobank.org/1BD2BC59-BCB2-4DC3-9003-9AFBE56AEEC7

Corresponding author: Chiu-Min Cheng (cmcheng@nkust.edu.tw)

Academic editor: Ronald Fricke ♦ **Received** 23 August 2021 ♦ **Accepted** 12 October 2021 ♦ **Published** 22 November 2021

Citation: Ho H-C, Tang C-N, Cheng C-M (2021) A southward range extension of a wreckfish, *Stereolepis doederleini* (Actinopterygii: Acropomatiformes: Polyprionidae), to tropical water off eastern Taiwan. Acta Ichthyologica et Piscatoria 51(4): 365–370. https://doi.org/10.3897/aiep.52.73207

Abstract

A wreckfish, *Stereolepis doederleini* Lindberg et Krasyukova, 1969, inhabits typical cold or temperate waters and was previously known from Great Bay (Sea of Japan), Korea, south to Kyuhu-Palau Ridge of Japan. In the present report, a specimen of this fish was collected from southeastern Taiwan representing the southernmost distribution of the cold-water genus *Stereolepis* in the Northern Hemisphere, with a southward extension into the tropical region. It is also the first record of a member of the family Polyprionidae from Taiwan. Here we document the species found in Taiwan, with a detailed description of the specimen.

Keywords

Actinopterygii, Acropomatiformes, biogeography, cold-water fish, distribution

Introduction

The wreckfish family Polyprionidae is a group of large marine fishes, growing up to 250 cm in length, and attaining high market values by some of its members (Froese and Pauly 2021). The family comprises 2 genera and 4 species, including *Polyprion americanus* (Bloch et Schneider, 1801) (nearly circumglobal; absent in Pacific coast of South America and northern Pacific), *Polyprion oxygeneios* (Schneider et Forster, 1801) (circumglobal in the Southern Ocean), *Stereolepis gigas* Ayres, 1859 (northern Pacific), and *Stereolepis doederleini* Lindberg et Krasyukova, 1969 (northwestern Pacific).

Of these species, *S. doederleini* was previously recorded from around Great Bay, Korea to Kyuhu-Palau Ridge of Japan (Sokolovskaâ et al. 1998; Choi et al. 2003; Nakabo 2013). However, not much morphological information regarding the species was available in the literature. Noichi et al. (1990) studied the ecology of juveniles of *S. doederleini* based on 106 individuals collected from Yanagihama beach of Nagasaki Prefecture, Japan. Kwun et al. (2018) reported juvenile *S. doederleini* collected from Jeju Island, southern Korea. Moon et al. (2011) studied the nutrition components of *S. doederleini* and suggested that it can potentially be a new aquaculture fish species.

Recently, a younger specimen of *S. doederleini* was collected from deep water by hook and line from off Fugang, Taitung, southeastern Taiwan. The finding reveals a southward extension of its distribution from cold or temperate into tropical water. A detailed description of this specimen is provided.

Materials and methods

Methods for counts and proportional measurements followed Hubbs and Lagler (1958). Standard length is expressed as SL. Standardization of morphometric data is expressed as a percentage of SL. All measurements were made with digital calipers to the nearest 0.1 mm. The cheek depth is the narrowest space between the lower margin of the eye and the lower margin of premaxilla. Osteological characters were determined by X-radiographs. The specimen is deposited at Pisces Collection of the National Museum of Marine Biology and Aquarium, Pingtung, Taiwan (NMMB-P).

Results

Family Polyprionidae

Stereolepis doederleini Lindberg et Krasyukova, 1969

Figs 1–3

Synonymy. *Stereolepis doederleini* Lindberg et Krasyukova, 1969; Lindberg and Krasûkova 1969: 69, fig. 130 (type locality: Sea of Japan). Mochizuki 1984: 124 (Hokkaido to Kochi and Ishikawa, Japan). Sokolovskaâ et al. 1998: 11 (Sea of Japan). Choi et al. 2003: 307, 589 (Korea). Nakabo 2013: 749 (Hokkaido to Kyushu-Palau Ridge, Korea, East China Sea, Peter the Great Gulf).

Specimen examined. NMMB-P32813, 385 mm SL, off Fugang (ca. 22°43′N 121°20′E), Taitung, southeastern Taiwan, March 2020, by deep-water longline, ca. 400 m, purchased at local auction.

Description of NMMB-P32813. Morphological measurements presented as a percentage of SL. Dorsal-fin elements XI, 10; anal-fin elements III, 7; pectoral-fin rays 19 (right side)/18 (left side), two dorsalmost rays unbranched, others branched; pelvic-fin rays I, 5; principal caudal-fin rays 9 (upper lobe) + 8 (lower lobe), procurrent caudal-fin rays 9 (dorsal)/8 (ventral), total caudal-fin rays 24. Gill rakers on first gill arch 4 + 13 = 16, 3 rudimental plus 1 developed on upper limb and 7 developed plus 6 rudimental on lower limb. Pored lateral-line scales 73, including 3 on caudal-fin base. Rows of cheek scales 11. Circumpeduncular scale rows 39. Scales above lateral line 15, counted slitting posteriorly from dorsal-fin origin. Scales below lateral line 28 (counted from anal-fin origin slitting up anteriorly to lateral line) or 23 (counted from anal-fin origin slitting up posteriorly to lateral line). Vertebrae: 12 precaudal + 14 caudal = 26 in total. Vertebral formula 0/0/0+2/1+1/1/1/1/1/1/1/1 (predorsal and spinous dorsal fin only).

Head length 2.7 times in SL (36.9% SL); body depth at pectoral-fin base depth 2.9 (34.2); body width at pectoral-fin base 5.2 (19.2); predorsal length 2.7 (36.4); prepectoral length 2.8 (36.4); prepelvic length 2.7 (37.1); distance between origins of pelvic and anal fins 2.8 (36.4); dorsal-fin base length 2.1 (48.1); anal-fin base 7.0 (14.2); caudal-peduncle length 5.2 (19.2); caudal-peduncle depth

Figure 1. *Stereolepis doederleini*, NMMB-P32813, 385 mm SL, off southeastern Taiwan. (**A**) preserved condition. (**B**) fresh condition at auction.

8.5 (11.8); pectoral-fin length 5.1 (19.6); pelvic-fin length 4.7 (21.1); pelvic-fin spine length 9.6 (10.4); caudal-fin length 4.8 (21.0).

Snout length 2.9 times (34.1% HL) in head length; fleshy eye diameter 5.5 (18.1); fleshy interorbital width 3.2 (30.9); bony interorbital width 3.6 (28.1); upper-jaw length 2.1 (46.9); post-orbital length 1.9 (52.5); distance from margin of eye to angle of subopercle 2.6 (38.1); suborbital height 7.7 (13.0); maxillary height 6.6 (including supramaxilla, maxilla, and premaxilla) (15.1); first dorsal-fin spine 8.4 (11.8); second dorsal-fin spines 3.5 (28.8); third dorsal-fin spine 2.3 (43.1); fourth dorsal-fin spine 2.0 (50.2); 11th dorsal-fin spine 4.9 (20.3); longest dorsal-fin ray 2.6 (39.2); first anal-fin spine 13.2 (7.6); second anal-fin spine 6.2+ (broken distally) (~16.1); third anal-fin spine 5.8 (17.3); longest anal-fin ray 2.7 (37.6).

Body moderately slender, deepest region at about middle of abdomen; less compressed. Dorsal profile smooth, nape slightly raised, dorsal-fin base straight at spinous region, slightly raised at soft-rayed region (Fig. 1A). Head moderately large; dorsal profile slightly more pronounced then ventral; dorsal profile barely convex from tip of snout to dorsal-fin origin (Fig. 2A). Posterior end of head below base of fourth dorsal-fin spine. Snout moderately long, blunt anteriorly, 1.9 times eye diameter. Eye small. Dorsal surface of skull with some smooth vermicular-like ridges. Middle of anterior portion of nape with long smooth ridge, its anterior portion branched (Fig. 2B).

Mouth moderately large, terminal, its gape slightly oblique, forming ca. 10° angle with horizontal body axis; lower jaw slightly overhanging upper jaw; posterior end of maxilla extending to vertical through middle of eye.

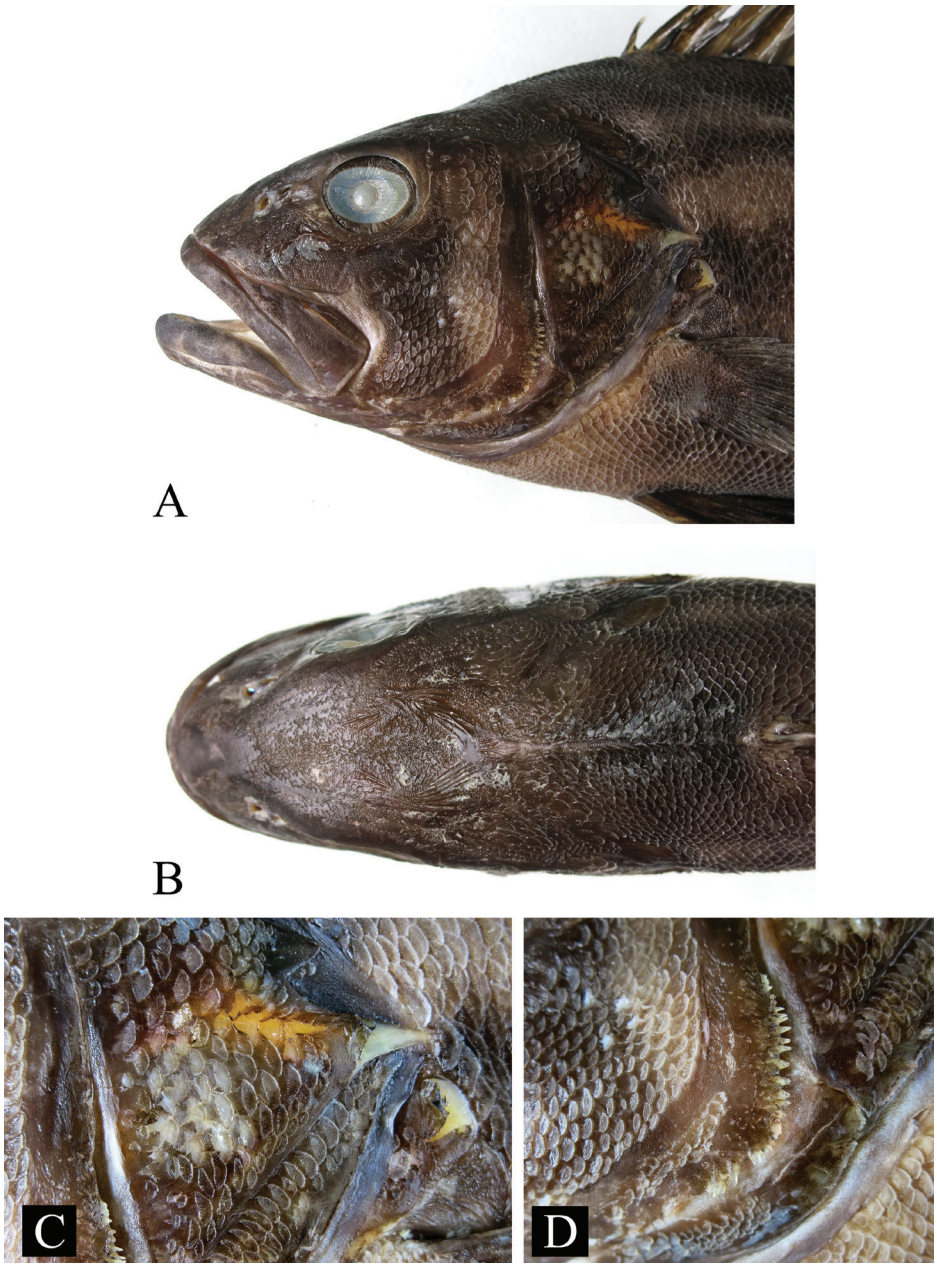

Figure 2. Close-up images of *Stereolepis doederleini*, NMMB-P32813. (**A**) Lateral view of head. (**B**) Dorsal view of head and nape. (**C**) Opercle. (**D**) Serration on preopercle. Anterior to left; not to scale.

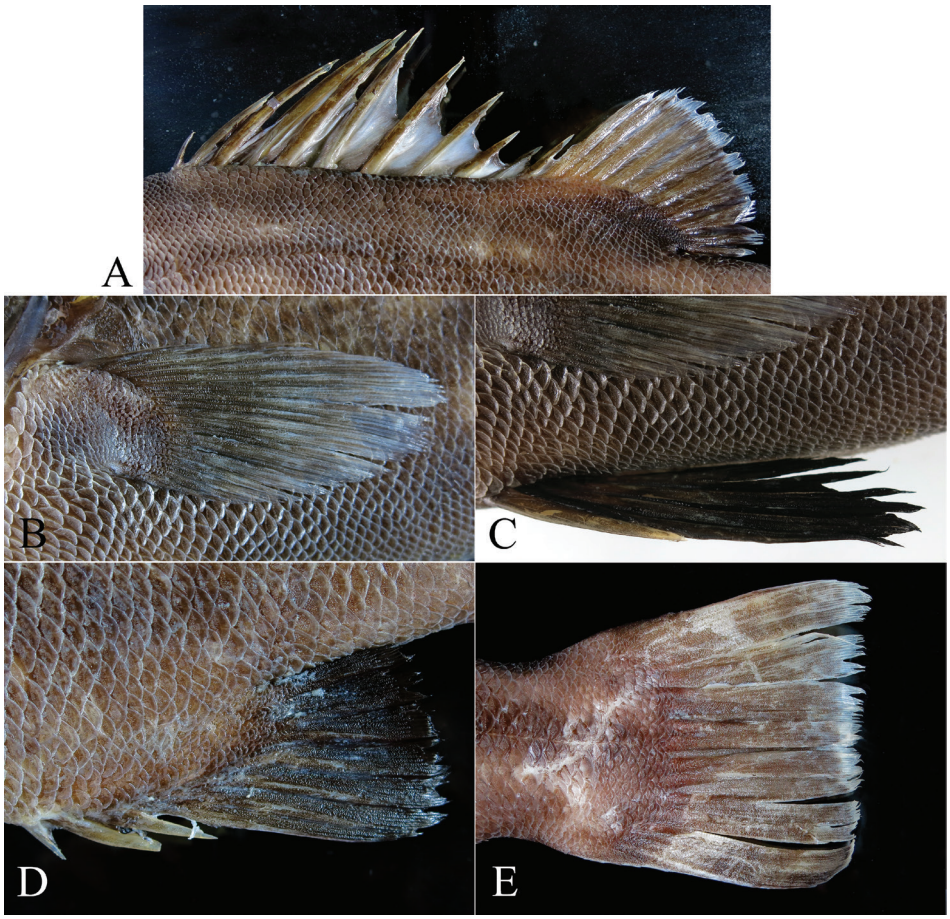

Figure 3. Close-ups of *Stereolepis doederleini*, NMMB-P32813. (**A**) Dorsal fin. (**B**) Pectoral fin. (**C**) Pelvic fin. (**D**) Anal fin. (**E**) Caudal fin. Anterior to left; not to scale.

First suborbital bone (lacrimal) well developed, slightly overlapped with anterior portion of maxilla, its lower margin smooth. Two nostrils well in front of eye. Anterior nostril rounded, bearing high rim with flap, its broader reaching anterior margin of posterior nostril when reflected. Posterior nostril elliptical, horizontal axis longer and slightly above the anterior nostril, with very low flashy rim along its lower margin (Fig. 2A).

Opercle with strong spine, pointed and rather distinct, mostly exposed from skin and extending to slightly overhanging posterior margin of opercle (Fig. 2C). Exposed margin of preopercle with strong stout spines, those along angle stronger and longer (Fig. 2D). Posterior margins of upper portion of subopercle smooth; lower margin of interopercle smooth. Posttemporal exposed, with weak serrations on posterior margin; upper portion cleithrum largely exposed; supracleithrum not exposed, covered by operculum totally.

Single dorsal fin with long base, deeply concaved at posterior third, spinous portion strongly arched with its base longer than that of soft-rayed portion, base of spinous portion 2.4 times base of soft-rayed portion (Fig. 3A). Dorsal-fin spines somewhat compressed; first spine short, the fourth spines longest, distinctly longer than third spine, rest spines gradually shorter posteriorly, except for last spine (11th, also leading spine of posterior lobe), which is slightly longer than penultimate spine. Second dorsal-fin ray longest, gradually shorter posteriorly.

Pectoral fin moderately large, long oval (Fig. 3B), its origin slightly below body axis and lower opercular spine, its tip reaching base of 9th dorsal-fin spine when addressed. Origin of pelvic fin (Fig. 3C) below origin of pectoral fin, about vertical through base of third dorsal-fin spine; its tip slightly behind middle of interspace between origins of pelvic and anal fins, its tip well before anus when pressed. Anal fin small with short base, first spine very short, all three spines shorter than second ray (also longest) (Fig. 3D); outer margin of anal fin straight. Caudal fin truncate, very slightly emarginated as middle (Fig. 3E).

Teeth villiform on jaws, vomer, and palatines; no teeth at symphysis of upper jaw. Vomer with wide triangular patch of small villiform teeth; no backward prolongation of vomerine tooth patch. Palatine with a narrow band of numerous rows of small teeth. No teeth on pterygoids or tongue. Pseudobranch present.

Gill rakers on first gill arch 3 (rudimental) + 1 (developed) on upper limb, 7 (developed) + 6 (rudimental) on lower lobe.

Scales weakly ctenoid, including those on cheek, interorbital, operculum, chest, nape, chest, and base of pectoral fin. No scale on snout and chin. Predorsal scales beginning in plane about halfway between posterior margin of orbit and upper end of gill slit.

Lateral line complete, lateral line scales not enlarged, each with simple sensory tubule. Rows of scales above and below lateral line parallel to it. Bases of soft-rayed portions of dorsal and anal fins covered by small scales. Pectoral and caudal fins with scales basally.

Coloration. When fresh, body yellowish brown dorsally and grayish ventrally with all fin darker, except for membranes of spinous dorsal fin translucent; 5 broad, irregular white stripes on lateral side of body; white bar on head and cheek right behind eye; soft dorsal fin and caudal fin with bright white margin. Body dark brown in general, with 5 broad pale stripes, uppermost one along dorsal-fin base, and other 4 on lateral side of body; fins darker, except for membranes of spinous dorsal fin pale; posterior margins of soft dorsal fin and caudal fin pale.

Distribution. Known from Russia (Sea of Japan) (Sokolovskaâ et al. 1998), Korea (Choi et al. 2003), and Japan (Mochizuki 1984; Nakabo 2013), at depths around 400–600 m. Newly collected from southeastern Taiwan off Taitung at depth around 400 m.

Remarks. The Taiwanese specimen is identified as *Stereolepis doederleini* based on the distinct coloration with 5 broad pale stripes on lateral sides of body among the family. It differs from the only other congener, *S. gigas*, co-occurring in the northwestern Pacific, by having the spinous dorsal fin distinctly higher than the soft dorsal fin (vs. the former distinctly lower than the later in *S. gigas*); the caudal fin truncate (vs. slightly concave or emarginated); 5 pale stripes on lateral sides of body (vs. black patches on lateral sides of body); lateral-line scales less than 73 (vs. about 80), scale rows below lateral 28–31 (vs. 35–40), and posterior end of maxilla reaching a vertical through posterior margin of eye (vs. reaching a vertical through anterior margin to middle of eye) (Mochizuki 1984; this study).

It is notable that Mochizuki (1984) reported 57–68 pored lateral-line scales for *S. doederleini*, whereas we counted 73 (including 3 on caudal-fin base) for our specimen which may represent the individual variation.

Discussion

The presently reported material of *Stereolepis doederleini* was caught by hook-and-line from deep water off Fugang fishing port, Taitung, eastern Taiwan. A portion of the local fisheries there are targeting high economical value demersal species such as *Doederleinia berycoides* (Hilgendorf, 1879) and *Atrobucca nibe* (Jordan et Thompson, 1911) and it is likely that S. *doederleini* was a bycatch with these species by deep water line fishery, where the habitat is assumed to be deep sandy or muddy sea floor (CNT, personal observation).

The discovery of *Stereolepis doederleini* in eastern Taiwan may represent a rare dispersal case of a cold-water species to southern and warmer regions. Similar cases were documented by Koeda and Muto (2019) and Chou and Tang (2021), where cold water species *Pholis fangi* (Wang et Wang, 1935) and *Sebastes thompsoni* (Jordan et Hubbs, 1925) were found in local catches of southwestern and northern Taiwan, respectively. Still, given the lack of further specimens, it remains uncertain whether the presently described specimen represented a rare local population or a rare dispersal event from the high latitude region.

Acknowledgments

We thank Mr. Yu-Hong Chuo for providing a photo and a specimen for our study and Dr. Keita Koeda for providing useful information. This study was supported by the National Museum of Marine Biology and Aquarium, Taiwan, and the National Kaohsiung University of Science and Technology, Taiwan.

References

Ayres WO (1859). […] on new fishes of this coast […] Proceedings of the California Academy of Natural Sciences, Volume 2: 25–32.

Bloch ME, Schneider JG (1801) M. E. Blochii, Systema Ichthyologiae Iconibus cx Ilustratum. Post obitum auctoris opus inchoatum absolvit, correxit, interpolavit Jo. Gottlob Schneider, Saxo. Sumtibus Auctoris Impressum et Bibliopolio Sanderiano Commissum, Berolini, 584 pp. [In Latin] https://doi.org/10.5962/bhl.title.5750

Choi Y, Kim J-H, Park J-Y (2003) [Marine fishes of Korea.] Kyuo-Hak, Seoul, Korea, 747 pp. [In Korean]

Chou T-K, Tang C-N (2021) Southward range extension of the goldeye rockfish, *Sebastes thompsoni* (Actinopterygii: Scorpaeniformes: Scorpaenidae), to northern Taiwan. Acta Ichthyologica et Piscatoria 51(2): 153–158. https://doi.org/10.3897/aiep.51.e68832

Froese R, Pauly D (Eds.) (2021) FishBase. World Wide Web electronic publication. www.fishbase.org, version 06/2021.

Hilgendorf FM (1879) Einige Beiträge zur Ichthyologie Japan's. Sitzungsberichte der Gesellschaft Naturforschender Freunde zu Berlin 1879: 78–81.

Hubbs CL, Lagler KF (1958) Fishes of the Great Lakes region. University of Michigan Press, Ann Arbor, MI, USA, 213 pp.

Jordan DS, Hubbs CL (1925) Record of fishes obtained by David Starr Jordan in Japan, 1922. Memoirs of the Carnegie Museum 10(2): 93–346.

Jordan DS, Thompson WF (1911) A review of the sciaenoid fishes of Japan. Proceedings of the United States National Museum 39(1787): 241–261. https://doi.org/10.5479/si.00963801.39-1787.241

Koeda K, Muto N (2019) An unexpected distribution record of the cold water fish *Pholis fangi* (Pholidae) from southern Taiwan. Zootaxa 4702(1): 87–93. https://doi.org/10.11646/zootaxa.4702.1.13

Kwun HJ, Park J, Kim HS, Kim JH, Park HS (2018) A juvenile *Stereolepis doederleini* (Polyprionidae) from a tidal pool at Jeju Island, Korea. Cybium, 42(4): 374–375. https://doi.org/10.26028/cybium/2018-424-008

Lindberg GU, Krasûkova ZV [Krasyukova ZV] (1969) [Fishes of the Sea of Japan and of adjacent areas of the Sea of Okhotsk and the Yellow Seas. Part 3.] Izdatel′stvo Nauka, Leningrad, USSR, 480 pp. [In Russian]

Mochizuki K (1984) *Stereolepis doederleini* Lindberg & Krasyukova. P. 124. In: Masuda H, Amaoka K, Araga C, Uyeno T, Yoshino T (Eds) The fishes of the Japanese Archipelago. Vol. 1. Tokai University Press, Tokyo, Japan, 437 pp.

Moon SK, Kim IS, Ko YS, Park JH, Kim GJ, Jeong BY (2011) [Food components of striped jewfish *Stereolepis doederleini*.] Korean Journal of Fisheries and Aquatic Sciences 44(5): 550–553. [In Korean] https://doi.org/10.5657/kfas.2011.0550

Noichi T, Kanbara T, Mito T, Sakamoto F, Kimura M, Senta T (1990) [Occurrence and ecology of juvenile striped jewfish *Stereolepis doederleini* (Family Percichthyidae) in Yanagihama beach, Nagasaki Prefecture.] Bulletin of the Faculty of Fisheries of Nagasaki University 68: 29–34. [In Japanese]

Nakabo T (2013) [Fishes of Japan with pictural keys to the species.] Tokai University Press, Tokyo, 2428 pp. [In Japanese]

Schneider JG, Forster JR (1801) [*Epinephelus*] 7. *Oxygeneios*. Pp. 301–302. In: Bloch ME, Schneider JG M. E. Blochii, Systema Ichthyologiae Iconibus cx Ilustratum. Post obitum auctoris opus inchoatum absolvit, correxit, interpolavit Jo. Gottlob Schneider, Saxo. Sumtibus Auctoris Impressum et Bibliopolio Sanderiano Commissum, Berolini, 584 pp. [In Latin]

Sokolovskaâ TG, Sokolovskij AS, Sobolevskij EI (1998) [A list of fishes of the Peter the Great Bay (the Sea of Japan).] Voprosy Ihtiologii 38(1): 5–15. [In Russian]

Wang K-F, Wang S-C (1935) Study of the teleost fishes of coastal region of Shangtung III. Contributions from the Biological Laboratory of the Science Society of China, Zoological Series 11(6): 165–237.

Acta Ichthyologica et Piscatoria 51(4), 2021, 371–378 | DOI 10.3897/aiep.51.74082

PENSOFT

ACTA ICHTHYOLOGICA ET PISCATORIA

Age and growth estimates from three hard parts of the spotted catfish, *Arius maculatus* (Actinopterygii: Siluriformes: Ariidae), in Songkhla Lake, Thailand's largest natural lake

Penprapa PHAEVISET[1], Pisit PHOMIKONG[2], Piyathap AVAKUL[3], Sontaya KOOLKALAYA[4], Wachira KWANGKHANG[2], Chaiwut GRUDPAN[1], Tuantong JUTAGATE[1]

1 *Faculty of Agriculture, Ubon Ratchathani University, Warin Chamrab, Ubon Ratchathani, Thailand*
2 *Department of Fisheries, Chatuchak, Bangkok, Thailand*
3 *Mahidol University, Nakhonsawan Campus, Nakhonsawan, Thailand*
4 *Faculty of Agricultural Technology, Rambhai Barni Rajabhat University, Muang, Chanthaburi, Thailand*

http://zoobank.org/6BF830BD-99D2-4F4D-B599-5F49B73F99F2

Corresponding author: Tuantong Jutagate (tuantng.j@ubu.ac.th)

Academic editor: Sanja Matić-Skoko ♦ **Received** 7 September 2021 ♦ **Accepted** 2 November 2021 ♦ **Published** 29 November 2021

Citation: Phaeviset P, Phomikong P, Avakul P, Koolkalaya S, Kwangkhang W, Grudpan C, Jutagate T (2021) Age and growth estimates from three hard parts of the spotted catfish, *Arius maculatus* (Actinopterygii: Siluriformes: Ariidae), in Songkhla Lake, Thailand's largest natural lake. Acta Ichthyologica et Piscatoria 51(4): 371–378. https://doi.org/10.3897/aiep.51.74082

Abstract

The spotted catfish, *Arius maculatus* (Thunberg, 1792), is a euryhaline fish that is economically important in the Indo-West Pacific. Population dynamics studies and stock assessments of this species have focused on marine stocks, but not those from fresh water. In this study, the age and growth of *A. maculatus* were, therefore, investigated for the inland stock in Songkhla Lake, Thailand. A total of 213 individuals ranging between 35 and 238 mm TL were used. The length–weight relation indicated positive allometry of this population. Three hard parts (otolith, dorsal- and pectoral-fin spines) were used for aging. The marginal increment ratio confirmed that an annulus was deposited once a year in all three hard parts. All of the samples were aged between 0+ and 6+ years. Verification of age estimates from three readers showed that the otolith was the most suitable part for age estimation. Three growth models (von Bertalanffy, Gompertz, and logistic) were applied in the study. The von Bertalanffy model best described the growth of this fish in Songkhla Lake. The obtained asymptotic length was 290.87 mm TL and the relative growth rate parameter was 0.166 year^{-1}. Our results will be applied as inputs for fish stock assessment models. The obtained growth parameters also can serve as a reference for *A. maculatus* stocks elsewhere.

Keywords

Arius maculatus, Dorsal-fin spine, otolith, pectoral-fin spine, Thailand, von Bertalanffy growth model

Introduction

The family Ariidae accommodates more than 140 species of catfishes, found mainly in marine and brackish waters (Froese and Pauly 2021). However, some species are euryhaline and can live in a wide range of environments, from freshwater to marine, including the spotted catfish, *Arius maculatus* (Thunberg, 1792), which is widely distributed across the Indo-West Pacific Region (Rainboth 1996). This species has been reported to grow as large as 80 cm TL, but the typical maximum size is 30 cm TL (Froese and Pauly 2021). The trophic level

of *A. maculatus* is estimated to be 3.4 ± 0.46, indicating carnivorous behavior. This fish feeds mainly on benthic invertebrates (Angsupanich et al. 2005), and plays an important role in the ecosystem; an imbalance in its abundance can trigger a trophic cascade (Froese and Pauly 2021). This fish is targeted for harvest in many countries, where the fisheries operations are mostly in either marine or brackish water environments (Arshad et al. 2008; Chu et al. 2012; Jumawan et al. 2020; Kutsyn et al. 2021). There is also a unique inland fishery for this species in Songkhla Lake, the largest natural lake in Thailand. The catch of *A. maculatus* was over 180 metric tons in 2011, following the restoration of the lake's fishery resources by declaring fish sanctuary zones and a stocking program for some indigenous species (Tanasomwang and Assava-aree 2013). The recent catch of this species in 2020 increased tremendously to 330 metric tons (Pattalung Inland Fisheries Research and Development Center, unpublished data), which was almost 1.5-fold higher than the previous record. This sharp rise in harvest implies that appropriate fisheries management of this resource is urgently required to prevent a collapse of this spotted catfish stock.

Effective fisheries management requires an understanding of the stock status and population dynamics of the targeted fish species, where the growth parameters (i.e., asymptotic length and curvature parameter) are among the crucial inputs (Isley and Grabowski 2007; Katsanevakis and Maravelias 2008). Accurate estimates of growth parameters are important for monitoring the stock status as well as for assessing management actions that have been applied to maintain the integrity of the fish stock (Zhang et al. 2020). To estimate growth, precise and accurate age data are required. Age can be estimated by several methods but counting natural growth rings of hard body parts is the most common and is generally reliable (Vitale et al. 2019). Many calcified structures, both inner parts (e.g., otoliths, vertebrae, and urohyal bone) as well as outer parts (e.g., scales, opercular bones, spines, and fin rays) have been shown to reliably reflect the age of fishes (Campana 2001; Morioka et al. 2019; Phomikong et al. 2019). As many hard parts are available for age determination, a comparison of multiple structures to determine the most suitable ones for a particular species or population is always recommended (Zhu et al. 2017). Khan et al. (2011) mentioned that selecting the most suitable hard part for aging is one of the problems in age and growth studies of fishes. They suggested comparing different bony structures of the targeted fish to obtain the most suitable one that has high precision and low aging error before further growth analysis. Moreover, if there is no significant difference in age reading between the inner and outer parts, the use of outer parts is recommended, since the fish does not need to be sacrificed; this is particularly desirable for long-lived species (Zhu et al. 2017).

Along with selecting suitable hard parts for aging, the most suitable model must be chosen for the length-at-age key, which can be determined by the shape of the growth curve and error component of the data (Zhu et al. 2017). Numerous growth curves, as well as their representative models, have been introduced and applied to explain fish growth. Growth models relate the age of fish in a population to their length or weight; the von Bertalanffy growth model is the most commonly adopted and widely used (Jones 2000; Katsanevakis and Maravelias 2008; Zhu et al. 2017). The von Bertalanffy model is commonly used because of the shape of the desired growth curve and from biological assumptions, one of which is that fish growth slows with age (Katsanevakis 2006). Other commonly used models include the Gompertz and logistic growth models (Katsanevakis 2006; Zhang et al. 2020). Both models are well suited to fishes, which exhibit low initial growth rates, but the regions above and below the inflection are asymmetrical in the Gompertz model, and symmetrical in the logistic models (Quist et al. 2012). The base assumption of all three of these models is that fish show asymptotic growth (Katsanevakis and Maravelias 2008).

The aim of this study was to provide length-at-age data and a growth model for the *A. maculatus* stock in Songkhla Lake, Thailand. We assess the suitability of hard parts for aging and evaluate three growth models to describe the relation between age and length, which can be used as a reference for other *A. maculatus* stocks. The results are also expected to be further used for stock assessment and fisheries management of the stock in Songkhla Lake for its sustainable exploitation.

Materials and methods

Study area and fish sampling. Songkhla Lake (Fig. 1) is a shallow coastal lagoon in southern Thailand (07°24′08″N, 100°15′42″E), with the mean depth of 2 m. The water body covers 1018 km^2 and is classified into three distinct zones: upper (459 km^2), middle (377 km^2), and lower (182 km^2). This lake hosts a high diversity of fishes (ca. 450 species), due in part to its range of physiological characteristics. For example, the upper zone is a freshwater environment, while the lower zone is brackish (maximum 15‰) at the mouth, where it enters the Gulf of Thailand (Damchoo et al. 2021). Meanwhile, the salinity in the middle zone fluctuates between 10‰ and 15‰ as it is a mixing zone between fresh and saline water (Tanasomwang and Assava-aree 2013). Samples of *A. maculatus* were collected from four landing sites (Fig. 1) in the upper and middle zones of Songkhla Lake (where the fishery is intensive) between January and December 2020. Individual fish were labeled, measured for standard length (SL), fork length (FL) total length (TL) to the nearest 0.1 cm, and weighed to the nearest 0.01 g *in situ*. Samples were then packed in ice and taken to the Pattalung Inland Fisheries Research and Development Center. Additionally, 15 *A. maculatus* representing various size classes were collected every three months for annual ring validation.

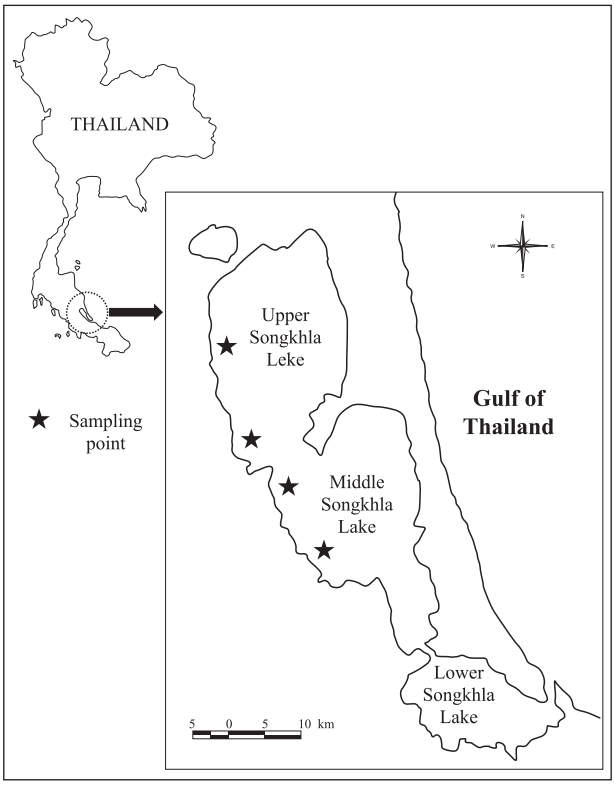

Figure 1. Location and map of Songkhla Lake, Thailand. Stars indicate fish landing points.

At the fisheries center, the largest pair of otoliths (i.e., lapilli) were removed, washed, and kept dry in a vial. Dorsal- and pectoral-fin spines were cut with bone-cutting forceps. Each hard part was embedded in resin and cut by a low-speed diamond saw (South Bay Technology Inc., model: 650). Bony parts were then polished by sandpaper (grit size ranging from 600 to 1500) until the core was seen. Each polished sample was photographed under 40× magnification, and annual rings were counted visually from the monitor and using the Image-J program. An annual ring was considered as the boundary between the inner edge of a wide opaque zone (i.e., corresponding to high growth rate) and the outer edge of a narrow translucent zone (i.e., corresponding to low growth rate) (Kutsyn et al. 2021). Three (3) readers, with no background information of the size of each individual fish, were assigned for aging each sample.

Data analysis. Length–length relations and length (TL)–weight relation (LWR) were examined by linear and curvilinear regressions. The estimated parameter "*b*" from LWR was tested for significant deviation from 3 by using a *t*-test. Annual ring formation was validated by marginal increment ratio (MIR) analysis (Beamish and McFarlane 1983) as

$$\mathrm{MIR} = \frac{(R - R_n)}{(R_n - R_{n-1})}$$

where R is the radius (distance between the center and the edge of hard part), R_n is the distance from center to outer edge of last complete band, and R_{n-1} is the distance from center to outer edge of next-to-last complete band. The difference in MIR among months of sampling was tested by Kruskal–Wallis test, and Dunn's post test was applied when a significant difference was found at $\alpha = 0.05$.

The percentage of agreement (PA) among the three readers was calculated as the ratio of the number of agreements among the three readings to the total number of readings made. Precision in age reading among the three readers of each hard part was tested by two methods (Campana 2001): mean percentage error (MPE)[1] and coefficient of variation (CV).

$$\mathrm{MPE} = \frac{\sum_{j=1}^{n} \mathrm{MPE}_j}{n}$$

where

$$\mathrm{MPE}_j = 100 \times \frac{\sum_{i=1}^{R} \frac{\left| x_{ij} - \bar{x}_j \right|}{\bar{x}_j}}{R}$$

where MPE_j is the mean percentage error for the j^{th} fish, x_{ij} is the i^{th} age estimate of the j^{th} fish, $\bar{x}_j$ is the mean age estimate for the j^{th} fish, R is the number of times that each fish was aged, and n is the number of samples.

$$\mathrm{CV} = \frac{\sum_{j=1}^{n} \mathrm{CV}_j}{n} \text{ where } \mathrm{CV}_j = 100 \times \frac{\sqrt{\frac{\sum_{i=1}^{R} \left(x_{ij} - \bar{x}_j \right)^2}{R-1}}}{\bar{x}_j}$$

where CV_j is the coefficient of variation for the j^{th} fish. The age readings of each fish sample and each hard part from the three readers were then averaged and rounded to the nearest integer. Two additional readers with extensive experience in fish aging reviewed each hard part and checked its designated age. The age-bias plot (Campana et al. 1995) was applied to visually assess potential aging differences among hard parts. Finally, three common growth models (Duarte-Neto et al. 2012), i.e., von Bertalanffy model (von Bertalanffy 1938), Gompertz model (Gompertz 1825), and Logistic model (Ricker 1975) were fitted to the observed length-at-age data:

$$L_t = L_\infty \left(1 - e^{-k(t - t_0)}\right)$$

von Bertalanffy model

$$L_t = L_\infty e^{-e^{-k(t - t_0)}}$$

Gompertz model

$$L_t = L_\infty \left(1 + e^{-k(t - t_0)}\right)^{-1}$$

Logistic model

1 It was originally (Campana 2001) "average percent error (APE)".

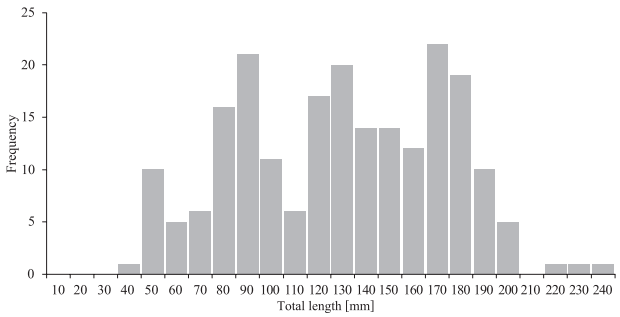

Figure 2. Length frequency distribution of *Arius maculatus* from Songkhla Lake, Thailand.

Results

A size distribution of the 213 *A. maculatus* samples used in this study is presented in Fig. 2, with a range between 35 and 238 mm TL (mean ± SD 128 ± 43 mm TL). Body weights ranged between 0.4 and 154.1 g, with mean ± SD of 26.4 ± 23.7 g. The length–length relations showed high correlation between measurements ($R^2 > 0.95$; Fig. 3A–B); meanwhile, the log-transformed LWR revealed positive allometric growth, i.e., parameter "*b*" of WLR was significantly higher than 3.0 ($P < 0.01$; Fig. 3C).

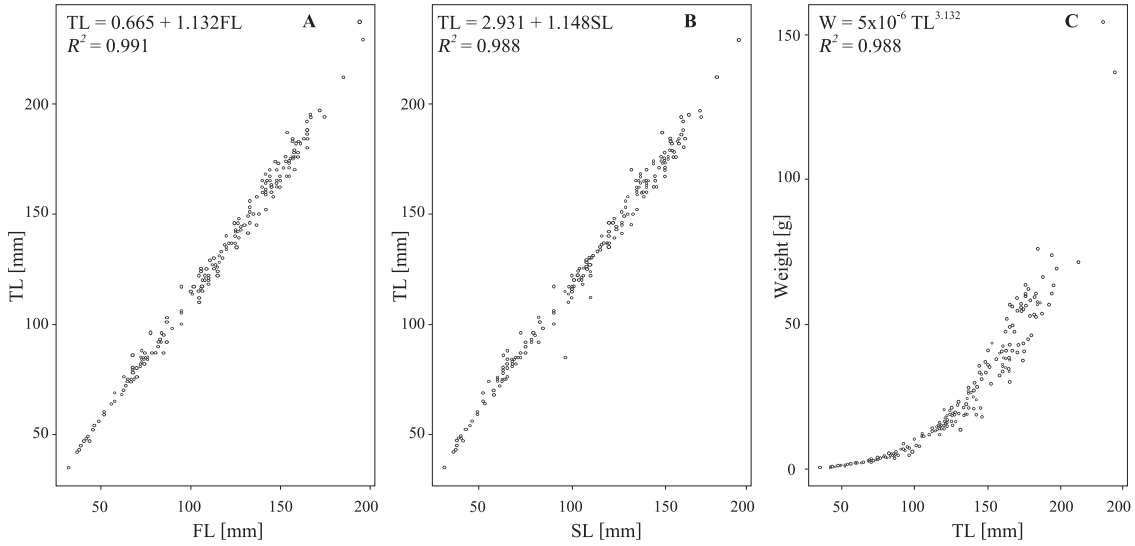

Figure 3. Length–length and length–weight relations of *Arius maculatus* from Songkhla Lake, Thailand. TL = total length, FL = form length, SL = standard length.

where L_t is the predicted length-at-age t, L_∞ is the asymptotic length, k is a relative growth rate parameter, and t_0 is the age when length is theoretically zero. The growth models were fitted to length-at-age data using nonlinear least-squares. The residual sum of squares (RSS) was used to measure the discrepancy between the data and an estimation model. The growth performance index (Ø′, Pauly and Munro 1984) of each growth model was estimated by

$$Ø' = \log(k) + 2\log(L_\infty)$$

The obtained L_∞ [cm] and k values were further used to estimate the natural mortality coefficient (M) by using Pauly's equation (Pauly 1980)

$$\log_{10}M = -0.0066 - 0.279\log_{10}L_\infty + 0.6543\log_{10}k + 0.4635\log_{10}T$$

where T is the annual mean water temperature, which was set at 30°C (International Lake Environment Committee Foundation 2021). Data analysis was conducted by using R-statistics (R Core Team 2020) under Package FSA (Ogle et al. 2021) and "fishmethods" (Nelson 2021).

The 60 *A. maculatus* samples for the MIR study ranged between 35 and 238 mm TL, with the mean ± SD of 128 ± 43 mm TL. The MIR results showed clear increasing trends from January (MIR near 0.5) to October (MIR near 1.0) in all three hard parts, and a significant difference was found between January and the other sampling months ($P < 0.05$; Fig. 4). The highest MIR was found in October for all hard

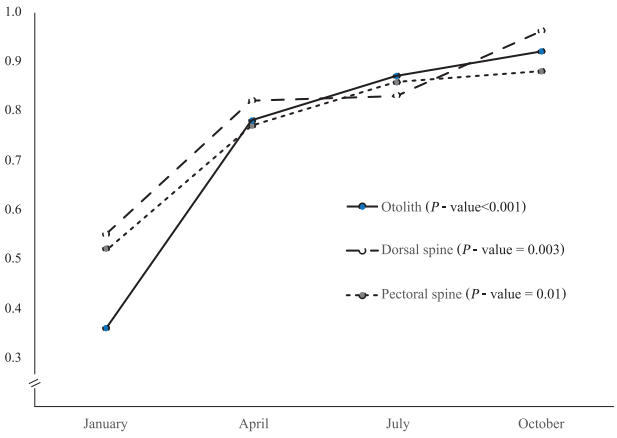

Figure 4. Marginal increment ratio (MIR) of *Arius maculatus* in Songkhla Lake, Thailand.

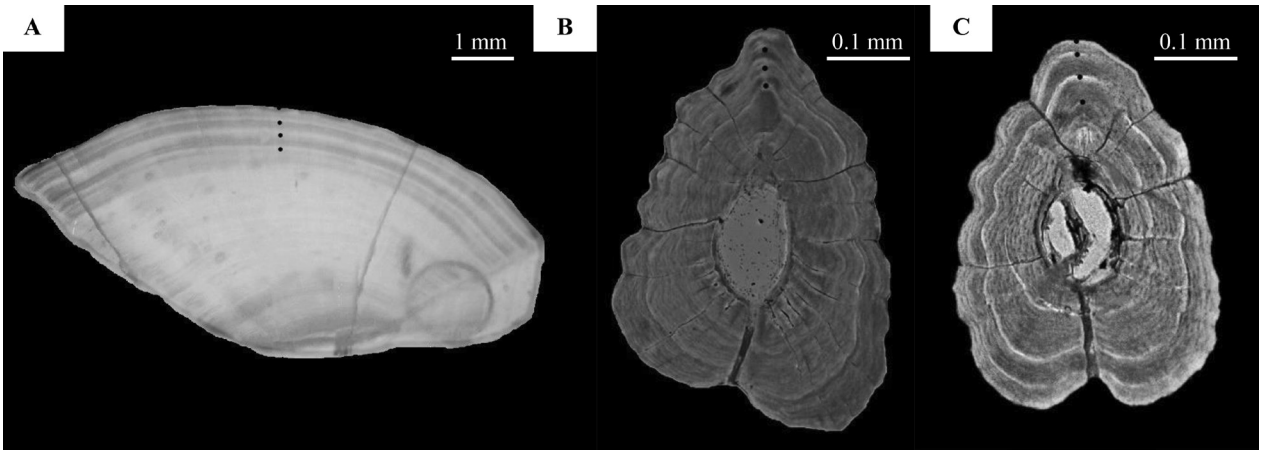

Figure 5. Cross-sections of three hard parts of *Arius maculatus* from Songkhla Lake, Thailand. (**A**) otolith, (**B**) dorsal spine and (**C**) pectoral spine. The black dots are labeled annuli.

parts and was almost double the MIR in January. The largest difference in MIR values between these two months was observed in otoliths. The significantly lower MIR in January implies that an annulus is deposited once a year.

Age estimates from the three hard parts ranged from less than 1 to a maximum of 6 years (Fig. 5). The percentage of agreement among the three readers was highest for otoliths (58.2%), resulting in the lowest MPE (9.5%) and CV (12.6%). Meanwhile, the pectoral-fin spine samples showed a higher percentage of agreement (and hence lower MPE and CV) than dorsal-fin spine samples (Table 1).

Table 1. Precision in age reading among three readers of *Arius maculatus* sampled from Songkhla Lake, Thailand.

Hard part	Agreement	MPE	CV
Otolith	58.2%	9.5%	12.6%
Dorsal-fin spine	50.3%	15.5%	16.0%
Pectoral-fin spine	55.9%	12.6%	14.4%

MPE = mean percentage error, CV = coefficient of variation.

The designated age of each hard part (i.e., by three readers in the first round) was checked by two highly experienced readers with a perfect agreement and thus was considered the observed age of each individual fish (Table 2). Biases of age reading from otoliths and spines were obvious at ages beyond 3 years, as the observed age from otoliths was a bit higher than the observed age from spines; meanwhile, less bias was found between the two spines (Fig. 6).

Parameter estimation in all models using the observed length-at-age data from the three hard parts is displayed in Table 3. It is clear that the asymptotic length (L_∞) estimated from the von Bertalanffy model (around 290 mm TL) was higher than from the other two models, for all hard parts. The larger L_∞ from the von Bertalanffy model was compensated by low k values, which consequently made Ø′ values for the three models relatively similar. The estimated natural mortality coefficient fluctuated between 0.573 and 1.631 year^{-1}, due to the estimated L_∞ and k values. In each growth model, the lowest sum of squares was obtained from the length-at-age data from otoliths. Therefore, this hard part was used to explain the growth of *A. maculatus* in Songkhla Lake as

$$L_t = 290.87(1 - e^{-0.166(t + 1.51)})$$
von Bertalanffy model

$$L_t = 229.82e^{-e^{-0.383(t - 0.598)}}$$
Gompertz model

$$L_t = 209.85(1 + e^{-0.604(t - 1.274)})^{-1}$$
Logistic model

Table 2. Observed age from three hard parts of *Arius maculatus* from Songkhla Lake, Thailand.

Length (TL) [mm]	Age [year]							Total
	0+	1+	2+	3+	4+	5+	6+	
31–50	11, 11, 11							33
51–70	10, 10, 11	1, 1, 0						33
71–90	19, 20, 21	18, 17, 16						111
91–110	0, 0, 1	11, 15, 14	5, 2, 2	1, 0, 0				51
111–130		12, 13, 16	22, 20, 20	3, 4, 1				111
131–150		1, 1, 2	13, 20, 17	13, 7, 9	1, 0, 0			84
151–170		0, 0, 1	2, 8, 6	23, 22, 22	9, 5, 6			105
171–190			0, 2, 4	9, 16, 11	16, 10, 13	3, 1, 1	1, 0, 0	87
191–210				0, 2, 1	2, 2, 3	1, 1, 1	2, 0, 0	15
211–230					1, 1, 1	1, 1, 1		6
231–250						0, 1, 1	1, 0, 0	3

Note: Numbers in each cell are the observed ages from otolith, dorsal- and pectoral-fin spines, respectively.

Table 3. Growth parameters from three hard parts of *Arius maculatus* from Songkhla Lake, Thailand.

Model	L_∞ [mm]	k [year^{-1}]	t_0 [year]	RSS	Ø′	M [year^{-1}]
Otolith						
von Bertalanffy	290.87	0.166	–1.51	58,029	2.148	0.573
Gompertz	229.82	0.383	0.598	57,467	2.306	1.058
Logistic	209.85	0.604	1.274	57,472	2.425	1.463
Dorsal-fin spine						
von Bertalanffy	292.20	0.184	–1.34	65,824	2.196	0.612
Gompertz	226.19	0.443	0.507	65,267	2.355	1.170
Logistic	205.21	0.706	1.072	65,211	2.473	1.631
Pectoral-fin spine						
von Bertalanffy	286.08	0.189	–1.389	59,626	2.189	0.627
Gompertz	226.11	0.435	0.451	59,753	2.347	1.156
Logistic	206.28	0.685	1.039	60,288	2.464	1.595

L_∞ = the asymptotic total length, k = relative growth rate parameter, t_0 = age when length is theoretically zero, RSS = residual sum of squares, Ø′ = phi prime value, M = natural mortality coefficient.

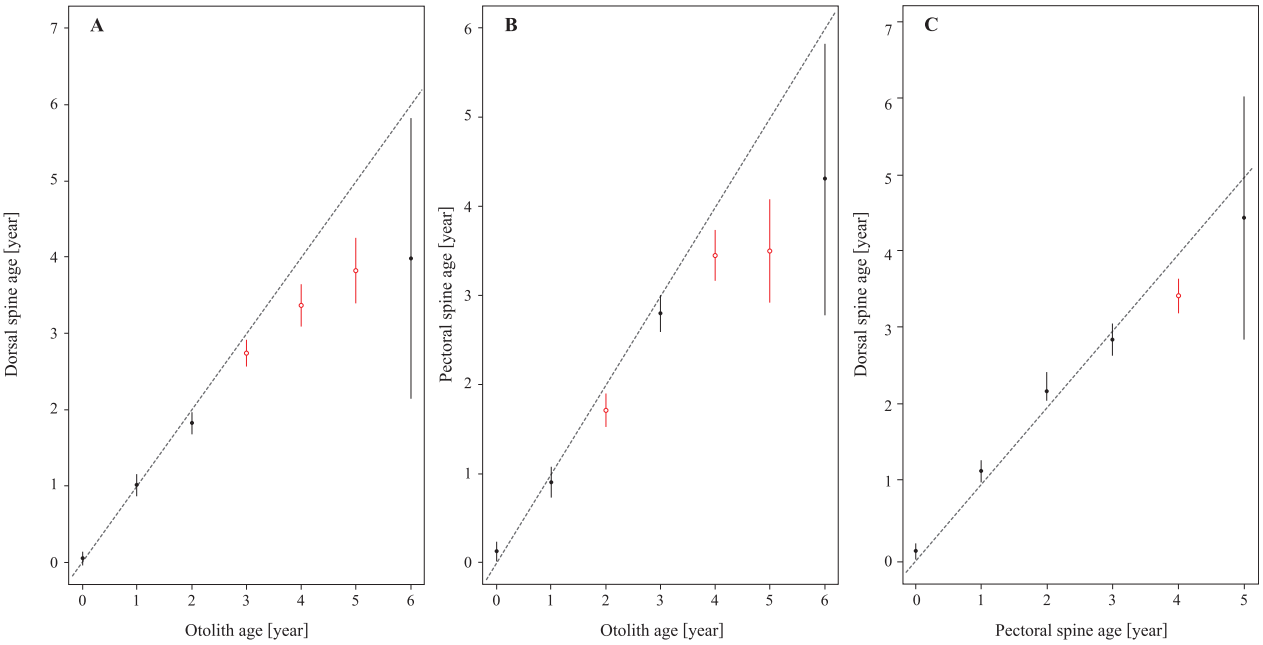

Figure 6. Age bias plots between hard parts of *Arius maculatus* from Songkhla Lake, Thailand. (**A**) otolith vs. dorsal spine, (**B**) otolith vs. pectoral spine and (**C**) pectoral spine vs. dorsal spine. Each error bar represents the 95% confidence interval. Red error bar indicates a significant difference in age agreement between two hard parts.

By applying the growth curves of the three models (Fig. 7), the estimated lengths at age 1 to 5 years were almost identical, whereas the estimated sizes from the von Bertalanffy model were larger at age 6 years old and above relative to the other models.

Figure 7. Growth curves of *Arius maculatus* in Songkhla Lake, Thailand, from three growth models.

Discussion

The age–length key and growth estimation of fishes and shellfishes can provide valuable insight into their life history and be further used to prescribe optimum fishing regulations for sustaining their fisheries (Isley and Grabowski 2007). In this study, the age–length key and growth of *A. maculatus* were assessed for the population in Songkhla Lake, Thailand. All the samples were from the upper or middle zones of the lake, implying that they can develop a stock in a low-salinity or freshwater habitat, contrary to the suggestion by Kutsyn et al. (2021) that this fish avoids the freshwater environment in the Mekong Delta.

The maximum length of *A. maculatus* in this study was 23.8 cm TL, which is similar to the maximum size from the Mekong Delta (25 cm TL; Kutsyn et al. 2021). Tran et al. (2021) reported that, in the Lower Mekong Basin, this fish can grow as large as 40 cm TL. The size (around 25 cm TL) found in fresh- and brackish-water habitats is substantially lower than in stocks from marine environments, such as 29 cm TL off the coast of Malaysia (Arshad et al. 2008) and 35 cm TL in Taiwan waters (Chu et al. 2012). Length–length relations showed high linearity with high correlation. The "*b*" coefficients (i.e., slope of the regression line) of SL–TL (1.15) and FL–TL (1.13) relations were similar to the values obtained for the stock off the coast of Taiwan for SL–TL (1.18) and FL–TL (1.06) (Chu et al. 2012). Meanwhile, the coefficient "*b*" for SL–TL relation of the *A. maculatus* stock from Peninsular Malaysia was 1.17 (Arshad et al. 2008). The similar values of "*b*" from various stocks indicate the similar body proportions of this fish, regardless of whether they are freshwater, brackish-water, or marine residents. The "*b*" coefficients of LWRs from this study were significantly higher than 3, indicating positive allometry (i.e., fish become heavier as length increases), and reflecting optimum conditions for growth (Froese 2006) as well as the suitability of habitat conditions (Damchoo et al. 2021). Interestingly, the "*b*" coefficients of LWRs from the marine stocks were lower than 3 (between 2.6 and 2.9) (Arshad et al. 2008; Chu et al. 2012), which could be explained either by climatic variation or resource competition (Dieb-Magalhães et al. 2015).

Age validation through MIR analysis provides relative certainty of annulus formation and confirms the growth zone deposition in *A. maculatus*. Low MIR was found in the early part of the year (January, winter) when the water temperature in the inner zone is normally less than 27°C; it is around 30°C during the rest of the year (Anonymous 2021). The maximum age (6 years) of *A. maculatus* found in this study is within the applicable range for age validation. MIR is not suitable for long-lived species

or older individuals (i.e., more than 10 years) (Campana 2001). A higher percentage of agreement in aging from otoliths than with other hard parts has also been reported by other researchers (Khan et al. 2011; Zhu et al. 2017). The percentage of agreement was 50%–60% in this study. Other studies that employed only two readers achieved rates of over 60% (e.g., Khan et al. 2011; Gebremedhin et al. 2021). Although the percentage of agreement was lower in this study, verification among the three readers through MPE and CV was still lower than the upper limit of 20% (Winter and Cliff 1996; Cruz-Martínez et al. 2004). More age bias was observed between otoliths and spines (both types) than between dorsal- and pectoral-fin spines. In older fish (i.e., beyond 3 years), the higher ages estimated from otoliths could be because the spine nucleus of many fish species is reabsorbed and replaced by a hole (i.e., vascularization), which eliminates or obscures the first annulus, causing underestimation of age from spines (Drew et al. 2006; Khan et al. 2011). For this reason, together with the greater consistency in aging among the three readers, otoliths were selected for growth estimation, similar to several other studies (e.g., Khan et al. 2011; Zhu et al. 2017; Almamari et al. 2021; Gebremedhin et al. 2021) that compare ages from various hard parts.

The growth models based on the age–length key from otolith reading revealed a lower residual sum of squares than for spines, which confirms the suitability of this hard part for *A. maculatus* aging. Higher L_∞ and lower k values from the von Bertalanffy model than from other growth models have been reported in many studies (e.g., Cruz-Martínez et al. 2004; Zhu et al. 2009; Duarte-Neto et al. 2012; Zhang et al. 2020). The obtained $Ø'$ values from all three growth models were within the range of values from stocks of *A. maculatus* elsewhere ($2.08 < Ø' < 3.14$), which were estimated either by otoliths or length-frequency data (Kutsyn et al. 2021). A suitable growth model should not only be selected by mathematical measures (Katsanevakis 2006; Katsanevakis and Maravelias 2008), but also biological as well as management points of view (Zhu et al. 2009; Haddon 2011). In a mathematical sense, the von Bertalanffy model was generally considered the most reliable candidate model for fish stocks (e.g., Zhu et al. 2009; Duarte-Neto et al. 2012; Zhang et al. 2020). From a management viewpoint, lower L_∞ and the higher k values of *A. maculatus* in Songkhla Lake from the Gompertz and Logistic models would result in an overestimated natural mortality coefficient, which would have drastic implications for fisheries management (Khan et al. 2011). For example, it could lead managers to increase fishing effort due to the high estimated natural mortality.

Conclusion

The age–length relation and growth of *A. maculatus* in Songkhla Lake, Thailand, were examined by using hard parts. Different aging structures and growth models were compared for biases in the results. Results showed that otoliths provided more precise age estimation among three readers. The von Bertalanffy model was judged to be the most suitable candidate for growth estimation because of the lowest residual sum of squares. The obtained growth parameters (i.e., L_∞ and k) can be used as inputs in other fish stock assessment models (e.g., the yield per recruit model) to investigate the optimum fishing level for this stock, which currently experiences high fishing pressure.

Acknowledgment

The first author is grateful for financial support towards his master's degree study from the Agricultural Research Development Agency (ARDA) Grant HRD6405081.

References

Almamari D, Rabia S, Park JM, Jawad LA (2021) Age, growth, mortality, and exploitation rate of blueline snapper, *Lutjanus coeruleolineatus* (Actinopterygii: Perciformes: Lutjanidae), from Dhofar Governorate, Sultanate of Oman. Acta Ichthyologica et Piscatoria 51(2): 159–166. https://doi.org/10.3897/aiep.51.63572

Angsupanich S, Somsak S, Phrommoon J (2005) Stomach contents of the catfishes *Osteogeneiosus militaris* (Linnaeus, 1758) and *Arius maculatus* (Thunberg, 1792) in the Songkhla Lake. Songklanakarin Journal of Science and Technology 27(Suppl. 1): 391–402.

Anonymous (2021) World lake database. International Lake Environment Committee Foundation. [version 01/2021] https://wldb.ilec.or.jp

Arshad A, Jimmy A, Nurulamin SM, Japarsidik B, Harah ZM (2008) Length–weight and length–length relationships of five fish species collected from seagrass beds of the Sungai Pulai estuary, Peninsular Malaysia. Journal of Applied Ichthyology 24(3): 328–329. https://doi.org/10.1111/j.1439-0426.2007.01026.x

Beamish RJ, McFarlane GA (1983) The forgotten requirement for age validation in fisheries biology. Transactions of the American Fisheries Society 112(6): 735–743. https://doi.org/10.1577/1548-8659(1983)112%3C735:TFRFAV%3E2.0.CO;2

Campana SE (2001) Accuracy, precision and quality control in age determination, including a review of the use and abuse of age validation methods. Journal of Fish Biology 59(2): 197–242. https://doi.org/10.1111/j.1095-8649.2001.tb00127.x

Campana SE, Annand MC, McMillan JI (1995) Graphical and statistical methods for determining the consistency of age determinations. Transactions of the American Fisheries Society 124(1): 131–138. https://doi.org/10.1577/1548-8659(1995)124%3C0131:GASMFD%3E2.3.CO;2

Chu WS, Hou YY, Ueng YT, Wang JP (2012) Correlation between the length and weight of *Arius maculatus* off the southwestern coast of Taiwan. Brazilian Archives of Biology and Technology 55(5): 705–708. https://doi.org/10.1590/S1516-89132012000500009

Cruz-Martínez A, Chiappa-Carrara X, Arenus-Fuentes V (2004) Age and growth of the bull shark, *Carcharhinus leucas*, from southern Gulf of Mexico. Journal of Northwest Atlantic Fishery Science 37: 367–374. https://doi.org/10.2960/J.v35.m481

Damchoo S, Grudpan C, Jutagate A, Grudpan J, Jutagate T (2021) Morphological investigation and length–weight relationships of long-snouted pipefish *Doryichthys boaja* (Syngnathidae) from two different environments. Agriculture and Natural Resources (Bangkok) 55: 664–673. https://doi.org/10.34044/j.anres.2021.55.4.17

Dieb-Magalhães L, Florentino AC, Soares MGM (2015) Length–weight relationships and length at first maturity for nine fish species of floodplain lakes in Central Amazon (Amazon basin, Brazil). Journal of Applied Ichthyology 31(6): 1182–1184. https://doi.org/10.1111/jai.12919

Drew K, Die DJ, Arocha F (2006) Understanding vascularization in fin spines of white marlin (*Tetrapturus albidus*). Bulletin of Marine Science 79(3): 847–852.

Duarte-Neto P, Higa FM, Lessa RP (2012) Age and growth estimation of bigeye tuna, *Thunnus obesus* (Teleostei: Scombridae) in the southwestern Atlantic. Neotropical Ichthyology 10(1): 149–158. https://doi.org/10.1590/S1679-62252012000100014

Froese R (2006) Cube law, condition factor and weight–length relationships: History, meta-analysis and recommendations. Journal of Ichthyology 22(4): 241–253. https://doi.org/10.1111/j.1439-0426.2006.00805.x

Froese R, Pauly D [Eds] (2021) FishBase. World Wide Web electronic publication. www.fishbase.org [version 06/2021]

Gebremedhin S, Bruneel S, Getahun A, Anteneh W, Goethals P (2021) Scientific methods to understand fish population dynamics and support sustainable fisheries management. Water 13(4): 574. https://doi.org/10.3390/w13040574

Gompertz B (1825) On the nature of the function expressive of the law of human mortality, and on a new mode of determining the value of life contingencies. Philosophical Transactions of the Royal Society of London 115: 513–583. https://doi.org/10.1098/rstl.1825.0026

Haddon M (2011) Modeling and quantitative methods in fisheries. 2nd edn. Champman and Hall/CRC, Boca Raton, FL, USA, 465 pp.

Isley JJ, Grabowski TB (2007) Age and growth. Pp. 187–228. In: Guy CS, Brown ML (Eds) Analysis and interpretation of freshwater fisheries data. American Fisheries Society, Bethesda, MD, USA.

Jones CM (2000) Fitting growth curves to retrospective size-at-age data. Fisheries Research 46(1–3): 123–129. https://doi.org/10.1016/S0165-7836(00)00139-9

Jumawan CQ, Metillo EB, Mutia MT (2020) Stock assessment of *Arius maculatus* (Thurnberg [sic], 1792) (Ariidae, Siluriformes) in Panguil Bay, northwestern Mindanao. The Philippine Journal of Fisheries 27(1): 40–53. https://doi.org/10.31398/tpjf/27.1.2019A0013

Katsanevakis S (2006) Modelling fish growth: Model selection, multi-model inference and model selection uncertainty. Fisheries Research 81(2–3): 229–235. https://doi.org/10.1016/j.fishres.2006.07.002

Katsanevakis S, Maravelias CD (2008) Modelling fish growth: Multi-model inference as a better alternative to a priori using von Bertalanffy equation. Fish and Fisheries 9(2): 178–187. https://doi.org/10.1111/j.1467-2979.2008.00279.x

Khan S, Khan MA, Miyan K (2011) Comparison of age estimates from otoliths, vertebrae, and pectoral-fin spines in African sharptooth catfish, *Clarias gariepinus* (Burchell). Estonian Journal of Ecology 60(3): 183–193. https://doi.org/10.3176/eco.2011.3.02

Kutsyn DN, Ablyazov ER, Truong BH, Cu ND (2021) The size–age structure, growth, and maturation of the spotted catfish *Arius maculatus* (Thunberg, 1792) (Siluriformes: Ariidae) from the Mekong Delta, Vietnam. Russian Journal of Marine Biology 47(1): 56–63. https://doi.org/10.1134/S1063074021010053

Morioka S, Vongvichith B, Marui J, Okutsu T, Phomikong P, Avakul P, Jutagate T (2019) Characteristics of two populations of Thai River sprat *Clupeichthys aesarnensis* from man-made reservoirs in Thailand and Laos, with aspects of gonad development. Fisheries Science 85(4): 667–675. https://doi.org/10.1007/s12562-019-01319-x

Nelson GA (2021) fishmethods: Fishery science methods and models. R package version 1.11-2. [version 07/2021] https://CRAN.R-project.org/package=fishmethods

Ogle DH, Doll JC, Wheeler P, Dinno A (2021) FSA: Fisheries stock analysis. R package version 0.9.1. [version 07/2021] https://CRAN.R-project.org/package=FSA

Pauly D (1980) On the interrelationships between natural mortality, growth parameters, and mean environmental temperature in 175 fish stocks. ICES Journal of Marine Science 39(2): 175–192. https://doi.org/10.1093/icesjms/39.2.175

Pauly D, Munro JL (1984) Once more on the comparison of growth in fish and invertebrates. ICLARM Fishbyte (2): 21.

Phomikong P, Seehirunwong S, Jutagate T (2019) A preliminary estimate of age and growth of two populations of dasyatid stingray *Urogymnus polylepis* in Thailand. Journal of Fisheries and Environment 43(3): 43–54.

Quist MC, Pegg MA, Devries DR (2012) Age and growth. Pp. 677–731. In: Zale AV, Parrish DL, Sutton TM (Eds) Fisheries techniques. American Fisheries Society, Bethesda, MD, USA.

R Core Team (2020) R: A language and environment for statistical computing. [version 01/2020] http://www.r-project.org/index.html

Rainboth WJ (1996) Fishes of the Cambodian Mekong: FAO Species Identification Field Guide for Fishery Purposes. FAO, Rome, 265 pp.

Ricker WE (1975). Computation and interpretation of biological statistics of fish populations. Bulletin of the Fisheries Research Board of Canada 191: 1–382.

Tanasomwang V, Assava-aree A (2013) [Fishery status and total catch in year 2011 and 2012 after restoration of fishery resources in Songkhla Lake.] Department of Fisheries, Bangkok, 44 pp. [In Thai with English abstract]

Tran DD, Shibukawa K, Nguyen PT, Ha HP, Tran LX, Mai HV, Utsugi K (2013) Mô tả định Loại Cá. Đồng Bằng Sông Cửu Long, Việt Nam. Fishes of the Mekong Delta, Vietnam. Can Tho University Publishing House, Can Tho, Vietnam, 174 pp.

Vitale F, Clausen LW, Chonchúir GN [Eds] (2019) Handbook of fish age estimation protocols and validation methods. International Council for the Exploration of the Sea, Copenhagen, 180 pp.

von Bertalanffy L (1938) A quantitative theory of organic growth (Inquires on growth law II). Human Biology 10(2): 181–213. https://www.jstor.org/stable/41447359

Winter SP, Cliff G (1996) Age and growth determination of the blacktip shark, *Carcharhinus limbatus*, from the east coast of South Africa. Fish Bulletin 94: 135–144.

Zhang K, Zhang J, Li J, Liao B (2020) Model selection for fish growth patterns based on a Bayesian approach: A case study of five freshwater fish species. Aquatic Living Resources 17(33). https://doi.org/10.1051/alr/2020019

Zhu L, Li L, Liang Z (2009) Comparison of six statistical approaches in the selection of appropriate fish growth models. Chinese Journal of Oceanology and Limnology 27(3): 457–467. https://doi.org/10.1007/s00343-009-9236-6

Zhu X, Wastle R, Leonard D, Howland K, Carmichael TJ, Tallman RF (2017) Comparison of scales, pectoral-fin fin rays, and otoliths for estimating age, growth, and mortality of lake whitefish, *Coregonus clupeaformis*, in Great Slave Lake. Canadian Science Advisory Secretariat, Ottawa, ON, Canada, 28 pp.

Acta Ichthyologica et Piscatoria 51(4), 2021, 379–383 | DOI 10.3897/aiep.51.75811

PENSOFT

ACTA ICHTHYOLOGICA ET PISCATORIA

New record of *Pterois* cf. *miles* (Actinopterygii: Scorpaeniformes: Scorpaenidae) from the eastern middle Adriatic Sea (Croatian waters): Northward expansion

Branko DRAGIČEVIĆ[1], Pero UGARKOVIĆ[2], Maja KRŽELJ[3], Damir ZURUB[4], Jakov DULČIĆ[1]

1 *Institute of Oceanography and Fisheries, Laboratory for Ichthyology and Coastal Fisheries, Split, Croatia*
2 *Velebitska 24, Split, Croatia*
3 *University Department of Marine Studies, University of Split, Split, Croatia*
4 *Vilima Korajca 23, Zagreb, Croatia*

http://zoobank.org/84EA2832-2CA8-4CF2-8E4C-D7D354DC70EC

Corresponding author: Branko Dragičević (brankod@izor.hr)

Academic editor: Paraskevi Karachle ♦ **Received** 27 September 2021 ♦ **Accepted** 29 October 2021 ♦ **Published** 29 November 2021

Citation: Dragičević B, Ugarković P, Krželj M, Zurub D, Dulčić J (2021) New record of *Pterois* cf. *miles* (Actinopterygii: Scorpaeniformes: Scorpaenidae) from the eastern middle Adriatic Sea (Croatian waters): Northward expansion. Acta Ichthyologica et Piscatoria 51(4): 379–383. https://doi.org/10.3897/aiep.51.75811

Abstract

A single specimen of *Pterois* cf. *miles* has been recorded in the eastern middle Adriatic Sea. It was observed near the island of Vis at a depth of 15 m. The location of the record is further north than previous Adriatic records and it constitutes the northernmost record of this species in the Mediterranean Sea to date. The record is based solely on photographs and video footage provided by a professional underwater photographer.

Keywords

invasion, Lessepsian migrant, lionfish, Mediterranean Sea, *Pterois miles*

Introduction

The devil firefish, *Pterois miles* (Bennett, 1828), commonly known as lionfish, is a fish species belonging to the family Scorpaenidae, native to the Indo-Pacific Ocean where it is distributed from the Red Sea to Sumatra. It is also present in the Mediterranean Sea which it most likely entered from the Red Sea through the Suez Canal (Bariche et al. 2017). The first record of this species in the Mediterranean dates back to 1991 when a single specimen was recorded from the Levantine coast (Golani and Sonin 1992). Subsequent records appeared after more than two decades when two specimens were collected in 2012 in Lebanon (Bariche et al. 2013). The first signs of an increase in the initially slow-paced expansion were documented in Cyprus when numerous specimens were recorded in the 2013–2015 period (Kletou et al. 2016). Substantial expansion both in abundance and space followed and *P. miles* spread to many coastal areas including Turkey and Greece in the north and Tunisia and Italy in the west (Turan and Öztürk 2015; Dailianis et al. 2016; Azzurro et al. 2017; Dimitriadis et al. 2020). Until 2019, the northernmost record of this species was indicated by Dimitriadis et al. (2020) near the Greek island of Corfu in the Ionian Sea. Subsequently, sightings of the lionfish were recorded in the Adriatic Sea near Lecce (Italy) and beach Dhermi (Albania) in July 2019 and in Torre Canne near Brindisi in August 2020 (Di Martino and Stancanelli 2021). Dynamics of the expansion in the eastern Mediterranean and invasive potential of *P. miles* led Karachle et al. (2017) to foresee its potential arrival in Albanian waters a few years prior to its first record in the area.

Figure 1. A specimen of *Pterois* cf. *miles* photographed at Rt Stupišće near Komiža (Vis Island, eastern middle Adriatic). Photo: D. Zurub.

The concerns associated with the occurrence of this species in the Mediterranean are mostly motivated by the western Atlantic scenario whereby a non-native lionfish (*Pterois miles*/*Pterois volitans* complex) severely impacted the biodiversity and ecological processes in invaded areas. For example, high predation rates of this generalist piscivore species negatively impact local fish communities by reducing their abundance and recruitment at invaded locations (Ballew et al. 2016; Goodbody-Gringley et al. 2019).

In this paper, we report the first observation of this species in the middle eastern Adriatic Sea, in Croatian waters.

Material and methods

A specimen of lionfish was observed and photographed (Fig. 1) by a professional underwater photographer during scuba diving on 13 August 2021 at a depth of 15 m, near Komiža at cape Stupišće (island Vis, Croatian waters, middle Adriatic; 43°0′18.25″N, 016°4′1.27″E) (Fig. 2). Diving was organized by the local diving center "Manta". Sea temperature at the site was measured at 24°C with Mares Genius diving computer.

Results and discussion

The length of the specimen was approx. 13–15 cm in total length. It was observed on the bottom consisting of large boulders overgrown with various algae including invasive *Caulerpa cylindracea* (Chlorophyta). The individual was slowly moving on the algal mat which allowed the photographer to take high-quality photos. Divers observed the fish at the same position on three consecutive days. Due to the nature of the record (photos and video), it was not possible to accurately count meristic characters which distinguish *P. miles* and *P. volitans*, so the species identification was tentatively assigned to *Pterois* cf. *miles*. Tentative identification was based on particular morphological traits of the specimen visible in provided photos such as distinctive coloration i.e., alternating brown and white vertical stripes throughout the body; large feather-like pectoral fins; conspicuously large dorsal fin spines and fleshy tentacles above the eyes and mouth; soft rays of dorsal, anal and caudal fins with dark spots (Golani and Sonin 1992; Bariche et al. 2013). If we consider the route of species spreading in the eastern Mediterranean, confidence in the species assignment is further strengthened as many of the records along the route were genetically confirmed as *P. miles* records (Bariche et al. 2017; Stern et al. 2018; Vavasis et al. 2020).

The area where the specimen was found is located on a protruding cape on a northwestern part of Vis island oriented toward the open sea and influenced by open sea currents (Fig. 2). The location itself is about 143 Nm farther than the closest previous Adriatic record reported from Italy (Torre Canne) by Di Martino and Stancanelli (2021). The present record also represents the northernmost record of this Lessepsian migrant both in the Adriatic Sea and the entire Mediterranean to date.

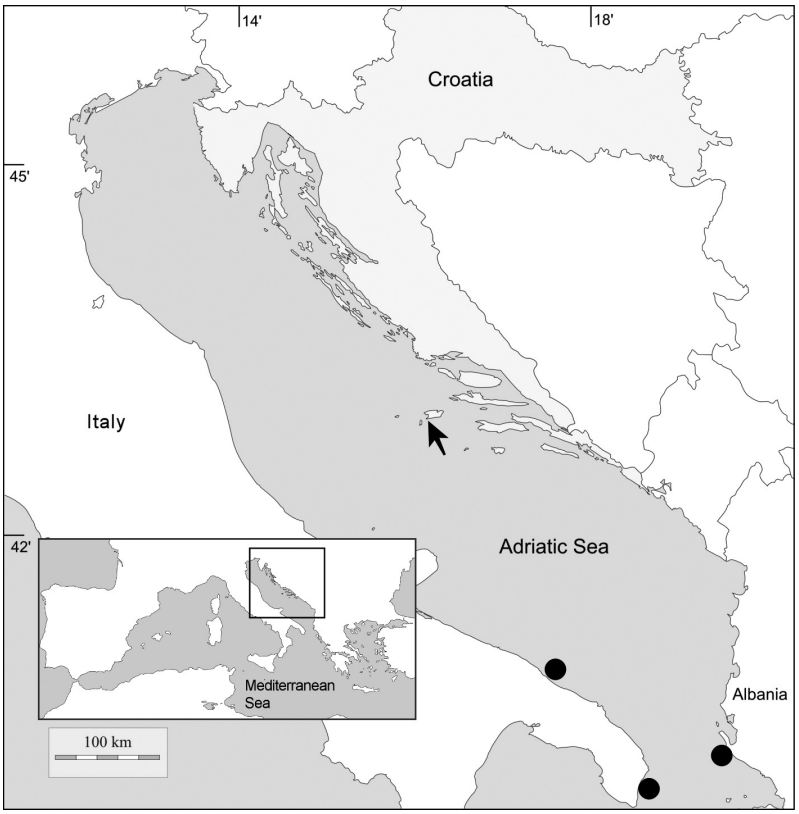

Figure 2. Map showing location of the present record (arrow) and previous Adriatic records (black circles; from Di Martino and Stancanelli 2021) of *Pterois miles*.

Predictions of the expansion of *P. miles* in the Mediterranean from various studies offer different future scenarios for the Adriatic Sea (D'Amen and Azzurro 2020; Dimitriadis et al. 2020; Poursanidis et al. 2020). Such differences mostly stem from diverse methodologies and parameters considered in driving the prediction models, but also due to differing time frames considered in predictions. Only the northernmost part of the Adriatic is consistently excluded as a distributional area in these predictions, while predictions for the middle and southern Adriatic vary. For example, the study by Dimitriadis et al. (2020) indicated a scenario with an increased risk of expansion towards the middle Adriatic until 2050. These authors considered the role of low winter temperatures as a limiting factor for the expansion and establishment of the species. On the other hand, for example, Poursanidis et al. (2020) considered the Adriatic to be an unfavorable area for the lionfish invasion based on habitat suitability modeling.

Kimball et al. (2004) experimentally determined that at a mean temperature of 16.1°C lionfish stop feeding while a mean 10°C was determined to be a chronic lethal temperature. At present, low winter temperatures in the middle Adriatic (Russo et al. 2012), which fall below the one at which lionfish cease to feed, can pose an obstacle for its successful invasion. However, it is suggested that lionfish can survive prolonged fasting which, in synergy with the possibility of climatic niche expansion and sea warming trends, can challenge this hypothesis (Parravicini et al. 2015; Côté and Smith 2018; Grbec et al. 2018). In any case, the present record clearly shows that the species reached the middle Adriatic, but its establishment and impact will need to be evaluated with future investigations.

As indicated by Azzurro et al. (2017) the majority of records of this species in the Mediterranean were made based on underwater footage provided by divers as is the case with the present record. Recently, Phillips and Kotrschal (2021) took advantage of this fact and, using diving centers' expertise, managed to detect additional lionfish sightings throughout the Mediterranean coast indicating the high potential of such methodology in the tracking of its expansion. Also, citizen science campaigns have been initiated throughout the Mediterranean to keep track of lionfish expansion (Azzurro et al. 2017; Giovos et al. 2019).

Due to the high negative impact of *P. miles* on native fish communities in invaded areas, campaigns aimed at population control of the species have been initiated in the eastern Mediterranean, particularly in Cyprus where such actions resulted in a significant decrease in lionfish numbers in areas targeted (Kleitou et al. 2021). Actions aimed at population control rather than eradication are more realistic in cases of marine invasions as instances of successful eradication are rare (Giakoumi et al. 2019). As early detection and rapid response in the first stages of invasion are considered crucial for successful mitigation and even eradication (see Campbell et al. 2018), we emphasize the need for immediate action in Croatia which should be coordinated among scientific institutions and relevant governmental bodies. For example, actions aimed at population control should be foreseen and

an appropriate legal and logistic basis for such actions should be established as soon as possible. Several citizen science campaigns have already been undertaken in Croatia in the last decade to heighten the general public's awareness about marine biological invasions (for example, in the course of LEKFishResCRO project founded by the Croatian Science Foundation) and to motivate citizens to indulge in monitoring efforts through reporting observations of unusual species. Also, the perils of the lionfish invasion, both in terms of its ecosystem impact and potential health hazard due to its venomousness, have already been conveyed to the general public through various news channels and social networks even before this record and similar efforts should be continued.

Acknowledgment

This work has been fully supported by the Croatian Science Foundation (HRZZ) under the project IP-2016-06-5251.

References

Azzurro E, Stancanelli B, Di Martino V, Bariche M (2017) Range expansion of the common lionfish *Pterois miles* (Bennett, 1828) in the Mediterranean Sea: An unwanted new guest for Italian waters. BioInvasions Records 6(2): 95–98. https://doi.org/10.3391/bir.2017.6.2.01

Ballew N, Bacheler N, Kellison G, Schueller A (2016) Invasive lionfish reduce native fish abundance on a regional scale. Scientific Reports 6(1): 32169. https://doi.org/10.1038/srep32169

Bariche M, Torres M, Azzurro E (2013) The presence of the invasive lionfish *Pterois miles* in the Mediterranean Sea. Mediterranean Marine Science 14(2): 292–294. https://doi.org/10.12681/mms.428

Bariche M, Kleitou P, Stefanos K, Bernardi G (2017) Genetics reveal the identity and origin of the lionfish invasion in the Mediterranean Sea. Scientific Reports 7(1): 6782. https://doi.org/10.1038/s41598-017-07326-1

Campbell ML, Leonard K, Primo C, Hewitt CL (2018) Marine biosecurity crisis decision-making: Two tools to aid "go"/"no go" decision-making. Frontiers in Marine Science 5: 331. https://doi.org/10.3389/fmars.2018.00331

Côté IM, Smith NS (2018) The lionfish *Pterois* sp. invasion: Has the worst-case scenario come to pass? Journal of Fish Biology 92(3): 660–689. https://doi.org/10.1111/jfb.13544

D'Amen M, Azzurro E (2020) Lessepsian fish invasion in Mediterranean marine protected areas: A risk assessment under climate change scenarios. ICES Journal of Marine Science 77(1): 388–397. https://doi.org/10.1093/icesjms/fsz207

Dailianis T, Akyol O, Babali N, Bariche M, Crocetta F, Gerovasileiou V, Ghanem R, Gökoğlu M, Hasiotis T, Izquierdo-Muñoz A, Julian D, Katsanevakis S, Lipej L, Mancini E, Mytilineou Ch (2016) New Mediterranean Biodiversity Records (July 2016). Mediterranean Marine Science 17(2): 608–626. https://doi.org/10.12681/mms.1734

Di Martino V, Stancanelli B (2021) The alien lionfish, *Pterois miles* (Bennett, 1828), enters the Adriatic Sea, Central Mediterranean Sea. Journal of the Black Sea/Mediterranean Environment 27(1): 104–108.

Dimitriadis C, Galanidi M, Zenetos A, Corsini-Foka M, Giovos I, Karachle P, Fournari - Konstantinidoy I, Kytinou E, Issaris Y, Azzurro E, Castriota L, Falautano M, Kalimeris A, Katsanevakis S (2020) Updating the occurrences of *Pterois miles* in the Mediterranean Sea, with considerations on thermal boundaries and future range expansion. Mediterranean Marine Science 21(1): 62–69. https://doi.org/10.12681/mms.21845

Giakoumi S, Katsanevakis S, Albano P, Azzurro E, De Jesus Cardoso A, Cebrian E, Deidun A, Edelist D, Francour P, Jimenez C, Macic V, Occhipinti-Ambrogi A, Rilov G, Sghaier Y (2019) Management priorities for marine invasive species. Science of the Total Environment 688: 976–982. https://doi.org/10.1016/j.scitotenv.2019.06.282

Giovos I, Kleitou P, Poursanidis D, Batjakas I, Bernardi G, Crocetta F, Doumpas N, Kalogirou S, Kampouris T, Keramidas I, Langeneck J, Maximiadi M, Mitsou E, Stoilas VO, Tiralongo F, Romanidis-Kyriakidis G, Xentidis NJ, Zenetos A, Katsanevakis S (2019) Citizen-science for monitoring marine invasions and stimulating public engagement—A case project from the eastern Mediterranean. Biological Invasions 21(12): 3707–3721. https://doi.org/10.1007/s10530-019-02083-w

Golani D, Sonin O (1992) New records of the Red Sea fishes, *Pterois miles* (Scorpaenidae) and *Pteragogus pelycus* (Labridae) from the eastern Mediterranean Sea. Japanese Journal of Ichthyology 39(2): 167–169. https://doi.org/10.1007/BF02906001

Goodbody-Gringley G, Eddy C, Pitt JM, Chequer AD, Smith SR (2019) Ecological drivers of invasive lionfish (*Pterois volitans* and *Pterois miles*) distribution across mesophotic reefs in Bermuda. Frontiers in Marine Science 6: 258. https://doi.org/10.3389/fmars.2019.00258

Grbec B, Matić F, Beg Paklar G, Morović M, Popović R, Vilibić I (2018) Long-term trends, variability and extremes of in situ sea surface temperature measured along the eastern Adriatic coast and its relationship to hemispheric processes. Pure and Applied Geophysics 175(11): 4031–4046. https://doi.org/10.1007/s00024-018-1793-1

Karachle PK, Corsini Foka M, Crocetta F, Dulčić J, Dzhembekova N, Galanidi M, Ivanova P, Shenkar N, Skolka M, Stefanova E, Stefanova K, Surugiu V, Uysal I, Verlaque M, Zenetos A (2017) Setting-up a billboard of marine invasive species in the ESENIAS area: Current situation and future expectancies. Acta Adriatica 58(3): 429–458. https://doi.org/10.32582/aa.58.3.4

Kimball M, Miller J, Whitfield P, Hare J (2004) Thermal tolerance and potential distribution of invasive lionfish (*Pterois volitans/miles* complex) on the east coast of the United States. Marine Ecology Progress Series 283: 269–278. https://doi.org/10.3354/meps283269

Kleitou P, Rees S, Cecconi F, Kletou D, Savva I, Cai LL, Hall-Spencer JM (2021) Regular monitoring and targeted removals can control lionfish in Mediterranean Marine Protected Areas. Aquatic Conservation: Marine and Freshwater Ecosystems 1–13. https://doi.org/10.1002/aqc.3669

Kletou D, Hall-Spencer J, Kleitou P (2016) A lionfish (*Pterois miles*) invasion has begun in the Mediterranean Sea. Marine Biodiversity Records 9: e46(2016). https://doi.org/10.1186/s41200-016-0065-y

Parravicini V, Azzurro E, Kulbicki M, Belmaker J (2015) Niche shift can impair the ability to predict invasion risk in the marine realm:

An illustration using Mediterranean fish invaders. Ecology Letters 18(3): 246–253. https://doi.org/10.1111/ele.12401

Phillips E, Kotrschal A (2021) Where are they now? Tracking the Mediterranean lionfish invasion via local dive centers. Journal of Environmental Management 298: 113354. https://doi.org/10.1016/j.jenvman.2021.113354

Poursanidis D, Kalogirou S, Azzurro E, Parravicini V, Bariche M, Dohna H (2020) Habitat suitability, niche unfilling and the potential spread of *Pterois miles* in the Mediterranean Sea. Marine Pollution Bulletin 154: 111054. https://doi.org/10.1016/j.marpolbul.2020.111054

Russo A, Carniel S, Sclavo M, Krželj M (2012) Climatology of the northern-central Adriatic Sea. Pp. 177–212. In: Wang S-Y, Gillies R (Eds) Modern climatology. InTech, London, UK. https://doi.org/10.5772/34693

Stern N, Jimenez C, Huseyinoglu MF, Andreou V, Hadjioannou L, Petrou A, Öztürk B, Golani D, Rothman SBS (2018) Constructing the genetic population demography of the invasive lionfish *Pterois miles* in the Levant Basin, Eastern Mediterranean. Mitochondrial DNA. Part A, DNA Mapping, Sequencing, and Analysis 30(29): 1–7. https://doi.org/10.1080/24701394.2018.1482284

Turan C, Öztürk B (2015) First record of the lionfish *Pterois miles* from the Aegean Sea. Journal of the Black Sea/Mediterranean Environment 21: 334–338.

Vavasis C, Simotas G, Spinos E, Konstantinidis E, Minoudi S, Triantifyllidis A, Perdikaris C (2020) Occurrence of *Pterois miles* in the Island of Kefalonia (Greece): The northernmost dispersal record in the Mediterranean Sea. Thalassas: An international Journal of Marine Science 36: 171–175. https://doi.org/10.1007/s41208-019-00175-x

Acta Ichthyologica et Piscatoria 51(4), 2021, 385–391 | DOI 10.3897/aiep.51.72676

PENSOFT

ACTA ICHTHYOLOGICA ET PISCATORIA

First record of exotic alligator gar, *Atractosteus spatula* (Actinopterygii: Lepisosteiformes: Lepisosteidae), from Ganga River system, India: A possible threat to indigenous riverine fish diversity

Ranjan Kumar MANNA[1], Archisman RAY[1], Supriti BAYEN[1], Tanushree BERA[1], Debashis PALUI[2], Basanta Kumar DAS[1]

1 *Central Inland Fisheries Research Institute (ICAR), Barrackpore, Kolkata, West Bengal, India*

2 *Directorate of Fisheries, Government of West Bengal, Kolkata, West Bengal, India*

http://zoobank.org/DD6EE48F-C7BF-4F98-B9ED-B060375CFED6

Corresponding author: Basanta Kumar Das (basantakumard@gmail.com)

Academic editor: Predrag Simonović ♦ **Received** 6 August 2021 ♦ **Accepted** 8 October 2021 ♦ **Published** 29 November 2021

Citation: Manna RK, Ray A, Bayen S, Bera T, Palui D, Das BK (2021) First record of exotic alligator gar, *Atractosteus spatula* (Actinopterygii: Lepisosteiformes: Lepisosteidae), from Ganga River system, India: A possible threat to indigenous riverine fish diversity. Acta Ichthyologica et Piscatoria 51(4): 385–391. https://doi.org/10.3897/aiep.51.72676

Abstract

A new record of an exotic alligator gar, *Atractosteus spatula* (Lacepède, 1803), from an open wetland of the Ganga River was presented in this paper and discussed along with the environmental parameters. Entry of the exotic fish into the natural system was probably a result of uncontrolled ornamental fish trading. Considering threats of this predatory fish to become invasive and disturb riverine fish diversity, possible ways to avoid such risk have been discussed.

Keywords

alligator gar, exotic fish, Ganga River, wetland

Introduction

Large rivers basins harbor a significant share of the world's aquatic biodiversity, providing important goods and services to the society, including fisheries. Ganga basin is the largest and most important river basin in India. The wetlands of the Ganga basin are mostly formed as a result of the meandering of the river or sloughs or tectonic depressions receiving huge surface runoff or freshwater from the river. The connection of the wetland to the river promotes aquatic biodiversity, especially a higher abundance of small indigenous fishes (Manna et al. 2018). However, the intrusion of exotic fishes into associated wetland exerts invariable threats upon native riverine fish biodiversity (Singh and Lakra 2006). The Ganga basin, which supports a wealthy fish diversity of more than 266 fish species (Talwar and Jhingran 1991), has already been invaded by more than 10 species of exotic fishes in almost its entire freshwater stretch (Sarkar et al. 2012) resulting in considerable damage to riverine fish diversity. The entry of exotics into the riverine system has been presumed mainly to have come about due to illegal or unwanted introduction from aquaculture practices or by other anthropogenic activities, including extreme climatic events like floods, etc. (Raj et al. 2021). Besides exotic carps, which have been legally brought for aquaculture enhancement in India, the Ganga River has experienced in recent years the appearance of a few exotic aquarium species like *Gambusia affinis* (Baird et Girard, 1853), *Pterygoplichthys pardalis* (Castelnau, 1855), and

Pterygoplichthys disjunctivus (Weber, 1991) (see Singh et al. 2013; Das et al. 2020). However, the occurrence of exotic alligator gar, *Atractosteus spatula* (Lacepède, 1803) has not been documented from the main channel or any of the water bodies associated with the largest river of the country. *Atractosteus spatula*, representing the family: Lepisosteidae, is a native to North America primarily from the Mississippi River basin (Raz-Guzmán et al. 2018). Alligator gar has been established worldwide as an outcome of the ornamental fish trade (Salnikov 2010). This highly predatory species has been reported recently from several water bodies of different Indian states like Assam (Anonymous 2020), West Bengal (Thakur 2016), Odisha (Anonymous 2017a), Andhra Pradesh (Vadlamudi 2021), Kerala (Kumar et al. 2019), and Maharashtra (Ghai 2018, Patil et al. 2019) displaying its probable congenial interaction with the varied environmental habitats (Fig. 1). The present paper documents the first record of the alligator gar from an open wetland connected to the Ganga River in West Bengal, India, along with a description of the aquatic environment.

Material and methods

A single specimen of *Atractosteus spatula* was captured from Chharaganga Beel (wetland) (23°27′48.87″N, 88°20′46.7592″E), Nabadwip, West Bengal using a gillnet (mesh 10–15 cm) on 23 July 2020 during the early morning hours of fishing activity. The fish was identified in line with the methodology of Bigelow et al. (1963).

Figure 1. Water bodies of India from where alligator gar, *Atractosteus spatula*, has recently been reported. The newly reported site is Chharaganga Beel.

The associated hydrological parameters were determined as a part of the assessment of the associated wetland of the Ganga River following standard methods (Baird and Bridgewater 2017).

Ethical statement. During the study, no harm was made to alligator gar which has been described in this paper. After the study, the fish was released in live condition into secured captivity so that it could not reach natural open water.

Results

The fish collected from Chharaganga wetland was identified as *Atractosteus spatula*, it weighed 2.25 kg, and was characterized by a long and cylindrical body (Figs 2–3). It had an elongated snout and rounded caudal fin. Both the dorsal and anal fins consisted of 7 rays respectively and were positioned close to the tail with the former slightly posterior to the latter. Body scales were hard, non-overlapping, and diamond in shape. Head and snout were devoid of scales. It could be easily distinguished by two rows of sharp series of teeth on the upper jaw. However, the second row of teeth was positioned within the mouth, which was different from the externally visible teeth. The pectoral fin ray count was 14 and the fin was situated in close proximity to the gill opening. The dorsal surface of the body was dark olivaceous while the lower abdominal portion of the body was characterized by whitish shades.

Discussion

Although the information on its habitat usage is scanty, *Atractosteus spatula* was reported to dwell in both freshwater and marine water habitats (Goodyear 1967). Reports from Indonesia (Hasan et al. 2020) and Texas (Buckmeier 2008) have provided evidence towards its wide tolerance of salinity gradients which has created an additional advantage for its survival, growth, and possible establishment. The presently described site of fish capture is freshwater in nature; however, since it is located at the head of Hooghly estuary, the lowermost stretch of the main channel of the river experiences minor tidal variations. The mean annual temperature [ºC] of the wetland is 27.87 ± 3.16 (Table 1) which is slightly higher than the temperature (24–26ºC) recorded from Vincente Guerrero Reservoir, Mexico (Garcia de Leon et al. 2001). Additional water quality parameters of the wetland, specifically its salinity (0.0167‰–0.079‰), and depth (mean 4.32 m) are at par with the values obtained from the water body of the USA (Boschung and Mayden 2004) indicating a somewhat agreeable environmental condition required for its survival, spawning, and maturation. Having a connection to the wetland, there remains a high chance of its entry into the river. However, the river water possesses a slightly different water quality status (Table 1). Significant differences in parameters like wa-

Figure 2. Alligator gar, *Atractosteus spatula*, recorded from Chharaganga Beel, Nabadwip, West Bengal (dorsal view).

Figure 3. Alligator gar, *Atractosteus spatula*, recorded from Chharaganga Beel, Nabadwip, West Bengal (anteroventral view showing the teeth).

ter turbidity and sediment soil organic carbon might be attributed to the dense growth of aquatic macrophytes, especially floating water hyacinth and different varieties of submerged macrophytes in the wetland (Table 2). Still, there is a high chance of the species establishing in the river as it is basically a riverine species of the Mississippi River system.

The alligator gar has been presumed to have been released by some aquarium hobbyists deliberately into the wetland which is a routine method to get rid of the pet when it attained a size large exciding the capacity of an indoor aquarium. Other than willful release by the hobbyist, extreme climatic events have often been identified for entry of the exotic fishes into Indian inland open waters (Raj et al. 2021) as a route of entry of alien fishes into the natural ecosystem. In the absence of any such climatic event in the studied area in the recent past, its entry through the aquarium trade may be considered. Aquarium trading has now created a miserable approach towards the non-native introduction of fishes (Krishnakumar et al. 2009) with more than 5000 species traded globally, which in turn has linked more than 200 countries of rapidly growing ornamental industry, associated with the second most popular hobby with about 100 million hobbyists in the world (Chan et al. 2020). Alligator gar has been illegally introduced into the Indian fishery system as it is not highlighted in the list of 92 different aquarium fish species considered for import (Kumar et al. 2019). The encroachment and establishment of several other exotic species, which thereby impact the local fishes, are reported from almost the entire riverine system in India (Knight 2010; Sandilyan 2016). As a consequence of ornamental fish trading, vermiculated sailfin catfish, *Pterygoplichthys disjunctivus*, has been recorded from various river systems of the country like the Ganga or Cauvery (Panikkar et al. 2015; Das et al. 2020). Suresh

Table 1. Water parameters of Chharaganga Beel adjacent to the Ganga River (at Nabadwip).

Parameter	Chharaganga Beel		Ganga River (Nabadwip)	
	Range	Mean ± SD	Range	Mean ± SD
Temperature [°C]	22.7–32.6	27.87 ± 3.16	18.2–33.7	27.69 ± 6.32
pH	6.8–9.2	7.97 ± 0.55	7.4–8.7	8.18 ± 0.44
Dissolved O_2 [ppm]	1.0–10.5	5.27 ± 2.15	5.4–9.5	7.01 ± 1.43
Turbidity (NTU)	0.03–56.20	4.19 ± 8.15	15.48–237.00	94.52 ± 76.16
Conductivity [$\mu S \cdot cm^{-1}$]	172–570	276.42 ± 64.56	177–338	249 ± 62.41
Alkalinity [ppm]	78–188	129.43 ± 22.09	67–134	99.91 ± 25.83
Hardness [ppm]	80–150	113.62 ± 19.15	60–140	91.5 ±28.81
Ca^{2+} [ppm]	12.65–44.08	26.30 ± 6.79	14.43–36.87	27.33 ± 7.32
Mg^{2+} [ppm]	4.70–28.56	13.42 ± 6.35	1.88–16.44	6.55 ± 4.79
Nitrate-N [ppm]	0.012–0.200	0.072 ± 0.05	0.120–0.512	0.304 ± 0.120
Total N [ppm]	0.074–2.297	0.616 ± 0.44	0.376–0.700	0.495 ± 0.110
Phosphate-P [ppm]	0.004–0.827	0.087 ± 0.17	0.026–0.070	0.043 ± 0.020
Silicate-Si [ppm]	1.6–24.2	6.028 ± 4.280	0.4–10.2	7.10 ± 3.47

SD = standard deviation.

Table 2. Soil parameters of Chharaganga Beel adjacent to the Ganga River (at Nabadwip).

Parameter	Chharaganga Beel		Ganga River (Nabadwip)	
	Range	Mean ± SD	Range	Mean ± SD
pH	7.01–8.24	7.68 ± 0.30	7.60–8.70	8.27 ± 0.39
Specific conductivity [$mS \cdot cm^{-1}$]	0.218–2.08	0.924 ± 0.470	0.058–0.274	0.192 ± 94.770
Organic C [%]	0.10–2.00	0.74 ± 0.51	0.09–0.54	0.34 ± 0.15
Total N [%]	0.01–0.30	0.10 ± 0.07	0.02–0.07	0.04 ± 0.02
Available N [$mg \cdot 100\ g^{-1}$ soil]	8.40–26.30	15.26 ± 3.53	2.80–7.84	5.79 ± 2.65
Available P [$mg \cdot 100\ g^{-1}$ soil]	0.13–0.54	0.31 ± 0.09	0.92–3.48	2.22 ± 1.35

SD = standard deviation.

et al. (2019) have even documented the species from an ecologically important East Kolkata Wetland (a Ramsar site) with an estimated annual production of 300 t. Kumar et al. (2020) has recently reported increasing availability of another ornamental three-spot cichlid, *Cichlasoma trimaculatum* (Günther, 1867), in the Cauvery River. The *C. trimaculatum* was ranked as posing a "high" risk of being invasive in the river as determined using the Aquatic Species Invasiveness Screening Kit. The alligator gar, *Atractosteus spatula*, though being recorded regularly beyond its native area, has not yet been recognized as a potential threat as it was not included in the list of 259 non-native freshwater fish species for which risk assessment has been conducted so far using Aquatic Species Invasiveness Screening Kit (Vilizzi et al. 2021). However, considering its possible potential biodiversity risks, an assessment of the species within the United States beyond its native range was attempted (Anonymous 2017b).

West Bengal occupies a major position in the ornamental fish trade with 55% of total production in India. Gupta (2012) has recorded the availability of 139 species of exotic fishes in the ornamental fish market (widely known as Galiff Street) of Kolkata. However, the presence of alligator gar in the market remained unmentioned. The presently reported survey noted that the trading of live alligator gar is performed extensively year-round in the ornamental fish market of the city. Each specimen is marketed at 700.00 Indian Rupee (=8 Euro) at a size range of 15–17 cm. Due to the aggressive nature of their behavior, alligator gar are marketed and maintained individually. Besides, as a part of the supply chain marketing system, this exotic fish is also transported to various local aquarium traders within the state. Exotic fishes with recreational and commercial purposes have now become potential threats to natural aquatic bodies. Many such fishes have already invaded rivers, reservoirs, wetlands, etc. and established themselves alongside the declined catch of other indigenous fish species. The invasion of *Clarias gariepinus* (Burchell, 1822), a highly carnivorous catfish in the Ganga River is one such example (Singh et al. 2013). Large-scale anthropogenic modification of the riverine habitat through water obstruction, pollution, etc. has provided a favorable habitat, allowing a competitive advantage for exotic varieties over native ones (Daga et al. 2016). The Ganga River has also observed an increasing number of barricades over the years, especially in the upper reaches of the river. The availability of the adult alligator gar in an open wetland certainly creates chances for ecological imbalance in the wetland as well as in the connected river by displacing the native fish species spectrum. As little is known about its population dynamics and breeding phenology, data regarding its juvenile availability in the local markets requires more attention. A strategy for developing legal ornamental fish trading is urgently needed. A detailed database on habitat preference, breeding habits, and other biological aspects must be developed before each individual fish being targeted is introduced into the ornamental sector.

Studying fish invasions in more than 1000 river basins on a global scale, Leprieur et al. (2008) opined that

more exotic invasions may occur in river basins of developing countries, including India. India is eighth in the world and third in Asia with 788 freshwater fish species where more than one-fourth is either vulnerable or in the endangered category (Kottelat and Whitten 1996, Gopi and Mishra 2015). With an increasing number of dams and barrages, exotic invasion can certainly aggravate the situation by causing a decline of precious fish diversity. The best approach to prevent non-native species is to identify the possible entry points rather than eradication methods. The list of fish species presently being imported into India should be critically revised based on their possibility of establishment and invasiveness, or if they reached natural water by chance. Alligator gar is yet to be included in the list of 14 freshwater invasive fish species compiled by Centre for Biodiversity Policy and Law (CEBPOL), National Biodiversity Authority (NBA) as updated in 2018. A priority list should be prepared including those exotic fishes which have the possibility to become invasive in the future. Existing laws like 'The Biological Diversity Act, 2002' also clearly mentioned about not importing any such fish species into India. The National Biodiversity Strategy and Action Plan has many important suggestions for the control and management of such detrimental invasive species (MOEFCC 2014). Strict monitoring and implementation/enforcement of the law are required but this necessitates national/institutional level monitoring. Awareness among local communities about the detrimental effect of identified invasive species can help to reduce their inclusion for species enhancement in aquaculture or as an ornamental fish to be reared as a pet.

Acknowledgments

We wish to thank the National Mission for Clean Ganga (NMCG), Ministry of Jal Shakti, Government of India for their funding support under Project No. T-17/2014 15/526/NMCG- Fish and Fisheries. Thanks to Ms. Manisha Bhor for the preparation of the fish distribution map given in the paper.

References

Anonymous (2017a) Exotic alligator gar fish rescued from Bindusagar in Odisha capital. Sambad English Bureau 23.06.2017. https://sambadenglish.com/exotic-alligator-gar-fish-rescued-from-bindusagar-in-odisha-capital/

Anonymous (2017b) Alligator gar (*Atractosteus spatula*) Ecological Risk Screening Summary US Fish and Wildlife Service, August 2017 Web Version, 11/29/2017, 14 pp. https://www.fws.gov/fisheries/ans/erss/uncertainrisk/ERSS-Atractosteus-spatula-Nov-2017-FINAL.pdf

Anonymous (2020) Rare North American fish species found in Mangaldai District. The Sentinel 20th May, 2020. https://www.sentinelassam.com/north-east-india-news/assam-news/rare-north-american-fish-species-found-in-mangaldai-district-477741

Baird R, Bridgewater L (2017) Standard methods for the examination of water and wastewater, 23rd ed. American Public Health Association.

Bigelow HB, Bradbury MG, Dymond JR, Greeley JR, Hildebrand SF, Mead GW, Miller RR, Rivas RL, Schroeder WL, Suttkus RD, Vladykov VD (1963) Fishes of the western North Atlantic. Part three. Memoir one. Soft-rayed bony fishes: Orders Acipenseroidei, Lepisostei, and Isospondyli: Sturgeons, gars, tarpons, ladyfish, bonefish, salmon, charrs, anchovies, herring, sheds, smelt, capelin, et al. Sears Foundation for Marine Research. Yale University Press, New Haven, CT, USA.

Boschung HT, Mayden RL (2004) Fishes of Alabama. Smithsonian Institution Press, Washington DC, USA.

Buckmeier DL (2008) Life history and status of alligator gar *Atractosteus spatula*, with recommendations for management. TPWD Inland Fisheries Report, Heart of the Hills Fisheries Science Center, TX, USA, 13 pp.

Chan FT, Beatty SJ, Gilles Jr ASJ, Hill JE, Kozic S, Luo D, Morgan DL, Pavia RTBJ Jr, Therriault TW, Verreycken H, Vilizzi L, Wei H, Yeo DCJ, Zeng Y, Zięba G, Copp GH (2020) Leaving the fishbowl: The ornamental trade as a global vector for freshwater fish invasions. Aquatic Ecosystem Health and Management 22(4): 417–439. https://doi.org/10.1080/14634988.2019.1685849

Daga VS, Debona T, Abilhoa V, Gubiani ÉA, Vitule JRS (2016) Non-native fish invasions of a Neotropical ecoregion with high endemism: A review of the Iguaçu River. Aquatic Invasions 11(2): 209–223. https://doi.org/10.3391/ai.2016.11.2.10

Das BK, Ray A, Manna RK, Roshith CM, Baitha R, Karna SK, Gupta SD, Bhor M (2020) Occurrence of exotic vermiculated sailfin catfish *Pterygoplichthys disjunctivus* from the lower stretch of River Ganga, West Bengal, India. Current Science 119(12): 2006–2009. https://doi.org/10.18520/cs/v119/i12/2006-2009

Garcia de Leon FJ, Gonzalez-Garcia L, Herrera-Castillo JM, Winemiller KO, Banda-Valdes A (2001) Ecology of the alligator gar, *Atractosteus spatula*, in the Vicente Guerrero Reservoir, Tamaulipas, Mexico. Southwestern Naturalist 46(2): 151–157. https://doi.org/10.2307/3672523

Ghai R (2018) Alligator gar discovery a signal to revise list of fish introduced to India. Down to Earth, New Delhi, India. https://www.downtoearth.org.in/news/wildlife-biodiversity/-alligator-gar-discovery-a-signal-to-revise-list-of-fish-introduced-to-india--62386

Goodyear CP (1967) Feeding habits of three species of gars, *Lepisosteus*, along the Mississippi gulf coast. Transactions of the American Fisheries Society 96(3): 297–300. https://doi.org/10.1577/1548-8659(1967)96[297:FHOTSO]2.0.CO;2

Gopi KC, Mishra SS (2015) Diversity of marine fish of India. Pp. 171–193. In: Venkataraman K, Sivaperuman C (Eds) Marine faunal diversity in India. Taxonomy, ecology and conservation. Elsevier, Amsterdam, the Netherlands.

Gupta S (2012) Present status of Galiff Street Market, the wholesale ornamental fish market of Kolkata. Fishing Chimes 32(5): 34–42.

Hasan V, Widodo MS, Islamy RA, Pebriani DA (2020) New records of alligator gar, *Atractosteus spatula* (Actinopterygii: Lepisosteiformes: Lepisosteidae) from Bali and Java, Indonesia. Acta Ichthyologica et Piscatoria 50(2): 233–236. https://doi.org/10.3750/AIEP/02954

Knight JDM (2010) Invasive ornamental fish: A potential threat to aquatic biodiversity in peninsular India. Journal of Threatened Taxa 2(2): 700–704. https://doi.org/10.11609/JoTT.o2179.700-4

Kottelat M, Whitten T (1996) Freshwater biodiversity in Asia with special reference to fish. World Bank Technical Paper No. 343, Washington, DC, USA, 59 pp. http://dx.doi.org/10.1596/0-8213-3808-0

Krishnakumar K, Raghavan R, Prasad G, Bijukumar A, Sekharan M, Pereira B, Ali A (2009) When pets become pests—Exotic aquarium fishes and biological invasions in Kerala, India. Current Science 97: 474–476.

Kumar AB, Raj S, Arjun CP, Katwate U, Raghavan R (2019) Jurassic invaders: Flood-associated occurrence of arapaima and alligator gar in the rivers of Kerala. Current Science 116: 1628–1630.

Kumar L, Kumari K, Gogoi P, Manna RK, Roshith CM (2020) Risk analysis of non-native three-spot cichlid, *Amphilophus trimaculatus* in the River Cauvery (India). Fisheries Management and Ecology 28(2): 158–166. https://doi.org/10.1111/fme.12467

Leprieur F, Beauchard O, Blanchet S, Oberdorff T, Brosse S (2008) Fish invasions in the world's river systems: When natural processes are blurred by human activities. PLoS Biology 6(2; e28): 0404–0410. https://doi.org/10.1371/journal.pbio.0060028

Manna RK, Aftabuddin Md, Suresh VR, Sharma AP (2018) Major factors influencing fish species spectrum in floodplain wetlands of Assam. Pp. 157–170. In: Mahapatra BK, Roy AK, Pramanick NC (Eds) Sustainable management of aquatic resources. Narendra Publishing House, Delhi, India.

MOEFCC (2014) National Biodiversity Action Plan (NBAP): Addendum 2014 to NBAP 2008, Ministry of Environment, Forest and Climate Change, Government of India, 75 pp. https://www. cbd.int/doc/world/in/in-nbsap-v3-en.pdf

Panikkar P, Jagadeesh TD, Krishna Rao DS, Sarkar UK, Naskar M (2015) First record of non-native loricariid catfish, *Pterygoplichthys disjunctivus* (Weber, 1991), (Siluriformes, Loricariidae) in Cauvery River of peninsular India. Bioscan 10(4): 1659–1663.

Patil TS, Yadav RB, Patil RJ, Muley DV (2019) On a record of exotic fish species *Atractosteus spatula* (Lepisosteiformes: Lepisosteidae) from the freshwater well of Kolhapur, Maharashtra, India. International Journal of Research and Analytical Reviews, Special issue: 566–568.

Raj S, Kumar AB, Tharian J, Raghavan R (2021) Illegal and unmanaged aquaculture, unregulated fisheries and extreme climatic events combine to trigger invasions in a global biodiversity hotspot. Biological Invasions 23(8): 2373–2380. https://doi.org/10.1007/s10530-021-02525-4

Raz-Guzmán A, Huidobro L, Padilla V (2018) An updated checklist and characterisation of the ichthyofauna (Elasmobranchii and Actinopterygii) of the Laguna de Tamiahua, Veracruz, Mexico. Acta Ichthyologica et Piscatoria 48(4): 341–362. https://doi.org/10.3750/AIEP/02451

Salnikov VB (2010) First finding of gar *Atractosteus* sp. (Actinopterygii, Lepisosteiformes, Lepisosteidae) in the Caspian Sea near the coast of Turkmenistan. Russian Journal of Biological Invasions 1(1): 17–20. https://doi.org/10.1134/S2075111710010042

Sandilyan S (2016) Occurrence of ornamental fishes: A looming danger for Inland fish diversity of India. Current Science 110(11): 2099–2104. https://doi.org/10.18520/cs/v110/i11/2099-2104

Sarkar UK, Pathak AK, Sinha RK, Sivakumar K, Pandian AK, Pandey A, Lakra WS (2012) Freshwater fish biodiversity in the River Ganga (India): Changing pattern, threats and conservation perspectives. Reviews in Fish Biology and Fisheries 22(1): 251–272. https://doi.org/10.1007/s11160-011-9218-6

Singh AK, Lakra WS (2006) Alien fish species in India: Impact and emerging scenario. Journal of Ecophysiology and Occupational Health 6: 165–174.

Singh AK, Kumar D, Srivastava SC, Ansari A, Jena JK, Sarkar UK (2013) Invasion and impacts of alien fish species in the Ganga River, India. Aquatic Ecosystem Health and Management 16(4): 408–414. https://doi.org/10.1080/14634988.2013.857974

Suresh VR, Ekka A, Biswas DK, Sahu SK, Yousuf A, Das S (2019) Vermiculated sailfin catfish, *Pterygoplichthys disjunctivus* (Actinopterygii Siluriformes: Loricariidae): Invasion, biology, and initial impacts in east Kolkata Wetlands, India. Acta Ichthyologica et Piscatoria 49(3): 221–233. https://doi.org/10.3750/AIEP/02551

Talwar PK, Jhingran AG (1991) Inland fishes of India and adjacent countries. Vol. 1 and Vol. 2, Oxford and IBH Publishing, New Delhi, Bombay and Calcutta, India.

Thakur J (2016) Discovery of predator fish that resembles an alligator concerns experts. Hindustan Times, 22nd June, https://www.hindustantimes.com/kolkata/kolkata-discovery-of-predator-fish-that-resembles-an-alligator-concernsexperts/story.html

Vadlamudi S (2021) Exotic aquarium fish species threatening lake biodiversity. The Hindu 22nd March, 2021. https://www.thehindu.com

Vilizzi L, Copp GH, Hill JE, Adamovich B, Aislabie L, Akin D, Al-Faisal AJ, Almeida D, Azmai MNA, Bakiu R, Bellati A, Bernier R, Bies JM, Bilge G, Branco P, Bui TD, Canning-Clode J, Cardoso Ramos HA, Castellanos-Galindo GA, Castro N, Chaichana R, Chainho P, Chan J, Cunico AM, Curd A, Dangchana P, Dashinov D, Davison PI, de Camargo MP, Dodd JA, Durland Donahou AL, Edsman L, Ekmekçi FG, Elphinstone-Davis J, Erős T, Evangelista C, Fenwick G, Ferincz Á, Ferreira T, Feunteun E, Filiz H, Forneck SC, Gajduchenko HS, Gama Monteiro J, Gestoso I, Giannetto D, Gilles AS Jr, Gizzi F, Glamuzina B, Glamuzina L, Goldsmit J, Gollasch S, Goulletquer P, Grabowska J, Harmer R, Haubrock PJ, He D, Hean JW, Herczeg G, Howland KL, İlhan A, Interesova E, Jakubčinová K, Jelmert A, Johnsen SI, Kakareko T, Kanongdate K, Killi N, Kim J-E, Kırankaya ŞG, Kňazovická D, Kopecký O, Kostov V, Koutsikos N, Kozic S, Kuljanishvili T, Kumar B, Kumar L, Kurita Y, Kurtul I, Lazzaro L, Lee L, Lehtiniemi M, Leonardi G, Leuven RSEW, Li S, Lipinskaya T, Liu F, Lloyd L, Lorenzoni M, Luna SA, Lyons TJ, Magellan K, Malmstrøm M, Marchini A, Marr SM, Masson G, Masson L, McKenzie CH, Mememdemin D, Mendoza R, Minchin D, Miossec L, Moghaddas SD, Moshobane MC, Mumladze L, Naddafi R, Najafi-Majd E, Năstase A, Năvodaru I, Neal JW, Nienhuis S, Nimtim M, Nolan ET, Occhipinti-Ambrogi A, Ojaveer H, Olenin S, Olsson K, Onikura N, O'Shaughnessy K, Paganelli D, Parretti P, Patoka J, Pavia RTB Jr, Pellitteri-Rosa D, Pelletier-Rousseau M, Peralta EM, Perdikaris C, Pietraszewski D, Piria M, Pitois S, Pompei L, Poulet N, Preda C, Puntila-Dodd R, Qashqaei AT, Radočaj T, Rahmani H, Raj S, Reeves D, Ristovska M, Rizevsky V, Robertson DR, Robertson P, Ruykys L, Saba AO, Santos JM, Sarı HM, Segurado P, Semenchenko V, Senanan W, Simard N, Simonović P, Skóra ME, Slovák

Švolíková K, Smeti E, Šmídová T, Špelić I, Srėbalienė G, Stasolla G, Stebbing P, Ševove B, Suresh VR, Szajbert B, Ta KAT, Tarkan AS, Tempesti J, Therriault TW, Tidbury HJ, Top-Karakuş N, Tricarico E, Troca DFA, Tsiamis K, Tuckett QM, Tutman P, Uyan U, Uzunova E, Vardakas L, Velle G, Verreycken H, Vintsek L, Wei H, Weiperth A, Weyl OLF, Winter ER, Włodarczyk R, Wood LE, Yang R, Yapıcı S, Yeo SSB, Yoğurtçuoğlu B, Yunnie ALE, Zhu Y, Zięba G, Žitňanová K, Clarke S (2021) A global-scale screening of non-native aquatic organisms to identify potentially invasive species under current and future climate conditions. Science of the Total Environment 788: 147868. https://doi.org/10.1016/j.scitotenv.2021.147868

Acta Ichthyologica et Piscatoria 51(4), 2021, 393–401 | DOI 10.3897/aiep.51.64061

PENSOFT

ACTA ICHTHYOLOGICA ET PISCATORIA

A new record of a rare labrid, *Suezichthys notatus* (Actinopterygii: Labridae), from Taiwan, with comparison to related species from Taiwan

Chi-Ngai TANG[1], Hong-Ming CHEN[2], Husan-Ching HO[3,4,5]

1 *Institute of Oceanography, National Taiwan University, Taipei, Taiwan*
2 *Department of Aquaculture, National Taiwan Ocean University, Keelung, Taiwan*
3 *National Museum of Marine Biology and Aquarium, Checheng, Taiwan*
4 *Institute of Marine Biology, National Dong Hwa University, Pingtung, Taiwan*
5 *Australian Museum, Sydney, Australia*

http://zoobank.org/7CAAC9BE-0F8F-41BC-904D-E412111FA6AA

Corresponding author: Chi-Ngai Tang (victorcntang@gmail.com)

Academic editor: Ronald Fricke ♦ **Received** 6 February 2021 ♦ **Accepted** 28 September 2021 ♦ **Published** 6 December 2021

Citation: Tang C-N, Chen H-M, Ho H-C (2021) A new record of a rare labrid, *Suezichthys notatus* (Actinopterygii: Labridae), from Taiwan, with comparison to related species from Taiwan. Acta Ichthyologica et Piscatoria 51(4): 393–401. https://doi.org/10.3897/aiep.51.64061

Abstract

Three specimens of a rare labrid, *Suezichthys notatus* (Kamohara, 1958) were recently collected from local markets, which were captured from deep-water off northern and southwestern Taiwan, and represent a new record for Taiwan. *Suezichthys notatus* can be distinguished from its congeners by a combination of characters: scale rows above lateral line 2½; low scaly sheath present at base of dorsal and anal fins; dorsal-fin element IX, 11; anal-fin elements III, 10; lateral line scales 25–26, each with simple, unbranched laterosensory canal tube; cheek scale rows behind and below eye 2 and 2–3 respectively; a group of prominent dark blotches extending from the interorbital region dorsoposteriorly; body depth at dorsal-fin origin 3.7–3.9 in standard length; short pelvic fin without filamentous extension, 2.2–2.5 in head length. *Suezichthys* resembles the labrid genus *Pseudolabrus*, comparison of Taiwanese species of *Suezichthys* with those of *Pseudolabrus* are given.

Keywords

biodiversity, Indo-Pacific, morphology, taxonomy

Introduction

The labrid fish genus *Suezichthys* was originally proposed by Smith (1957) as *Suezia* (a name preoccupied in Crustacea), and subsequently replaced by *Suezichthys* (see Smith 1958). *Suezichthys* is a group of small, sexually dimorphic fishes occurring on sandy bottoms and rocky reefs of the Indo-Pacific and the southwestern Atlantic region. Some of the species are found on deep bottoms or mesophotic reefs, e.g., *Suezichthy notatus* (Kamohara 1958), which have been collected at deeper than 119 m (Shimada 2013).

The genus currently comprises 12 valid species. Russell and Westneat (2013) recognized 11 species, including a new species, *Suezichthys rosenblatti* Russell et Westneat, 2013, from Juan Fernandez and Isla San Felix off the coast of Chile. Another species, *Suezichthys devisi*

(Whitley, 1941), although not recognized by Russell and Westneat (2013), was regarded as valid by Kuiter (1993). *Suezichthys* was redefined by Russell (1985) and Russell and Westneat (2013). It superficially resembles the labrid genus *Pseudolabrus*, but is distinctive in some osteological characters. *Suezichthys* is also morphologically similar to *Halichoeres*, but differs by having cheeks scaly (vs. naked); gill membranes forming a free fold across the isthmus (vs. broadly attached); and anal-fin elements III, 10–12 (mostly III, 10 vs. III, 11–13) (Russell 1985; Russell and Westneat 2013).

In Taiwan, only one species, *Suezichthys gracilis* (Steindachner et Döderlein, 1887) has been documented (e.g., Shen et al. 1993). It is found in coastal marine habitats, often occurring on shallow reefs and adjacent sandy bottoms. Recently, the first author obtained specimens of a rare labrid from local fish markets, which occurred in the catches of deep-water line fisheries off northern and southwestern Taiwan. This species was subsequently recognized as *Suezichthys notatus*, the second species of *Suezichthys* recognized in Taiwan. In this work, a detailed description of specimens of *S. notatus* from Taiwan, comparisons with *S. gracilis*, and comments on species of *Pseudolabrus* from Taiwan are given.

Methods and materials

Counts, measurements, and terminology generally follow Russell and Randall (1981) and Russell (1985), except where indicated. The format of the description generally follows Randall and Kotthaus (1977). Definition of the initial phase (IP) and terminal phase (TP) follow Warner and Robertson (1978). Measurements were taken by digital or analog calipers based on the length of the measured items, recorded to the nearest 0.1 mm. Standard length (SL) and head length (HL) were used throughout. Pectoral-fin counts are given as the total number. Caudal-fin length was measured from the posterior edge of the hypural plate to the uppermost tip of the fin. Osteological characters were determined by X-radiographs. For the determination of associations of the hemal (haemal) arch and caudal vertebrae, the X-radiographs were taken by putting the specimen at an angle of ca. 45 degrees between the lateral surface and the X-ray source. Counts were recorded from the left side of the specimens unless otherwise indicated. Specimens of *S. notatus* were deposited at the Pisces Collection of National Marine Museum of Biology and Aquarium, Taiwan (NMMB-P).

Specimen examined. NMMB-P34163, 119.5 mm SL, northern Taiwan, near the "Three Northern Islands" region (e.g., Pinnacle Islet, Crag Islet, and Agincourt Islet), ca. 100–150 m depth, captured by hook-and-line, purchased from Keelung Fish Market, 16 Apr. 2020, coll. CNT. NMMB-P35255, 121.5 mm SL, same as NMMB-P34163, 28 Mar. 2021. NMMB-P35256, 110.4 mm SL, Kaoshiung, southwestern Taiwan, by hook-and-line, purchased from Chienchen Fishing Port, 1 Apr. 2021.

Comparative materials. *Suezichthys gracilis*: NMMB-P5157, 5 specimens, 85–113 mm SL, An-pin, Tainan, Taiwan, 01 Jan. 1965; NMMB-P26423 and NMMB-P26425, 60 and 67 mm SL respectively, Ke-tzu-liao, Kaohsiung, Taiwan, 18 Jun. 2017; *Pseudolabrus eoethinus*, NMMB-P2194, 118 mm SL, Hou-bi-hu, Pingtung, Taiwan, 01 Nov. 2011; NMMB-P4106, 3 specimens, 105–133 mm SL, Hou-bi-hu, Pingtung, Taiwan, 31 Aug. 2002; NMMB-P27484, 117 mm SL, Hengchun, Pingtung, Taiwan, 02 Nov. 2017; NMMB-P34434, 3 specimens, 112–140 mm SL, Ao-di, northeastern Taiwan, purchased in Keelung Fish Market, 01 Mar. 2020. *Pseudolabrus sieboldi*, 5 specimens, 140–151 mm SL, Pom-cha-yu, 20 Dec. 2006; NMMB-P20794, 136 mm SL, Da-shi, Yilan, Taiwan 12 Nov. 2012; NMMB-P20796, 133 mm SL, Da-shi, Yilan, Taiwan, 12 Nov. 2012; NMMB-P34433, 125 mm SL, Ao-di, northeastern Taiwan, purchased in Keelung Fish Market, 01 Mar. 2020; NMMB-P34720, 137 mm SL, Keelung Fish Market, northern Taiwan, 30 Oct. 2020.

Results

Family Labridae

Suezichthys Smith, 1958

Suezichthys notatus (Kamohara, 1958)

Figs. 1–4, Tables 1–2

New Chinese name: 斑頭蘇彝士隆頭魚

Pseudolabrus notatus Kamohara, 1958: pl. 3, fig. 2 (type-locality: Okinoshima, Japan).

Suezichthys tripunctatus Randall et Kotthaus, 1977: 34, figs. 1–3 (type-locality: Oahu, Hawaiian Islands)

Description of Taiwanese specimens. Proportional measurements are given in Table 1. Dorsal-fin elements IX, 11, all soft rays segmented and branched; anal-fin elements III, 10, all soft rays segmented and branched; pectoral-fin rays 13, uppermost rudimentary and second uppermost unbranched; pelvic-fin elements I, 5, all soft rays segmented and branched; caudal-fin rays 6 (dorsal unsegmented) + 2 (dorsal segmented and unbranched) + 12 (branched) + 2 (ventral segmented and unbranched) + 5–6 (ventral unsegmented); lateral line complete, bent abruptly downward beneath 10th dorsal-fin ray, with pored and tubed scales 25–26 (including enlarged and pointed pored scale on base of caudal fin; pored scale attached to opercular membrane excluded), simple and unbranched; scales above lateral line to origin of dorsal fin 2½; scales below lateral line to origin of anal fin 7½; low scaly sheath present at base of dorsal and anal fins; predorsal scales rows 5; cheek scale rows behind eye 2, scale rows below eye 2–3; circumpeduncular scales 15–16; total gill rakers 17–20; pseudobranchial filaments 19; branchiostegal rays 6; vertebrae 9 (precaudal) + 16 (caudal) = 25; ribs present from 3rd to 9th

Table 1. Morphometric proportions of *Suezichthys notatus*, *S. gracilis*, *Pseudolabrus eoethinus*, and *P. sieboldi*.

Character	*Suezichthys notatus*		*S. gracilis*		*Pseudolabrus eoethinus*		*P. sieboldi*	
	n = 3 (3 TP)		*n* = 6 (1 IP; 5 TP)		*n* = 5 (I IP, 4 TP)		*n* = 6 (1 IP, 5 TP)	
Standard length [mm]	110.4–121.5		60.2–112.5		105.3–133.3		125.4–151.1	
	% in standard length							
	Mean (range)	SD	Mean (range)	SD	Mean (range)	SD	Mean (range)	SD
Head length	34.5 (33.4–35.4)	1.0	30.8 (29.8–31.8)	0.7	35.5 (34.3–36.7)	0.9	34.5 (33–35.3)	0.8
Body depth at D-fin origin	26.3 (25.9–26.8)	0.5	22.7 (21.1–24.5)	1.4	34.2 (32.5–36.7)	1.5	35.2 (33.8–36.4)	1.0
Body width	11.0 (10.0–11.9)	1.0	10.5 (9.0–12.2)	1.1	15.2 (14.0–16.1)	0.7	15.7 (15.0–17.1)	0.8
Snout length	9.1 (8.6–9.5)	0.5	8.2 (7.6–8.9)	0.4	10.8 (10.1–11.5)	0.4	10 (9.3–10.5)	0.5
Orbit diameter	7.9 (7.7–8.2)	0.3	6.6 (5.6–7.3)	0.7	7.6 (7.2–8.3)	0.4	7.8 (7.4–8.3)	0.3
Postorbital length	18.4 (17.9–18.9)	0.5	16.5 (15.4–17.7)	0.9	18.4 (17.4–19.1)	0.6	18.3 (17.1–19.3)	0.7
Bony interorbital width	5.3 (5.0–5.4)	0.2	4.4 (4.2–4.9)	0.3	6.9 (6.6–7.4)	0.3	6.7 (6.1–7.0)	0.3
Suborbital width	4.3 (4.1–4.5)	0.2	3.0 (2.3–3.4)	0.4	5.2 (4.0–5.9)	0.6	5.1 (4.6–5.4)	0.3
Upper jaw length	8.5 (8.4–8.5)	0.1	7.1 (6.8–7.3)	0.2	9.8 (8.6–10.8)	0.8	9.3 (8.8–10.3)	0.5
Caudal peduncle length	13.6 (13.3–14.2)	0.5	14.6 (13.7–15.3)	0.6	15.0 (14.0–16.1)	0.7	15.7 (15.2–16.1)	0.3
Caudal peduncle depth	12.5 (12.1–13.0)	0.5	10.9 (10.6–11.3)	0.3	14.6 (13.3–16.3)	0.9	15.6 (14.5–16.5)	0.8
Pre-dorsal length	32.5 (31.2–33.3)	1.1	29.6 (28.5–30.6)	0.9	35.8 (34.0–37.7)	1.3	35.4 (34.3–36.5)	0.8
Pre-anal length	57.6 (55.4–58.7)	1.9	54.7 (51.8–56.6)	2.0	62.3 (60.0–64.4)	1.9	61.2 (59.1–63.9)	1.5
Pre-pelvic length	31.9 (31.3–32.3)	0.5	32.1 (29.7–33.4)	1.5	38.6 (37.5–40.8)	1.2	38 (36.1–40.7)	1.8
Snout to pre-scaled area on head	18.7 (17.9–19.4)	0.8	17.3 (16.6–18.7)	0.8	19.8 (18.5–21.8)	1.2	19.2 (17.3–21.0)	1.2
D-fin base length	58.5 (57.2–59.5)	1.2	60.6 (58.8–62.9)	1.3	57.9 (55.4–59.5)	1.5	58.3 (56.7–59.9)	1.3
1st D-fin spine	5.0 (4.7–5.4)	0.4	4.5 (3.8–5.3)	0.5	6.9 (6.5–7.7)	0.4	7.5 (6.9–8.2)	0.5
Longest D-fin spine (9th)	10.1 (9.1–10.7)	0.8	9.1 (8.5–10.0)	0.6	12.1 (10.9–13.6)	1.1	11.7 (11.1–12.8)	0.6
Last segmented D-fin ray	12.0 (10.9–13.0)	1.1	11.8 (11.0–12.8)	0.6	14.8 (14.1–15.7)	0.6	14.4 (13.8–15.1)	0.4
Longest D-fin ray (6th)	13.0 (12.0–13.5)	0.8	14.2 (13.2–15.9)	1.1	15.7 (15.0–16.3)	0.5	15.5 (14.8–16.6)	0.7
Last D-fin ray	11.6 (11.4–11.7)	0.1	12.3 (9.6–13.8)	1.7	12.6 (10.7–14.8)	1.3	13.5 (12.5–14.7)	0.6
Anal-fin base length	34.1 (33.2–35.1)	1.0	33.1 (31.4–34.6)	1.2	30.4 (29.5–31.1)	0.6	31.3 (29.3–33.0)	1.3
1st A-fin spine	3.6 (3.4–3.8)	0.2	3.7 (3.2–4.0)	0.3	5.7 (4.3–7.6)	1.2	4.9 (4.2–5.7)	0.5
2nd A-fin spine	5.3 (5.0–5.6)	0.4	5.8 (4.7–7.1)	0.8	8.9 (7.6–10.0)	1.0	7.9 (7.4–8.9)	0.5
3rd A-fin spine	7.8 (7.5–8.2)	0.3	7.2 (6.6–8.2)	0.6	10.7 (9.4–12)	1.0	9.6 (8.5–10.7)	0.7
1st segmented A-fin ray	11.0 (10.1–11.8)	0.8	11.0 (10.0–11.9)	0.8	13.6 (12.9–14.8)	0.7	13.4 (12.6–14.2)	0.6
Longest A-fin ray (4th)	11.9 (11.6–12.5)	0.5	12.9 (10.3–15.1)	1.7	14.1 (13.1–15.1)	0.7	13.5 (12.2–14.8)	0.9
Caudal fin length	21.7 (21.6–21.9)	0.2	21.1 (20.1–22.4)	1.0	25.7 (22.8–26.7)	1.3	27.0 (26.2–28.0)	0.6
Pectoral fin length	18.5 (18.1–18.8)	0.4	18.4 (17.0–19.8)	1.1	24.1 (23.2–24.7)	0.5	24.0 (23.4–25.5)	0.8
Pelvic fin spine length	7.6 (7.2–8.2)	0.5	8.2 (7.6–9.5)	0.8	11.0 (10.0–11.9)	0.7	10.2 (9.4–10.8)	0.5
Pelvic-fin length	14.9 (14.1–16.0)	1.0	18.0 (13.6–23.8)	3.7	17.3 (16.3–17.9)	0.5	16.4 (15.7–18.3)	0.9

D = dorsal; A = anal. TP = terminal phase; IP = initial phase.

vertebra; epineural bones ending on 12th vertebra; hemal arches associated with anterior caudal vertebrae of 10th to 12–13th vertebrae forming large hemal canal (Fig 4A).

Body moderately elongate, its depth at dorsal-fin origin 3.7–3.9 in SL; moderately compressed, width behind gill opening 2.8–3.6 in HL. Head small, its length 2.8–3.0 in SL; snout short, length 3.5–4.0 in HL; orbital diameter 4.2–4.5 in HL; bony interorbital width 6.4–6.7 in HL; suborbital depth 7.4–8.5 in HL. Least depth of caudal peduncle 2.7–2.8 in HL; length of caudal peduncle 2.4–2.7 in HL. Caudal fin slightly rounded, its length 1.6 in HL. Pectoral-fin length 1.8–1.9 in HL, reaching level of 7th dorsal-fin spine. Pelvic fin short, 2.2–2.5 in HL, first pelvic-fin ray not elongated. Length of dorsal-fin base 1.7–1.8 in SL; dorsal-fin spines progressively longer; first spine 6.4–7.3 in HL; last spine (9th) longest, 3.2–3.9 in HL; longest dorsal-fin ray (6th) 2.6–2.8 in HL. Length of anal-fin base 2.9–3.0 in SL; first anal-fin spine 9.3–9.9 in HL; third spine longest, 4.2–4.5 in HL; longest anal-fin ray (4th) 2.8–3.0 in HL.

(Based on NMMB-P34163) Mouth terminal, horizontal, and small, posterior end of maxilla reaching vertical through posterior nostril; lips moderately fleshy; upper lip with 6 longitudinal plicae and lower lip with 1; upper jaw with two pairs of enlarged canines at front, anteriormost pair of canine largest and recurved, second one about half length of first; 15/16 progressively smaller canine teeth laterally in upper jaw, with inner row of 6 (on left)/4 (on right) small canines behind anteriormost teeth; enlarged and antrorse canine at posterior end of upper jaw; lower jaw with 2 pairs of enlarged anterior canines, second canine slightly shorter than first; 11/13 progressively smaller lateral teeth in lower jaw, with inner row of 6/6 pairs of smaller canines behind anteriormost teeth; no teeth on palatine.

Nostrils small, in two pairs just in front of orbit; anterior nostril terminating in small membranous tube; posterior nostril without flap or prominent ridge at margin. Gill membranes not attached to isthmus, forming free fold posteriorly. Gill rakers short, longest less than half length of longest gill filament. Preopercle entire, free posterior margin reaching just above level of lower rim of orbit, free lower membrane extending forward to below level of middle of lower rim of orbit. Opercular membrane broadly rounded, extending posterior to pectoral-fin base. About 26 pores in lateralis system around orbit; ca. 22 pores along free edge of preopercle (based on NMMB-P34163).

Table 2. Meristic data of *Suezichthys notatus*, *S. gracilis*, *Pseudolabrus eoethinus*, and *P. sieboldi*.

Character	*Suezichthys notatus*			*S. gracilis*	*Pseudolabrus eoethinus*	*P. sieboldi*
	NMMB-P34163 (TP)	NMMB-P35255 (TP)	NMMB-P35256 (TP)	*n* = 6 (1 IP; 5 TP)	*n* = 6 (1 IP, 5 TP)	*n* = 6 (1 IP, 5 TP)
Standard length [mm]	119.5	121.5	110.4	60.2–112.5	105.3–133.3	125.4–151.1
Dorsal-fin rays	IX, 11	IX, 11	IX, 11	IX, 11	IX, 11	IX, 11
Anal-fin rays	III, 10	III, 10	III, 10	III, 10	III, 10	III, 10
Pectoral-fin rays	13	13	13	13–14	13	13
Pelvic-fin rays	I, 5	I, 5	I, 5	I, 5	I, 5	I, 5
Caudal fin rays	6 + 2 + 12 + 2 + 5	6 + 2 + 12 + 2 + 5	6 + 2 + 12 + 2 + 6	5–6 + 2 + 12–13 + 2 + 5	6 + 2 + 12 + 2 + 5–6	5–6 + 2 + 12 + 2 + 5
Pored LL scale	26	26	25	25	25	25–26
Scale rows above LL	2½	2½	2½	1½	3–4	3.5
Scale rows below LL	7½	7½	7½	7½	7–9	8½–9
Predorsal scale row	5	—	—	5	4–5	5–7
cheek SRs behind eye	2	2	3	2	2	2
cheek SRs below eye	3	2	3	3	4–5	5–6
Circumpedunclar scales	15	16	16	15	15–16	16–17
Gill rakers	20	17	19	17–20	17–20	17–20
Pseudobranchial filaments	19	19	—	16–17	16–21	18–25

LL = lateral line.

Figure 1. Fresh coloration of *Suezichthys notatus* from Taiwan. (**A**) NMMB-P34163, 119.5 mm SL, TP individual. (**B**) NMMB-P35255, 121.5 mm SL. (**C**) NMMB-P35256, 110.4 mm SL.

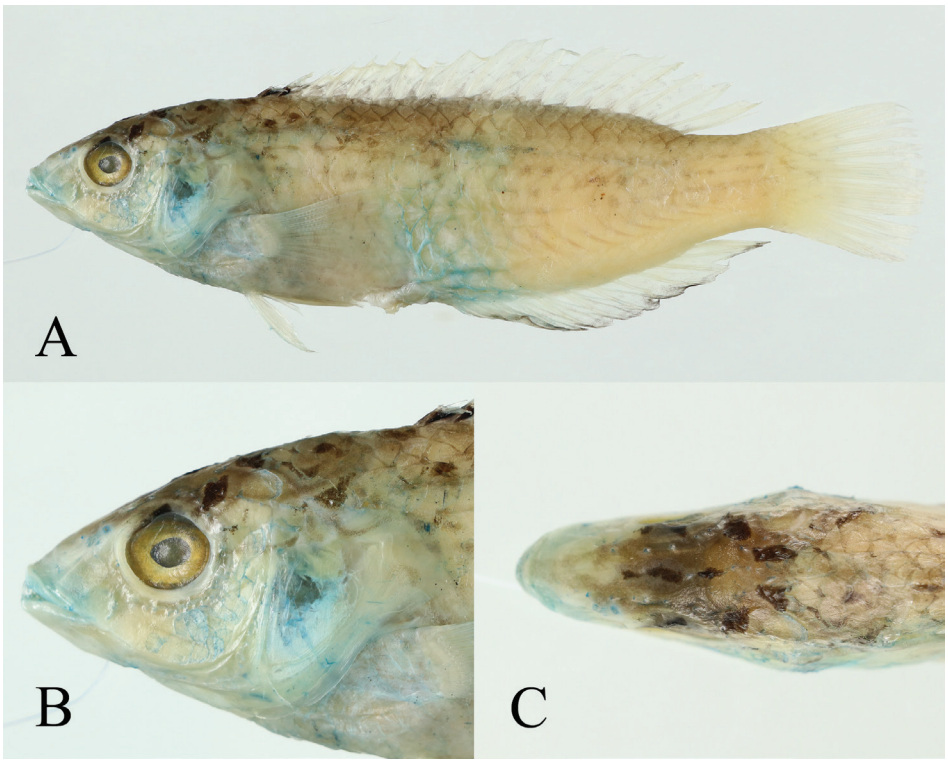

Figure 2. Preserved specimen of *Suezichthys notatus*, NMMB-P34163. (**A**) lateral view; (**B**) lateral side of head; (**C**) dorsal view of head and pre-dorsal region.

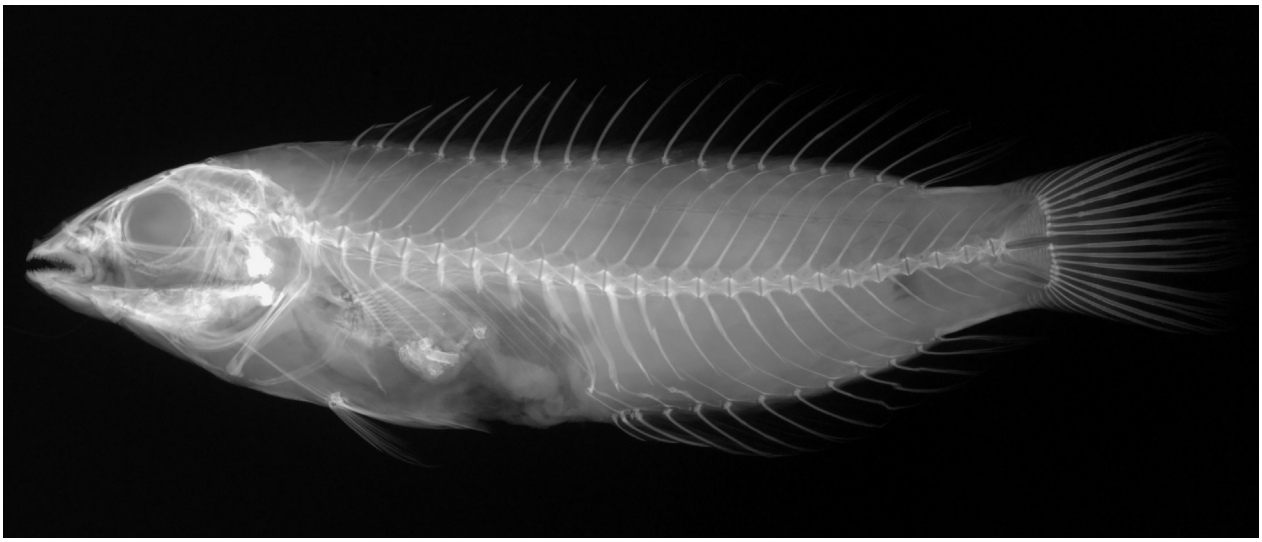

Figure 3. Radiograph of *Suezichthys notatus*, NMMB-P34163.

Opercle with 6 large scales posteriorly, almost extending to posterior margin of preopercle. Preopercle with 2 rows of cheek scales behind eye, and 2–3 rows below eye, extending forward to beneath middle of lower rim of orbit. Thorax fully scaled, scales about one half to three quarters of size of body scales. Basal portion of caudal fin scaled; forehead, snout, ventral side of head naked; subopercle naked. Body scales large, cycloid.

Dorsal-fin origin above upper pectoral-fin base; anal-fin origin below first dorsal-fin soft ray; pelvic-fin base slightly anterior to pectoral-fin base.

Coloration. (TP individuals) When fresh (Fig. 1A–C), body color pink to purple, paler on abdomen. Faint yellow reticulated pattern on lateral body. Group of prominent dark blotches extending from interorbital region dorsoposteriorly. Snout yellow, extending on operculum as two yellow stripes. Three faint yellow stripes gradually narrower extending from behind operculum to caudal peduncle. Dorsal fin pinkish to purple, yellow wavy lines above base and on upper edge of fin. Black spot between membrane of first and second dorsal-fin spine. Anal fin pinkish to purple, its edge yellow. Caudal fin yellow, with

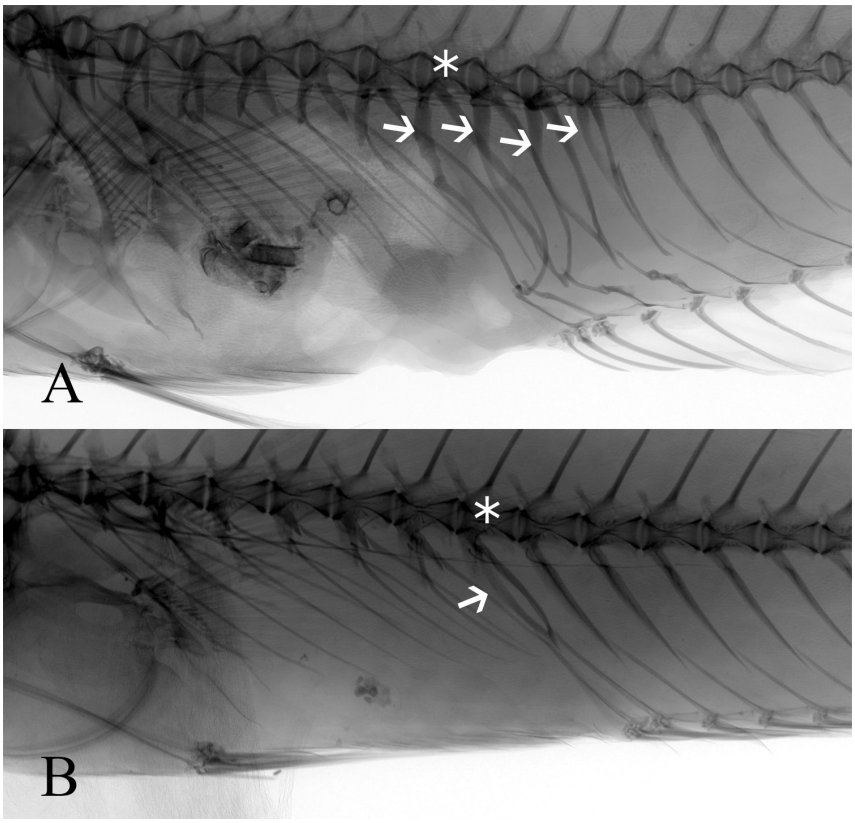

Figure 4. Radiographs showing the hemal arch formation associated with the anterior caudal vertebrae, arrows and asterisks are indicating the hemal arch on the 10th vertebra (anterior-most caudal vertebra) of two *Suezichthys*. (**A**) *S. notatus*, NMMB-P34163, on 10th to 13th vertebrae; (**B**) *S. gracilis*, NMMB-P26425, on the 10th vertebra.

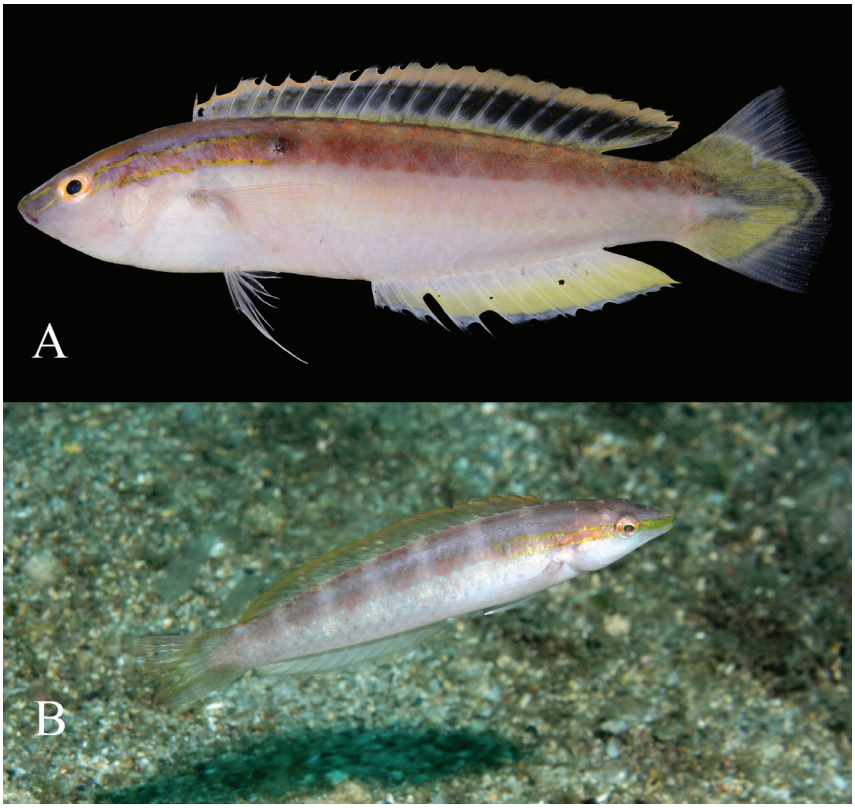

Figure 5. Fresh and live coloration of *Suezichthys gracilis*. (**A**) TP individual, KAUM-I.113342, 91 mm SL, collected from Ke-tzu-liao, Kaoshiung, southwestern Taiwan (photo by Keita Koeda, credit to the Kagoshima University Museum); (**B**) IP, at Long-dong, northeastern Taiwan, depth ca. 12 m (photo by Chen-Lu Lee).

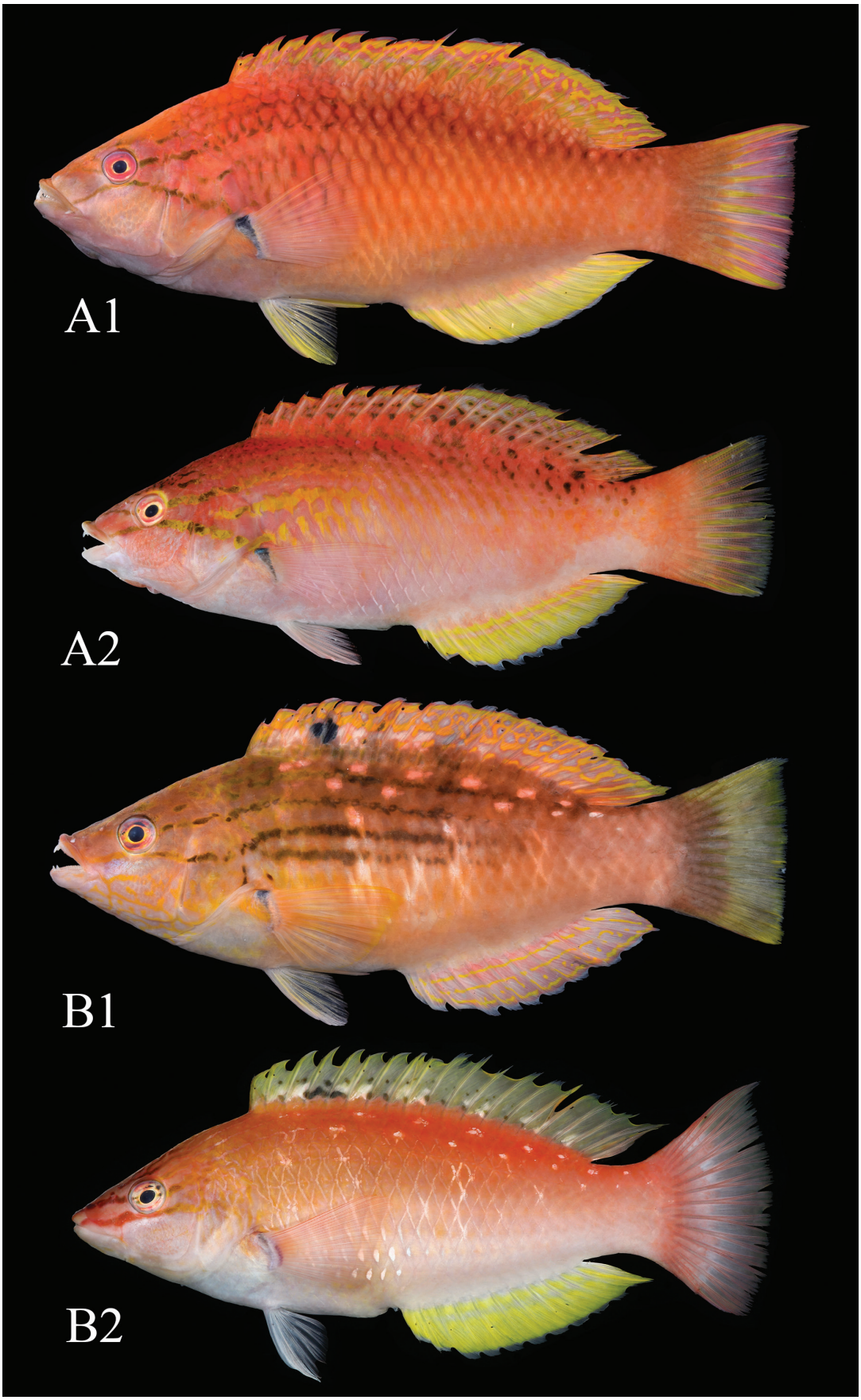

Figure 6. Fresh coloration of *Pseudolabrus eoethinus* (**A1–A2**) and *P. sieboldi* (**B1–B2**), captured off northeastern Taiwan. (A) *P. eoethinus*, NMMB-P34434 (both specimens), A1: TP individual, 140.5 mm SL; A2: IP, 111.8 mm SL; (B) *P. sieboldi*, NMMB-P34433, B1: TP, 124.5 mm SL; B2: NMMB-P34720, IP, 137.1 mm SL.

2–3 vertical purple stripes. Pectoral fin translucent pink. Pelvic fin white.

When preserved (Fig. 2), body pale. Prominent black blotches or spots on forehead and dorsal fin consistent with fresh condition. Forehead and dorsal-fin base dusky. Few faint dusky lines along, above and below lateral line. Edge of anal fin black.

Distribution. *Suezichthys notatus* is known from scattered localities across the Pacific Ocean and the easternmost Indian Ocean. Its type locality is Okinoshima, Kochi Prefecture of Japan. *Suezichthys notatus* also occurs in deep waters off northwestern Australia and Oahu, of the Hawaiian Archipelago. In the Hawaiian Archipelago, *S. notatus* has been observed along the edges of sand patches near irregular, hard surfaces, and foraging by picking at objects on rocks and sand at depths of 119–272 m (Russell 1985; Chave and Mundy 1994). The Taiwanese specimens described here were caught off the coast of Keelung, near the "Northern Three Islands", at depths of ca. 100–150 m, and off Kaoshiung, southwestern Taiwan (depth unknown); its habitat was assumed to be deep sandy-rocky bottom.

Discussion

Suezichthys notatus (Kamohara, 1958) was briefly described from a single specimen collected from Okinoshima, Kochi Prefecture, Japan. Russell (1985) noted the holotype of *S. notatus* had been re-examined by Takeshi Yamakawa, who reported a 16 total gill rakers, instead of 4 + 1 + 9 = 14 as given by Kamohara (1958). The specimen from Taiwan has more gill rakers, e.g., 17–20, on the first gill arch.

Species of *Suezichthys* share similar meristic counts; they have a combination of the following characters: Dorsal-fin rays IX, 11 (rarely 12–13); anal-fin rays III, 10–12; caudal-fin rays (5–6 + 2 + 12–13 + 2 + 5–6); total pectoral-fin rays 12–14 (mostly 13, the uppermost 2 rays unbranched, the dorsalmost rudimentary); lateral line scales 25–26 (usually 25); scales rows below lateral line 7½ (Russell 1985, Russell and Westneat 2013; this study). *Suezichthys notatus* can be classified into the species group with 2½ scales above the lateral line, and distinguished from these close congeners by the following combination of characters: dorsal-fin rays IX, 11 (only IX, 12–13 in *Suezichthys ornatus* (Carmichael, 1819)); lateral-line scales with unbranched laterosensory canal tube (unbranched in the whole genus except *Suezichthys bifurcatus* Russell, 1986); IP and TP with black blotch or blotches above dorsoposterior margin of eye (Fig. 2B, C).

Kamohara (1958) compared *S. notatus* with *S. gracilis* and noted the former has more lateral-line scales and fewer scale rows on the cheek. However, the counts of these characters in Russell (1985) and our study do not differ greatly between the two species.

In Taiwan, only two species of *Suezichthys* are recognized. The Taiwanese specimens of *S. notatus* and *S. gracilis* (Fig. 5) differ in various characters: a longer head in *S. notatus* (2.8–3.0 vs. 3.1–3.4 in SL in *S. gracilis*); greater body depth at the origin of dorsal fin (3.7–3.9 vs. 4.1–4.7 in SL); greater predorsal length (3.0–3.2 vs. 3.3–3.5); pelvic fin short (2.2–2.5 vs. 1.3–2.2 in HL); pelvic fin of terminal phase individual short, when appressed its tip not reaching the anus (vs. long, with a slightly filamentous extension, when appressed its tip reaching the anus or slightly beyond the origin of anal fin); scale rows above lateral line 2½ (vs. 1½); a low scaly sheath presents on the base of dorsal and anal fin (vs. without).

In coloration, *S. notatus* and *S. gracilis* are both overall pinkish and have a black spot present on the fin membrane between the 1st and 2nd spine in TP specimens. However, both IP and TP of *S. notatus* do not possess a lateral stripe on the body (vs. present on both phases of *S. gracilis*, red in IP and olive-green in TP); presence of black spots on the interorbital region dorsoposteriorly in *S. notatus* in TP (Fig. 2), or a large black spot at posterior end of dorsal-fin base (vs. none of these present in both phases of *S. gracilis*).

The morphology of hemal spines of caudal vertebrae differs between *S. notatus* and *S. gracilis* from Taiwan (Fig. 4). The hemal arches form a large hemal canal associated with anterior caudal vertebrae of the 10th to 12–13th vertebrae in *S. notatus* (Fig. 4A); in contrast *S. gracilis* has only a single hemal arch with a large hemal canal, associated with the 10th vertebra (Fig. 4B). Russell (1985) stated that the hemal arches with large hemal canal are on the 10th to 12th vertebrae of *S. notatus*, but in one of our specimens (NMMB-P34163) the 13th vertebra also has a large hemal canal.

As stated in previous literature, *Suezichthys* superficially resembles *Pseudolabrus*. In Taiwan, two species of *Pseudolabrus* are also recorded (Shen and Wu 2011): *Pseudolabrus eoethinus* (Richardson, 1846) and *Pseudolabrus sieboldi* Mabuchi et Nakabo, 1997 (Fig. 6). Meristic and morphometric data were obtained from Taiwanese specimens of *Pseudolabrus* species to compare with the two Taiwanese *Suezichthys* species (Tables 1, 2). *Suezichthys* species differ from *Pseudolabrus* species (based on Taiwanese specimens) as follows: fewer rows of scales above lateral line in *Suezichthys*, 1½–2½ (vs. 3–4 in *Pseudolabrus*); fewer cheek scale rows + below eye (3 vs. 4–6); shallower body depth at dorsal-fin origin (3.7–4.7 vs. 2.8–3.1 in SL); narrower bony interorbital width (6.4–7.4 vs. 4.9–5.4 in SL); shorter 1st dorsal-fin spine (5.8–8.0 vs. 4.4–5.6 in SL). However, as mentioned in Russell (1985), these characters do not clearly separate the two genera. More significantly, *Suezichthys* is distinct from *Pseudolabrus* in having the following characters: anterior preneural zygopophyses fused, slightly expanded (vs. separate, small); urohyal with a posteroventral spike-like extension (vs. no spike); and laterosensory canal tube of lateral line simple tubular, bifurcate or branched (vs. only bifurcate or multi-branched).

Acknowledgments

This study was supported by National Museum of Marine Biology and Aquarium, Pingtung (NMMBA), National Taiwan Ocean University, Keelung (NTOU), and the National Museum of Marine Science and Technology, Keelung (NMMST). We express our sincere thanks to Dr Barry Russell (Museum and Art Gallery of the Northern Territory, Australia) for providing comments on the manuscript, Dr Hiroyuki Motomura (the Kagoshima University Museum), and Dr Keita Koeda (the Kuroshio Biological Research Foundation, Kochi Prefecture, Japan) for kindly providing the color specimen image, Dr Chen-Lu Lee (NMMST) for providing underwater photography and ecological information, and Chia-Ho Chan (NMMBA) for the curatorial assistance.

References

Chave EH, Mundy BC (1994) Deep-sea benthic fish of the Hawaiian Archipelago, Cross Seamount, and Johnston Atoll. Pacific Science 48(4): 367–409.

Kamohara T (1958) A review of the labrid fishes found in the waters of Kochi Prefecture, Japan. Reports of the Usa Marine Biological Station 5(2): 1–8.

Kuiter RH (1993) Coastal fishes of south-eastern Australia. University of Hawaii Press, Honolulu, USA.

Mabuchi K, Nakabo T (1997) Revision of the genus *Pseudolabrus* (Labridae) from the east Asian waters. Ichthyological Research 44(4): 321–334. https://doi.org/10.1007/BF02671984

Randall JE, Kotthaus A (1977) *Suezichthys tripunctatus,* a new deep-dwelling Indo-Pacific labrid fish. Meteor Forschungsergebnisse. Reihe D. Biologie 24: 33–36.

Richardson J (1846) Report on the ichthyology of the seas of China and Japan. Report of the British Association for the Advancement of Science (1845): 187–320. https://doi.org/10.5962/bhl.title.59530

Russell BC (1985) Revision of the Indo-Pacific labrid fish genus *Suezichthys*, with descriptions of four new species. Indo-Pacific Fishes 2: 1–21.

Russell BC, Randall JE (1981) The labrid fish genus *Pseudolabrus* from islands of the southeastern Pacific, with description of a new species from Rapa. Pacific Science 34(4): 433–440.

Russell BC, Westneat MW (2013) A new species of *Suezichthys* (Teleostei: Perciformes: Labridae) from the southeastern Pacific, with a redefinition of the genus and a key to species. Zootaxa 3640(1): 88–94. https://doi.org/10.11646/zootaxa.3640.1.7

Shen SC, Lee SC, Shao KT, Mok HK, Chen CH, Chen CC, Tzeng CS (1993) [Fishes of Taiwan.] Department of Zoology, National Taiwan University, Taipei, Taiwan, 960 pp. [In Chinese]

Shen SC, Wu KY (2011) [Fishes of Taiwan.] National Museum of Marine Biology and Aquarium, Checheng, Taiwan, 896 pp. [In Chinese]

Shimada K (2013) Labridae. Pp. 1088–1136 and 2045–2056. In: Nakabo T (Ed.) Fishes of Japan with pictorial keys to the species. 3rd edn. Tokai University Press, Tokyo, Japan. [In Japanese.]

Smith JLB (1957) List of the fishes of the family Labridae in the western Indian Ocean with new records and five new species. Ichthyological Bulletin, Department of Ichthyology, Rhodes University 7: 99–114.

Smith JLB (1958) Rare fishes from South Africa. South African Journal of Science 54(12): 319–323.

Steindachner F, Döderlein L (1887) Beitrage zur Kenntnis der Fische Japan's. (IV). Denkschriften der Kaiserlichen Akademie der Wissenschaften, Mathematisch-Naturwissenschaftliche Classe, Wien 53: 257–296.

Warner RR, Robertson DR (1978) Sexual patterns in the labroid fishes of the western Caribbean, I: The wrasses (Labridae). Smithsonian Contributions to Zoology 254(254): 1–27. https://doi.org/10.5479/si.00810282.254

Whitley GP (1941) Ichthyological notes and illustrations. Australian Zoologist 10(1): 1–50.

Acta Ichthyologica et Piscatoria 51(4), 2021, 403–412 | DOI 10.3897/aiep.51.69363

PENSOFT

ACTA ICHTHYOLOGICA ET PISCATORIA

Morphometric variation of Middle-American cichlids: *Theraps–Paraneetroplus* clade (Actinopterygii: Cichliformes: Cichlidae)

Yanet Elizabeth AGUILAR-CONTRERAS[1], Alfonso A. GONZÁLEZ-DÍAZ[2], Omar MEJÍA[3], Rocío RODILES-HERNÁNDEZ[2]

1 *Maestría en Ciencias en Recursos Naturales y Desarrollo Rural, El Colegio de la Frontera Sur, San Cristóbal de Las Casas, Chiapas, México*

2 *Colección de Peces, El Colegio de la Frontera Sur, Departamento Conservación de la Biodiversidad, San Cristóbal de Las Casas, Chiapas, México*

3 *Departamento de Zoología, Escuela Nacional de Ciencias Biológicas, Instituto Politécnico Nacional, Ciudad de México, México*

http://zoobank.org/8C816018-3B79-4D6B-A199-EA2E74CE0955

Corresponding author: Alfonso A. González-Díaz (agonzalez@ecosur.mx)

Academic editor: Felipe Ottoni ♦ **Received** 28 May 2021 ♦ **Accepted** 4 November 2021 ♦ **Published** 22 December 2021

Citation: Aguilar-Contreras YE, González-Díaz AA, Mejía O, Rodiles-Hernández R (2021) Morphometric variation of Middle-American cichlids: *Theraps–Paraneetroplus* clade (Actinopterygii: Cichliformes: Cichlidae). Acta Ichthyologica et Piscatoria 51(4): 403–412. https://doi.org/10.3897/aiep.51.69363

Abstract

This study assesses the patterns of variation in body shape, and relations of morphological similarity among species of the *Theraps–Paraneetroplus* clade in order to determine whether body shape may be a trait in phylogenetic relations. A total of 208 specimens belonging to 10 species of the *Theraps–Paraneetroplus* clade were examined. The left side of each specimen was photographed; in each photograph, 27 fixed landmarks were placed to identify patterns in body shape variation. Images were processed by using geometric morphometrics, followed by a phylogenetic principal component analysis. The phylogenetic signal for body shape was then calculated. To determine the relations in morphological similarity, a dendrogram was created using the unweighted pair group method and arithmetic mean values, while a Procrustes ANOVA and post-hoc test were used to evaluate significant differences between species and habitats. We found three morphological groups that differed in body length and depth, head size, and the position of the mouth and eyes. The body shape analysis recovered the morphotypes of seven species, and statistical differences were demonstrated in eight species. Based on traits associated with cranial morphology, *Wajpamheros nourissati* (Allgayer, 1989) differed the most among the species examined. No phylogenetic signal was found for body shape; this trait shows independence from ancestral relatedness, indicating that there is little congruence between morphological and genetic interspecific patterns. As evidenced by the consistently convergent morphology of the species in the *Theraps–Paraneetroplus* clade, the diversification of the group is related to an ecological opportunity for habitat use and the exploitation of food resources. Although no phylogenetic signal was detected for body shape, there appears to be an order associated with cranial morphology-based phylogeny. However, it is important to evaluate the intraspecific morphologic plasticity produced by ecological segregation or partitioning of resources. Therefore, future morphological evolutionary studies should consider cranial structures related to the capture and processing of food.

Keywords

diversification, geometric morphometrics, morphological convergence, phylogenetic signal, Usumacinta province

Introduction

Among Neotropical freshwater fishes, evidence of diversity suggests that allopatric speciation models frequently apply to several clades and that there are few cases of sympatric speciation stemming from adaptive processes (Albert et al. 2020). The main historical processes include river capture and sea-level oscillations, which fragment and merge fluvial networks. In this scenario involving geographic changes and ecological heterogeneity, phenotypic variation has been an important attribute in morphological diversification and environmental adaptation (Albert et al. 2020). Freshwater fish orders such as Siluriformes, Characiformes, Cyprinodontiformes, Gymnotiformes, and Cichliformes are the best examples of morphological diversity in the Neotropical region due to their high species richness and abundance (Albert et al. 2020; Elías et al. 2020).

In Neotropical cichlids, the ability to use new or newly available resources (i.e., ecological opportunity) has been an important mechanism in diversification (Arbour and López-Fernández 2016; Říčan et al. 2016). Studies related to morphological diversity in South American cichlids have demonstrated that body shape and size variation have been the main axes of diversification, most notably the constant presence of morphological convergence between lineages (López-Fernández et al. 2010, 2013). Morphological convergence is interpretable as evidence that natural selection has selected similar traits, thus providing strong evidence for the adaptive quality of said traits (Elmer and Meyer 2011; Losos 2011; Burress 2015).

Despite advances in knowledge regarding the evolution of diverse groups of cichlids worldwide, there are still lineages with incipient research, such as Middle American heroine cichlids. Middle America harbors approximately 124 cichlid species (Říčan et al. 2011; Matamoros et al. 2015) and includes areas considered to be centers of endemism and high diversity, such as the San Juan and Usumacinta ichthyological provinces (*sensu* Říčan et al. 2016). From evolutionary evidence, it has been assumed that their diversification was promoted by ecological opportunity and resource partitioning (López-Fernández et al. 2012; Burress 2016; Říčan et al. 2016). This is supported by the diversity of body shapes and the specialization of trophic anatomy, particularly of the oral and pharyngeal jaws (Liem 1973; Meyer 1993; Salzburger 2009; Burress 2016). Notably, this has promoted frequent cases of morphological convergence and the low phylogenetic signal of diagnostic characters. This is the main reason for the unclear and complex taxonomy of cichlids in Middle America (Stiassny 1991; Říčan et al. 2008, 2016; McMahan et al. 2013).

Among Middle American cichlids, the *Theraps–Paraneetroplus* clade (*sensu* Říčan et al. 2016) is notable due to the presence of species therein with highly variable and frequently convergent morphology, which is most evident in their body shapes and characteristics associated with food capture (Soria-Barreto and Rodiles-Hernández 2008; Soria-Barreto et al. 2011, 2019). This group of fish is estimated to have originated under sympatric conditions approximately 7.3 mya (Miller et al. 2005; Říčan et al. 2016) and is thought to result from the event of ancient adaptive radiation (Arbour and López-Fernández 2016; Albert et al. 2020). The *Theraps–Paraneetroplus* clade includes 25 species belonging to 10 genera. Moreover, the distribution of this clade is located in the Usumacinta ichthyological province, comprising the hydrological basins of Papaloapan, Coatzacoalcos, Grijalva, Usumacinta, and northern Belize (Říčan et al. 2016).

In addition to ecomorphological evidence indicating that the phenotypic expression of morphological attributes in some clade members is associated with habitat type and feeding (Soria-Barreto et al. 2019), studies on the systematics and evolution of Middle American cichlids have demonstrated the existence of convergent morphological characters between several species of the *Theraps–Paraneetroplus* clade (López-Fernández et al. 2014; McMahan et al. 2015; Říčan et al. 2016). As the same body shape patterns are recurrent among species that exploit similar habitats (McMahan et al. 2015; Říčan et al. 2016), the existence of lentic and lotic ecomorphological patterns has been previously proposed; species of the genera *Cincelichthys*, *Kihnichthys*, *Oscura*, and *Vieja* represent the lentic ecomorphotype (i.e., with short and deep bodies), and the species *Theraps*, *Wajpamheros*, *Chuco*, *Rheoheros*, and *Paraneetroplus* represent the lotic ecomorphotype (i.e., with elongated and slender bodies). Notably, both ecomorphotypes are present in the genus *Maskaheros* (see Říčan et al. 2016).

In the *Theraps–Paraneetroplus* clade, convergent morphological characteristics seem to support the hypothesis of diversification via ecological opportunity and resource partitioning, which contrasts with the hypothesis proposed by phylogenetic systematics and the theory of evolutionary non-independence (Felsenstein 1985). In the non-independence hypothesis, it would be expected that body shapes within the species and genera of this clade would have a diversification pattern similar to that of phylogeny and taxa sharing an ancestor that is most morphologically similar. In this way, species with a lotic body shape should share an ancestor, which should be similarly true for the lentic body shape. In contrast, if the non-independence hypothesis is rejected, then the morphological patterns should not be statistical dependents of the common ancestry (Revell et al. 2008). Therefore, the presently reported study aims to describe and compare the body shape variation patterns in 10 species of the *Theraps–Paraneetroplus* clade. Furthermore, the phylogenetic signal is obtained to measure the statistical non-independence of the morphologic trait values of the species due to their phylogenetic relatedness (Revell et al. 2008).

For this purpose, geometric morphometrics and comparative phylogenetic methods are used as analytical tools because they are commonly used to study the evolution of biological morphology. Geometric morphometrics can be

used to identify variation in the pure shape of organisms, and separate the variation and size of individuals by analyzing shapes in multivariate space (Adams et al. 2004; Zelditch et al. 2004; Aguirre and Jiménez-Prado 2018). Notably, comparative phylogenetic methods can be used to analyze morphological characteristics and their significance in species diversification from a phylogenetic perspective (Pagel and Harvey 1988; Adams and Collyer 2018; Borges et al. 2019; Villalobos-Leiva and Benítez 2020). Recently, phylogenetic approaches have made it possible to understand the significance of morphological variation and changes in the dynamics of biological communities, particularly in speciation, adaptation, and extinction. This is essential to predict the effect of natural and anthropogenic changes on ecosystem processes. It also represents a fundamental step towards the management and conservation of biodiversity on the planet (Cavender-Bares et al. 2009).

Methods

To analyze the morphological variation among members of the *Theraps–Paraneetroplus* clade, the presently reported study included a total of 208 specimens (females and males of similar size) that correspond to 10 species, representative of each genus in the clade. All the specimens were deposited at the Fish Collection of El Colegio de la Frontera Sur, San Cristóbal (ECOSC). *Theraps* clade: *Chuco intermedium* (Günther, 1862) (abbreviation and number of specimens: Chin, *n* = 21); *Cincelichthys pearsei* (Hubbs, 1936) (Cipe, *n* = 24); *Kihnichthys ufermanni* (Allgayer, 2002) (Kiuf, *n* = 23); *Theraps irregularis* Günther, 1862 (Thir, *n* = 20); *Wajpamheros nourissati* (Allgayer, 1989) (Wano, *n* = 24); *Paraneetroplus* clade: *Maskaheros argenteus* (Allgayer, 1991) (Maar, *n* = 25); *Oscura heterospila* (Hubbs, 1936) (Oshe, *n* = 20); *Paraneetroplus bulleri* Regan, 1905 (Pabu, *n* = 3); *Rheoheros lentiginosus* (Steindachner, 1864) (Rhle, *n* = 25); *Vieja hartwegi* (Taylor et Miller, 1980) (Viha, *n* = 23).

Museum catalogue information. *Chuco intermedium* (Chin) ECOSC 103, 314(4), 334, 395(5), 440, 473(3), 815(2), 12747(2), 4892(2); *Cincelichthys pearsei* (Cipe) ECOSC 204, 229(2), 299, 300, 337, 444, 719(4), 849, 1049, 1512(3), 1055, 2352, 2546, 2575, 4422(2), 4436 (2); *Kihnichthys ufermanni* (Kiuf) ECOSC 90, 186, 233, 406, 409, 613, 675, 769, 1729, 1230, 1536(3), 1548, 1557(2), 1867, 1873, 2118(2), 2298, 4687, 7618; *Maskaheros argenteus* (Maar) ECOSC 386, 698, 741, 1280, 1448,1472, 1481, 1502, 1606, 1747, 1771, 1998, 2020, 2163, 2174, 2395, 2555, 2577, 4716, 4747(2), 4806(2), 4821, 7774; *Oscura heterospila* (Oshe) ECOSC 2338, 2720, 3053, 3054, 3491, 3505, 3777, 4563, 6709, 7826, 8465, 9070, 9080, 9267, 9318, 9816, 9849, 10164, 10165, 13757; *Paraneetroplus bulleri* (Pabu) ECOSC 12018(3); *Rheoheros lentiginosus* (Rhle) ECOSC 646, 853(3), 869(2), 1471(2), 1503(2), 1874, 1900, 2296(4), 2389, 2515(3), 2549, 2559, 7789, 4695, 12748; *Theraps irregularis* (Thir) ECOSC 245, 254, 817(2), 1255, 1780, 1967, 2133, 2626, 4725, 4729, 4809(9); *Vieja hartwegi* (Viha) ECOSC 4445(3), 4546, 6838, 6857(4), 7468, 7542(4), 7543(4), 7548(2), 7549(2), 12340; *Wajpamheros nourissati* (Wano) ECOSC 532(2), 684(2), 820(2), 893, 1237, 1288(2), 1546(2), 1847, 1289(2), 2082(2), 2105, 2280, 2651, 4744, 4888, 7336, 7453.

Morphometric analysis. Specimens were photographed on their left side using a Canon (EOS 70D) digital camera. The camera was mounted on a tripod to standardize the distance from the specimen. A 1-cm scale was placed on each photograph. To describe and compare body shapes, a geometric morphometric analysis was performed. In each photo, 27 fixed landmarks were placed using the configuration provided by Mejía et al. (2015) with two additional landmarks (Fig. 1). Image digitization and processing were performed using the software tpsUtil ver. 1.70 (Rohlf 2018) and tpsDig ver. 2.26 (Rohlf 2017).

Then, in order to eliminate variation caused by the size, rotation, and displacement of the specimens, a generalized Procrustes analysis (Goodall 1991) was performed (Aguirre and Jiménez-Prado 2018). The mean body shape configuration of each species was obtained in the same manner. In both cases, the "gpagen" function of the Geomorph ver. 4.0.0 library (Adams and Otárola-Castillo 2013; Adams et al. 2016) was used in R software (R Core Development Team 2017).

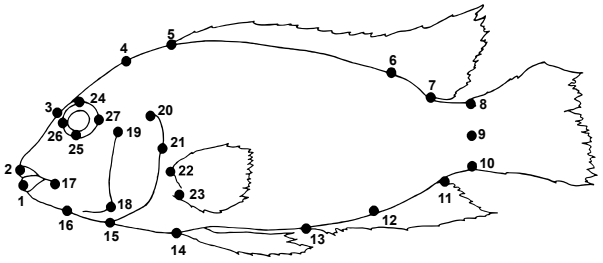

Figure 1. Location of fixed landmarks in species of the *Theraps–Paraneetroplus* clade (image modified from Mejía et al. 2015). 1. Anterior end of the lower maxilla, **2.** Anterior end of the upper maxilla, **3.** Length of the ascending premaxillary process, **4.** End of the supraoccipital bone, **5.** Start of the dorsal fin, **6.** Last spine of the dorsal fin, **7.** End of the dorsal fin, **8.** Upper boundary of the caudal fin, **9.** Center of the caudal fin, **10.** Base of the caudal fin, **11.** End of the anal fin, **12.** Last spine of the anal fin, **13.** Origin of the anal fin, **14.** Origin of the pelvic fin, **15.** Cleitral fusion, **16.** Posterior end of the lower maxilla, **17.** Posterior end of the upper lip, **18.** Maximum point of curvature at the preoperculum, **19.** Upper end of the preoperculum, **20.** Upper end of the operculum, **21.** Most posterior end at the operculum, **22.** Dorsal insertion of the pectoral fin, **23.** Ventral insertion of the pectoral fin, **24.** Upper extreme of the sphenotic orbit, **25.** Base of the sphenotic orbit, **26.** Left extreme of the sphenotic orbit, **27.** Right extreme of the sphenotic orbit.

Shape analysis. To reduce morphological variation related to phylogeny and differences in specimen size (allometry), regression of the Procrustes coordinates and centroid size was conducted using the "phyl.resid" function of the Phytools package ver. 0.7–80 in R software (Revell 2009, 2012). In order to then identify patterns in body shape variation, a phylogenetic principal component analysis (pPCA) was performed based on the Procrustes coordinates of the mean configurations of the 10 species. The nDNA molecular phylogeny based on ddRAD sequences proposed by Říčan et al. (2016) for Middle American cichlids was used in both instances. The body shape variation of the species was displayed on the first three pPCA axes. Additionally, deformation grids were obtained to visualize and describe the morphological variation among species in morphospace. All analyses were conducted in R software using the Phytools package ver. 0.7–80 (Revell 2009, 2012).

Additionally, the phylogenetic signal for body shape was computed by using the Kmult statistic (*K*) across 1000 permutations via the Geomorph package 4.0.0 in R software (Adams et al. 2021), *K* values <1 indicate a low phylogenetic signal, while *K* values >1 indicate a strong phylogenetic signal (Adams 2014). To determine the relation involved with morphological similarity among the 10 species, a dendrogram was constructed using the unweighted pair group method using mean values in Past 4.05 software (Hammer et al. 2001) based on the Mahalanobis distances obtained in MorphoJ 1.07a software (Klingenberg 2011).

Finally, to determine whether significant differences in body shape exist among species and between lentic (LE) and lotic (LO) habitats, a Procrustes ANOVA was used as implemented in Geomorph 4.0.0 (Adams et al. 2021) using the procD.lm function over 1000 permutations with the Procrustes coordinates and centroid size. Furthermore, to establish whether there are significant differences in body shape among species, a pairwise comparison test was performed using the pairwise function as implemented in library RRPP (Collyer and Adams 2018) over 1000 permutations.

Results

The pPCA indicated that the first three components explained 80% of the total variance (PC1: 52.6%; PC2: 17.6%; PC3: 11.6%). Species located on the positive axis of PC1 include *T. irregularis*, *P. bulleri*, and *R. lentiginosus*; *O. heterospila*, *M. argenteus*, *C. pearsei*, and *K. ufermanni* were located on the negative axis; and *C. intermedium*, *V. hartwegi*, and *W. nourissati* were located on the middle axis. The deformation grids showed variation among species on the positive axis related to decreased body height, elongation of the caudal peduncle, a convex base of the anal fin, and a narrow distal section. Species on the negative axis showed a deep body height, shortened caudal peduncle, and concave base of the anal fin. According to the morphotypes, the lotic species *T. irregularis*, *P. bulleri*, and *R. lentiginosus* were on the positive axis, while lentic species on the negative axis included *O. heterospila*, *M. argenteus*, *C. pearsei*, and *K. ufermanni.* However, the lotic species *C. intermedium* and *W. nourissati*, as well as the lentic species *V. hartwegi*, were in the middle of the axis (Fig. 2A, B)

In PC2, species found in the positive axis included *C. pearsei*, *K. ufermanni*, *C. intermedium*, *T. irregularis*, and *V. hartwegi*, while *O. heterospila*, *W. nourissati*, *R. lentiginosus*, *M. argenteus*, and *P. bulleri* were found on the negative axis (Fig. 2A). The deformation grids showed that the most remarkable deformation occurred in the cephalic region. Species on the positive axis exhibited heads with straight profiles and mouths in a terminal position, while the eyes were displaced posteriorly and slightly enlarged.

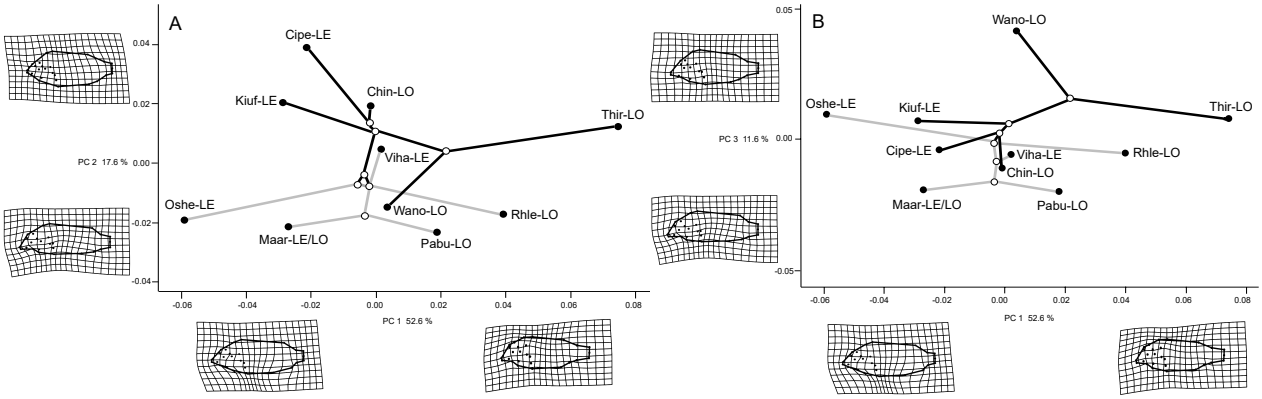

Figure 2. A) Phylomorphospace formed by PC1 and PC2. **B**) Phylomorphospace formed by PC1 and PC3. Black circles represent the mean body shape configuration for each species, and white circles the ancestral state. Black lines represent *Theraps* clade, and grey lines *Paraneetroplus* clade. LE represent lentic ecomorphotype, LO represent lotic ecomorphotype, LE/LO represent both ecomorphotypes. Deformation grids are associated to the most negative and positive values of the PC1 and PC2. Abbreviations: Chin-LO = *Chuco intermedium*; Cipe-LE = *Cincelichthys pearsei*; Kiuf-LE = *Kihnichthys ufermanni*; Thir-LO = *Theraps irregularis*; Wano-LO = *Wajpamheros nourissati*; Maar-LE/LO = *Maskaheros argenteus*; Oshe-LE = *Oscura heterospila*; Pabu-LE = *Paraneetroplus bulleri*; Rhle-LO = *Rheoheros lentiginosus*; Viha-LE = *Vieja hartwegi*.

Species on the negative axis showed rounded heads and a ventral mouth position, while the eyes were both smaller in size and were displaced anteriorly (Fig. 2A, 2B).

In PC3, *W. nourissati* was the most differentiated on the positive axis, exhibiting accentuated variation in the cephalic region with increased head size and a notable anteroventral displacement of the mouth. Additionally, the eyes and pectoral fins of *W. nourissati* were displaced posteriorly. On the negative axis, the remaining species were equally distributed with short heads, rounded profiles, and small mouths (Fig. 2B).

The dendrogram based on Mahalanobis distances showed that *C. intermedium* differed the most in body shape, followed by the *C. pearsei* and *K. ufermanni* groups. The remaining species formed two groups—one composed of *P. bulleri*, *R. lentiginosus*, and *T. irregularis* and another composed of *M. argenteus* and *O. heterospila*. The second most similar species were *W. nourissati* and *V. hartwegi.* The phylogenetic signal value of the Kmult statistic was 0.765, with a significance value of $P = 0.308$ and displaying no significant effect of phylogeny on body shape under the Brownian motion evolutionary model (Fig. 3).

The Procrustes ANOVA identified significant differences in body shape among species ($F = 34.62$, $R^2 = 0.59$, $P < 0.01$) and habitats for the comparison of Procrustes coordinates ($F = 56.24$, $R^2 = 0.20$, $P < 0.001$). However, the comparison using the centroid size of each species failed to recover significant differences among species ($F = 1.06$, $R^2 = 0.043$, $P = 0.181$) and habitats ($F = 1.20$, $R^2 = 0.005$, $P = 0.264$). However, the pairwise comparison test showed statistical differences between all the species ($P < 0.05$) excluding *V. hartwegi* and *P. bulleri* ($P = 0.055$) (Table 1).

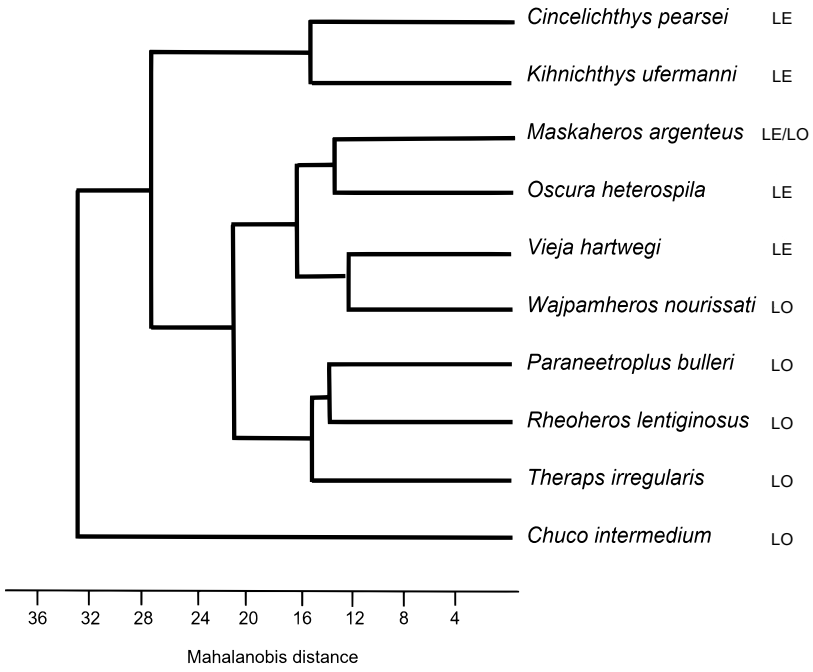

Figure 3. Dendrogram based on Mahalanobis distances (Cophenetic correlation = 0.79). LE represent lentic ecomorphotype, LO represent lotic ecomorphotype, combined LE/LO represent both ecomorphotypes.

Table 1. Procrustes distances (above diagonal) and *p* values (below diagonal) to pairwise comparison test between all cichlid species of Middle-American *Theraps–Paraneetroplus* clade. Bold letters indicate no significant differences between species.

	Chin	Cipe	Kiuf	Maar	Oshe	Pabu	Rhle	Thir	Viha	Wano
Chin	—	0.047	0.051	0.059	0.079	0.061	0.071	0.085	0.045	0.068
Cipe	0.001	—	0.034	0.066	0.074	0.081	0.087	0.102	0.049	0.077
Kiuf	0.001	0.004	—	0.057	0.055	0.075	0.083	0.105	0.044	0.066
Maar	0.001	0.001	0.001	—	0.052	0.058	0.077	0.111	0.049	0.071
Oshe	0.001	0.001	0.001	0.001	—	0.090	0.102	0.137	0.073	0.077
Pabu	0.006	0.001	0.001	0.009	0.001	—	0.057	0.077	0.046	0.067
Rhle	0.001	0.001	0.001	0.001	0.001	0.011	—	0.061	0.061	0.071
Thir	0.001	0.001	0.001	0.001	0.001	0.001	0.001	—	0.078	0.086
Viha	0.001	0.001	0.001	0.001	0.001	**0.055**	0.001	0.001	—	0.056
Wano	0.001	0.001	0.001	0.001	0.001	0.001	0.001	0.001	0.001	—

Abbreviations: Chin = *Chuco intermedium*; Cipe = *Cincelichthys pearsei*; Kiuf = *Kihnichthys ufermanni*; Thir = *Theraps irregularis*; Wano = *Wajpamheros nourissati*; Maar = *Maskaheros argenteus*; Oshe = *Oscura heterospila*; Pabu = *Paraneetroplus bulleri*; Rhle = *Rheoheros lentiginosus*; Viha = *Vieja hartwegi*.

Discussion

In the pPCA, species were placed in morphospace based on body length and depth, followed by variation in the cephalic region based on changes in head size and profile, mouth position, and eye position and size. Additionally, some morphological changes were evident based on the position and size of the fins. The variation observed in these morphological characteristics has been closely associated with the environments, locomotion, and feeding of fish (Wootton 1990; Muschick et al. 2012; Feilich 2016; Fugi unpublished*). In African and South American cichlids, variation in these morphological characteristics has been fundamental in adaptive radiation events because it facilitates phenotypic and lineage diversification through the exploitation of ecological opportunities (Kocher et al. 1993; Cooper et al. 2010; Muschick et al. 2014; Arbour and López-Fernández 2016). The morphological body variation patterns observed in South American cichlids are similar to those observed in species of the *Theraps–Paraneetroplus* clade, which supports the hypothesis of Middle American cichlid diversification via ecological opportunity as proposed in previous works (Arbour and López-Fernández 2016; Feilich 2016; Říčan et al. 2016).

In the morphospace and similarity analysis, the most notable groupings were *T. irregularis*, *R. lentiginosus*, and *P. bulleri*, all of which presented elongated bodies and caudal peduncles as well as pelvic fins that were positioned ventrally. Ecomorphological studies have reported that these characteristics are functionally associated with high-velocity current environments (Lowe-McConnell 1991; Lauder and Tytell 2005; Pease et al. 2012; Feilich 2016). Elongated bodies are more hydrodynamic, while fins in the ventral position permit fish to maintain stability (Drucker et al. 2005; Lauder and Tytell 2005; Pease et al. 2012; Feilich 2016; Han et al. 2020). Soria-Barreto and Rodiles-Hernández (2008) reported the same morphological pattern for *T. irregularis* and *R. lentiginosus* in the Lacandon rainforest (Montes Azules Biosphere Reserve, Mexico), and Gómez-González et al. (2018) in *V. hartwegi*. Additionally, the mouth positions of the three species tend to be sub-terminal or ventral, which is associated with foraging for algae and invertebrates on the bottom, particularly on the surfaces of rocks with silt and sand substrates (Keast and Webb 1966; Miller et al. 2005; Artigas-Azas 2005b).

The group comprising *O. heterospila*, *K. ufermanni*, *M. argenteus*, and *C. pearsei* occupies another part of the morphospace. These species displayed deep bodies, short heads, shortened caudal peduncles, and mouths that were generally in a terminal position. These morphological characteristics are associated with environments where current velocity ranges from medium to slow, and have different types of substrates (i.e., rock, gravel, sand, and mud) (Berbel-Filho et al. 2016; Feilich 2016; Říčan et al. 2016). Although these species are generally herbivorous and omnivorous, some may be detritivorous (Miller et al. 2005; Soria-Barreto et al. 2019; Říčan et al. 2016). Furthermore, *V. hartwegi*, *C. intermedium*, and *W. nourissati* have an intermediate morphology with shallow elongated bodies and shortened caudal peduncles. These three species likely share ecological niches and inhabit areas with moderate-to-high velocities (Miller et al. 2005; Pease et al. 2012; McMahan et al. 2015; Říčan et al. 2016; Gómez-González et al. 2018). Additionally, these species present more ventral snouts, facilitating feeding on aquatic invertebrates, detritus, algae, and vegetation (Soria-Barreto et al. 2019).

Wajpamheros nourissati, the outlier of the cichlids analyzed, is the only species that has long and thick lips. This is a characteristic associated with feeding between cracks, on rock surfaces, and on the substrate (Winemiller et al. 1995; Artigas-Azas 2005a; López-Fernández et al. 2014; Říčan et al. 2016). This characteristic has been reported in Middle and South American cichlids, which feed on benthic components and live in habitats with a variety of substrates including sand, silt, and organic matter in fine and coarse particles (Barlow and Munsey 1976; Moreira and Zuanon 2002; Hahn and Cunha 2005; Elmer et al. 2010; López-Fernández et al. 2012). Additionally, *W. nourissati* has well-developed pectoral fins that provide stability in habitats with currents of moderate velocity (Allgayer 1989). These morphological traits can be functionally important for exploiting specific habitats and alimentary resources while reducing competition with other sympatric cichlids.

The variation associated with the cephalic region revealed that the majority of species occupy a position in the morphospace that corresponds to their respective clades. For example, members of the *Theraps* clade (i.e., *C. pearsei*, *C. intermedium*, *K. ufermanni*, and *T. irregularis*) are positioned toward the superior part of the morphospace, while members of the *Paraneetroplus* clade (i.e., *M. argenteus*, *O. heterospila*, *P. bulleri*, and *R. lentiginosus*) are located toward the lower region. However, convergence between the two clades was also observed, largely in the variation of the cephalic characteristics of *V. hartwegi* and *W. nourissati*. This notably coincides with the variation of the cephalic characteristic in members of the opposite clade in both cases. Comparative studies have revealed patterns of rapid diversification between lineages and phenotypes through habitat- and diet-related morphological diversity (Arbour and López-Fernández 2016; Feilich 2016). Furthermore, it has been shown that the early radiation of certain Neotropical cichlid tribes in South America occurred rapidly, which resulted in a pattern of conflicting divergence (López-Fernández et al. 2013; Astudillo-Clavijo et al. 2015).

* Fugi R (1993) Estratégias alimentares utilizadas por cinco espécies de peixes comedoras de fundo do alto rio Paraná/PRMS. Dissertação de Mestrado. Universidade Federal de São Carlos. São Carlos, SP, Brasil.

Evidence of the low phylogenetic signal of the body shape thus disproves the hypothesis of evolutionary non-independence. However, as the value of the phylogenetic signal can be determined by several processes and evolutionary rates (Revell et al. 2008), it raises the question of what specific causes determine body shape. In the evolution of quantitative traits, there is evidence that a low phylogenetic signal is related to speciation events caused by divergent selection and adaptive processes (Revell et al. 2008). In several Neotropical cichlid clades, this is the main cause for diversification events related to ecological opportunity (López-Fernández et al. 2012, 2013; McMahan et al. 2015; Feilich 2016; Říčan et al. 2016).

In this context, some species of both clades (*Theraps–Paraneetroplus*) exhibited high convergence in the variation associated with body length and depth, fins position, and eye size and position. This is evident in *C. intermedium*, *V. hartwegi*, and *W. nourissati*, which showed similar body shapes despite being considered as different ecomorphotypes. The remaining species exhibited a morphological pattern consistent with what was expected from the corresponding habitat. The lentic species (*C. pearsei*, *K. ufermanni*, *M. argenteus*, and *O. heterospila*) showed a clear morphologically divergent pattern with respect to the lotic species (*R. lentiginosus*, *T. irregularis*, and *P. bulleri*). In the case of *C. intermedium*, *V. hartwegi*, and *W. nourissati*, it is probable that habitat preference is determined by other morphological traits that are likely linked to the cephalic region and associated with feeding behavior. This adaptive process has been documented in other fish groups; for example, in the Pomacentridae family, variations in cephalic traits explain feeding behavior and diet and are an important predictor of trophic habit (Aguilar-Medrano et al. 2011).

Based on the analysis of body shape and head characteristics, the lack of congruence in the order of species in morphospace does not fully support the ecomorphological classification described by Říčan et al. (2016). However, the results support the hypothesis of functional independence between the cephalic and postcranial regions identified for Middle American cichlids (Říčan et al. 2016). In regard to the cephalic region, the occurrence of five ecomorphotypes associated with feeding behavior was identified. Meanwhile, the postcranial region showed the lentic and lotic ecomorphotypes associated with their respective environments. In both instances, molecular phylogeny supported the recurrent evolution of diverse cephalic and postcranial ecomorphotypes among Middle American cichlids (Říčan et al. 2016). Additionally, modularity has been considered an evolutionary factor leading to patterns of variation among cichlids. Modularity studies in African cichlids have centered on modules associated with feeding: cichlid species that feed by suction have functional modules and those that feed by foraging have developmental modules (Parsons et al. 2012).

Species of the *Theraps–Paraneetroplus* clade show highly varied and convergent morphologies that are largely promoted by ecological opportunities associated with habitat and feeding preferences (Albertson and Kocher 2001; McKaye et al. 2002; Kassam et al. 2003; López-Fernández et al. 2013; Feilich 2016; Říčan et al. 2016). Body size and depth are features that appear unrelated to phylogenetic relations, whereas the head features of the majority of species exhibit patterns of variation associated with their phylogeny. However, further analyses of the shape, role, and evolution of these morphological attributes are necessary to understand their significance in the diversification of Middle American cichlids.

Conclusions

In this paper, the morphological variation of the *Theraps–Paraneetroplus* clade was divided into three groups within the morphospace. These variations are related to body length, body height, head shape, mouth position, and eye size and position. In particular, *W. nourissati* was the most divergent species due to its cranial characteristics, which are largely related to the shape of the head and the position of the mouth. Body size and height were the variables that best described the position of the species in the morphospace. This facilitates the recovery of lotic and lentic ecomorphotypes for seven species, with only *C. intermedium*, *V. hartwegi*, and *W. nourissati* showing incongruity. The presence of the phylogenetic signal disproves the non-independence hypothesis, but evidence suggests that body shape results from adaptive processes related to ecological opportunity. Although the results of the ANOVA with Procrustes distances and size of the centroid were contradictory, groupings in the morphospace and dendrogram were consistent with the ecomorphotypes and phylogeny. The pairwise comparison test showed statistical differences between all species, with the exception of *V. hartwegi–P. bulleri*. The morphological patterns found support the taxonomical validity of each species and can be used to describe body shape at the genus level. Future morphological evolution studies should consider cranial structures related to the capture and processing of food.

Acknowledgments

We thank the anonymous reviewers who provided helpful comments that improved the manuscript. Financial support for this study was received from the Project: “Conectividad y diversidad funcional de la cuenca del río Usumacinta” (Fondo de Investigación Científica y Desarrollo Tecnológico de El Colegio de la Frontera Sur, FID-784), coordinated by RRH. This manuscript is the result of the master thesis of YEAC.

References

Adams DC (2014) A generalized *K* statistic for estimating phylogenetic signal from shape and other high-dimensional multivariate data. Systematic Biology 63(5): 685–697. https://doi.org/10.1093/sysbio/syu030

Adams DC, Collyer ML (2018) Multivariate phylogenetic comparative methods: Evaluations, comparisons, and recommendations. Systematic Biology 67(1): 14–31. https://doi.org/10.1093/sysbio/syx055

Adams DC, Otárola-Castillo E (2013) Geomorph: An R package for the collection and analysis of geometric morphometric shape data. Methods in Ecology and Evolution 4(4): 393–399. https://doi.org/10.1111/2041-210X.12035

Adams DC, Rohlf FJ, Slice DE (2004) Geometric morphometrics: Ten years of progress following the "revolution". Italian Journal of Zoology 71(1): 5–16. https://doi.org/10.1080/11250000409356545

Adams DC, Collyer ML, Sherratt E (2016) geomorph: Software for geometric morphometric analyses. R package version 3.0. 2016 https://rune.une.edu.au/web/handle/1959.11/21330

Adams DC, Collyer M, Kaliontzopoulou A, Baken E (2021) Geometric morphometric analyses of 2D/3D Landmark Data. https://cran.csiro.au/web/packages/geomorph/geomorph.pdf

Aguilar-Medrano R, Frédérich B, De Luna E, Balart EF (2011) Patterns of morphological evolution of the cephalic region in damselfishes (Perciformes: Pomacentridae) of the eastern Pacific. Biological Journal of the Linnean Society. Linnean Society of London 102(3): 593–613. https://doi.org/10.1111/j.1095-8312.2010.01586.x

Aguirre W, Jiménez-Prado P (2018) Guía práctica de morfometría geométrica. Aplicaciones en la Ictiología: Pontificia Universidad Católica del Ecuador Sede Esmeraldas Ecuador, 106 pp.

Albert JS, Tagliacollo VA, Dagosta F (2020) Diversification of Neotropical freshwater fishes. Annual Review of Ecology, Evolution, and Systematics 51(1): 27–53. https://doi.org/10.1146/annurev-ecolsys-011620-031032

Albertson CR, Kocher DT (2001) Assessing morphological differences in an adaptive trait: A landmark-based morphometric approach. Journal of Experimental Zoology 289(6): 385–403. https://doi.org/10.1002/jez.1020

Allgayer R (1989) Révision et redescription du genre *Theraps* Günther, 1862. Description de deux espèces nouvelles du Mexique (Pisces, Perciformes, Cichlidae). Revue Française des Cichlidophiles 10(90): 4–30. https://cichlidae.com/reference.php?id=144&lang=es

Arbour HJ, López-Fernández H (2016) Continental cichlid radiations: Functional diversity reveals the role of changing ecological opportunity in the Neotropics. Proceedings of the Royal Society B: Biological Sciences 283(1836): 1–9. https://doi.org/10.1098/rspb.2016.0556

Artigas-Azas JM (2005a) *Amphilophus nourissati* (Allgayer, 1989) the big-lipped eartheater from Mexico. Cichlid News 14(1): 6–12.

Artigas-Azas JM (2005b) The corrientera—*Theraps irregularis* Günther, 1862. Cichlid News 14(4): 14–18.

Astudillo-Clavijo V, Arbour JH, López-Fernández H (2015) Selection towards different adaptive optima drove the early diversification of locomotor phenotypes in the radiation of Neotropical geophagine cichlids. BMC Evolutionary Biology 15(1): 1–13. https://doi.org/10.1186/s12862-015-0348-7

Barlow GW, Munsey JW (1976). The red devil—Midas-arrow cichlid species complex in Nicaragua. Investigations of the Ichthyofauna of Nicaraguan Lakes. 24. https://core.ac.uk/download/pdf/188046345.pdf

Berbel-Filho WM, Martínez PA, Ramos TPA, Torres RA, Lima SMQ (2016) Inter- and intra-basin phenotypic variation in two riverine cichlids from northeastern Brazil: Potential ecoevolutionary damages of São Francisco interbasin water transfer. Hydrobiologia 766(1): 43–56. https://doi.org/10.1007/s10750-015-2440-9

Borges R, Machado PJ, Gomes C, Rocha AP, Antunes A (2019) Measuring phylogenetic signal between categorical traits and phylogenies. Bioinformatics 35(11): 1862–1869. https://doi.org/10.1093/bioinformatics/bty800

Burress ED (2015) Cichlid fishes as models of ecological diversification: Patterns, mechanisms, and consequences. Hydrobiologia 748(1): 7–27. https://doi.org/10.1007/s10750-014-1960-z

Burress ED (2016) Ecological diversification associated with the pharyngeal jaw diversity of Neotropical cichlid fishes. Journal of Animal Ecology 85(1): 302–313. https://doi.org/10.1111/1365-2656.12457

Cavender-Bares J, Kozak H, Fine KH, Paul VA, Kembel SW (2009) The merging of community ecology and phylogenetic biology. Ecology Letters 12(7): 693–715. https://doi.org/10.1111/j.1461-0248.2009.01314.x

Collyer ML, Adams DC (2018) RRPP: An R package for fitting linear models to high-dimensional data using residual randomization. Methods in Ecology and Evolution 9(7): 1772–1779. https://doi.org/10.1111/2041-210X.13029

Cooper WJ, Parsons K, Mclntyre A, Kern B, McGee-Moore A, Albertson RC (2010) Bentho-pelagic divergence of cichlid feeding architecture was prodigious and consistent during multiple adaptive radiations within African rift-lakes. PLoS One 5(3): e9551. https://doi.org/10.1371/journal.pone.0009551

Drucker EG, Walker JA, Westneat M (2005) Mechanics of pectoral fin swimming in fishes. Fish Physiology 23: 369–423. https://doi.org/10.1016/S1546-5098(05)23010-8

Elías DJ, McMahan CD, Matamoros WA, Gómez-González AE, Piller KR, Chakrabarty P (2020) Scale(s) matter: Deconstructing an area of endemism for Middle American freshwater fishes. Journal of Biogeography 47(5): 1–19. https://doi.org/10.1111/jbi.13941

Elmer KR, Meyer A (2011) Adaptation in the age of ecological genomics: Insights from parallelism and convergence. Trends in Ecology and Evolution 26(6): 298–306. https://doi.org/10.1016/j.tree.2011.02.008

Elmer K, Lehtonen T, Kautt A, Harrod C, Meyer A (2010) Rapid sympatric ecological differentiation of crater lake cichlid fishes within historic times. Biomed Central Biology 8(60): 1–15. https://doi.org/10.1186/1741-7007-8-60

Feilich KL (2016) Correlated evolution of body and fin morphology in the cichlid fishes. Evolution 70(10): 2247–2267. https://doi.org/10.1111/evo.13021

Felsenstein J (1985) Phylogenies and the comparative method. American Naturalist 125(1): 1–15. https://doi.org/10.1086/284325

Gómez-González AE, Álvarez F, Matamoros WA, Velázquez-Velázquez E, Schmitter-Soto JJ, González-Díaz AA, McMahan CD (2018) Redescription of *Vieja hartwegi* (Taylor & Miller 1980) (Teleostei: Cichlidae) from the Grijalva River basin, Mexico and Guatemala, with description of a rheophilic morph. Zootaxa 4375(3): 371–391. https://doi.org/10.11646/zootaxa.4375.3.5

Goodall CR (1991) Procrustes methods in the statistical analysis of shape. Journal of the Royal Statistical Society. Series B. Methodological 53(2): 285–339. https://doi.org/10.1111/j.2517-6161.1991.tb01825.x

Hahn NS, Cunha F (2005) Feeding and trophic ecomorphology of *Satanoperca pappaterra* (Pisces, Cichlidae) in the Manso Reservoir, Mato Grosso State, Brazil. Brazilian Archives of Biology and Technology 48(6): 1007–1012. https://doi.org/10.1590/S1516-89132005000800017

Hammer Ø, Harper DAT, Ryan PD (2001) PAST: Paleontological statistics software package for education and data analysis. Paleontología Electrónica 4(1): 1–9 https://palaeo-electronica.org/2001_1/past/past.pdf

Han P, Lauder GV, Dong H (2020) Hydrodynamics of median-fin interactions in fish-like locomotion: Effects of fin shape and movement. Physics of Fluids 32(1): 011902. https://doi.org/10.1063/1.5129274

Kassam DD, Adams CD, Ambali AJD, Yamaoka K (2003) Body shape variation in relation to resource partitioning within cichlid trophic guilds coexisting along the rocky shore of Lake Malawi. Animal Biology 53(1): 59–70. https://doi.org/10.1163/157075603769682585

Keast A, Webb D (1966) Mouth and body form relative to feeding ecology in the fish fauna of a small lake, Lake Opinicon, Ontario. Journal of the Fisheries Research Board of Canada 23(12): 1845–1874. https://doi.org/10.1139/f66-175

Klingenberg CP (2011) MorphoJ: An integrated software package for geometric morphometrics. Molecular Ecology Resources 11(2): 353–357. https://doi.org/10.1111/j.1755-0998.2010.02924.x

Kocher TD, Conroy JA, McKaye KR, Stauffer JR (1993) Similar morphologies of cichlid fish in Lakes Tanganyika and Malawi are due to convergence. Molecular Phylogenetics and Evolution 2(2): 158–165. https://doi.org/10.1006/mpev.1993.1016

Lauder GV, Tytell ED (2005) Hydrodynamics of undulatory propulsion. Fish Physiology 23: 425–468. https://doi.org/10.1016/S1546-5098(05)23011-X

Liem KF (1973) Evolutionary strategies and morphological innovations: Cichlid pharyngeal jaws. Systematic Zoology 22(4): 425–441. https://doi.org/10.2307/2412950

López-Fernández H, Winemiller KO, Honeycutt RL (2010) Multilocus phylogeny and rapid radiations in Neotropical cichlid fishes (Perciformes: Cichlidae: Cichlinae). Molecular Phylogenetics and Evolution 55(3): 1070–1086. https://doi.org/10.1016/j.ympev.2010.02.020

López-Fernández H, Winemiller KO, Montaña C, Honeycutt RL (2012) Diet–morphology correlations in the radiation of South America geophagine cichlids (Perciformes: Cichlidae: Cichlinae). PLoS One 7(4): e33997. https://doi.org/10.1371/journal.pone.0033997

López-Fernández H, Arbour JH, Winemiller KO, Honeycutt RL (2013) Testing for ancient adaptive radiations in Neotropical cichlid fishes. Evolution 67(5): 1321–1337. https://doi.org/10.1111/evo.12038

López-Fernández H, Arbour J, Willis S, Watkins C, Honeycutt LR, Winemiller KO (2014) Morphology and efficiency of a specialized foraging behavior, sediment sifting, in Neotropical cichlid fishes. PLoS One 9(3): e89832. https://doi.org/10.1371/journal.pone.0089832

Losos JB (2011) Convergence, adaptation, and constraint. Evolution. 65(7): 1827–1840. https://doi.org/10.1111/j.1558-5646.2011.01289.x

Lowe-McConnell RH (1991) Ecology of cichlids in South American and African waters, excluding the African Great Lakes. Pp. 60–85. In: Keenleyside MHA (Ed.) Cichlid fishes. Behaviour, ecology and evolution. Chapman and Hall, London, UK.

Matamoros WA, McMahan CD, Chakrabarty P, Albert JS, Schaefer JF (2015) Derivation of the freshwater fish fauna of Central America revisited: Myers's hypothesis in the twenty-first century. Cladistics 31(2): 177–188. https://doi.org/10.1111/cla.12081

McKaye RK, Stauffer RJjr, Van den Berghe PE, Vivas R, Lopez-Perez JL, McCrary KJ, Waid R, Konings A, Woo-Jai L, Kocher TD (2002) Behavioral, morphological and genetic evidence of divergence of the Midas cichlid species complex in two Nicaraguan crater lakes. Cuadernos de investigación de la U.C.A. (12): 19–47. http://www.bio-nica.info/Biblioteca/McKaye2002.pdf

McMahan CD, Chakrabarty P, Sparks JS, Smith WML, Davis MP (2013) Temporal patterns of diversification across global cichlid biodiversity (Acanthomorpha: Cichlidae). PLoS One 8(8): e71162. https://doi.org/10.1371/journal.pone.0071162

McMahan CD, Matamoros WA, Piller KR, Chakrabarty P (2015) Taxonomy and systematics of the herichthyins (Cichlidae: Tribe Heroini), with the description of eight new Middle American genera. Zootaxa 3999(2): 211–234. https://doi.org/10.11646/zootaxa.3999.2.3

Mejía O, Pérez-Miranda F, León-Romero Y, Soto-Galera E, De Luna E (2015) Morphometric variation of the *Herichthys bartoni* (Bean, 1892) species group (Teleostei: Cichlidae): How many species comprise *H. labridens* (Pellegrin, 1903)? Neotropical Ichthyology 13(1): 61–67. https://doi.org/10.1590/1982-0224-20140067

Meyer A (1993) Phylogenetic relationships and evolutionary processes in east African cichlid fishes. Trends in Ecology and Evolution 8(8): 279–284. https://doi.org/10.1016/0169-5347(93)90255-N

Miller R, Minckley W, Norris SM (2005) Freshwater fishes of México. University of Chicago Press, Chicago, IL, USA, 652 pp.

Moreira SS, Zuanon J (2002) Dieta de *Retroculus lapidifer* (Perciformes: Cichlidae), um peixe reofílico do rio Araguaia, estado do Tocantins, Brasil. Acta Amazonica 32(4): 691–705.

Muschick M, Indermaur A, Salzburger W (2012) Convergent evolution within an adaptive radiation of cichlid fishes. Current Biology 22(24): 2362–2368. https://doi.org/10.1016/j.cub.2012.10.048

Muschick M, Nosil P, Roesti M, Dittmann MT, Harmon L, Salzburger W (2014) Testing the stages model in the adaptive radiation of cichlid fishes in east African Lake Tanganyika. Royal Society Publishing 281(1795): e20140605. https://doi.org/10.1098/rspb.2014.0605

Pagel MD, Harvey PH (1988) Recent developments in the analysis of comparative data. Quarterly Review of Biology 63(4): 413–440. https://doi.org/10.1086/416027

Parsons KJ, Márquez E, Albertson RC (2012) Constraint and opportunity: The genetic basis and evolution of modularity in the cichlid mandible. American Naturalist 179(1): 64–78. https://doi.org/10.1086/663200

Pease AA, González-Díaz A, Rodiles-Hernández R, Winemiller KO (2012) Functional diversity and trait–environment relationships of stream fish assemblages in a large tropical catchment. Freshwater Biology 57(5): 1060–1075. https://doi.org/10.1111/j.1365-2427.2012.02768.x

R Core Development Team (2017) R: A language and environment for statistical computing. Vienna, Austria.

Revell LJ (2009) Size-correction and principal components for interspecific comparative studies. Evolution 63(12): 3258–3268. https://doi.org/10.1111/j.1558-5646.2009.00804.x

Revell LJ (2012) Phytools: An R package for phylogenetic comparative biology (and other things). Methods in Ecology and Evolution 3(2): 217–223. https://doi.org/10.1111/j.2041-210X.2011.00169.x

Revell LJ, Harmon LJ, Collar DC (2008) Phylogenetic signal, evolutionary process, and rate. Systematic Biology 57(4): 591–601. https://doi.org/10.1080/10635150802302427

Říčan O, Zardoya R, Doadrio I (2008) Phylogenetic relationships of Middle American cichlids (Cichlidae, Heroini) based on combined evidence from nuclear genes, mtDNA, and morphology. Molecular Phylogenetics and Evolution 49(3): 941–957. https://doi.org/10.1016/j.ympev.2008.07.022

Říčan O, Piálek L, Almirón A, Casciotta J (2011) Two new species of *Autraloheros* (Teleostei: Cichlidae), with notes on diversity of the genus and biogeography of the Río de la Plata basin. Zootaxa 2982(1): 1–26. https://doi.org/10.11646/zootaxa.2982.1.1

Říčan O, Piálek L, Dragová K, Novák J (2016) Diversity and evolution of the Middle American cichlid fishes (Teleostei: Cichlidae) with revised classification. Vertebrate Zoology 66(1): 1–102. https://www.senckenberg.de/wp-content/uploads/2019/08/01_vertebrate_zoology_66-1_rican_1-102.pdf

Rohlf FJ (2017) TpsDig, versión 2.31. TpsSeries. Department of Ecology and Evolution, University of New York at Stony Brook, Stony Brook, NY, USA.

Rohlf FJ (2018) TpsUtil, file utility program, versión 1.76. Department of Ecology and Evolution, University of New York at Stony Brook, NY, USA.

Salzburger W (2009) The interaction of sexually and naturally selected traits in the adaptive radiations of cichlid fishes. Molecular Ecology 18(2): 169–185. https://doi.org/10.1111/j.1365-294X.2008.03981.x

Soria-Barreto M, Rodiles-Hernández R (2008) Spatial distribution of cichlids in Tzendales River, Biosphere Reserve Montes Azules, Chiapas, Mexico. Environmental Biology of Fishes 83(4): 459–469. https://doi.org/10.1007/s10641-008-9368-0

Soria-Barreto M, Rodiles-Hernández R, González-Díaz AA (2011) Morfometría de las especies de *Vieja* (Cichlidae) en ríos de la cuenca del Usumacinta, Chiapas, México. Revista Mexicana de Biodiversidad 82(2): 569–579. https://doi.org/10.22201/ib.20078706e.2011.2.460

Soria-Barreto M, Rodiles-Hernández R, Winemiller KO (2019) Trophic ecomorphology of cichlid fishes of Selva Lacandona, Usumacinta, Mexico. Environmental Biology of Fishes 102(7): 985–996. https://doi.org/10.1007/s10641-019-00884-5

Stiassny MLJ (1991) Phylogenetic interrelationship of the family Cichlidae. Pp. 1–31. In: Keenlyside MHA (Ed.) Cichlid fishes. Behavior, ecology and evolution. Chapman and Hall, London, UK.

Villalobos-Leiva A, Benítez HA (2020) Morfometría geométrica y sus nuevas aplicaciones en ecología y biología evolutiva. Parte 2. International Journal of Morphology 38(6): 1818–1836. https://doi.org/10.4067/S0717-95022020000601818

Winemiller KO, Kelso-Winemiller LC, Brenkert AL (1995) Ecomorphological diversification and convergence in fluvial cichlid fishes. Environmental Biology of Fishes 44(1–3): 235–261. https://doi.org/10.1007/BF00005919

Wootton RJ (1990) Ecology of teleost fishes. Chapman and Hall, New York, NY, USA, 404 pp. https://doi.org/10.1007/978-94-009-0829-1

Zelditch ML, Swiderski DL, Sheets HD, Fink WL (2004) Geometric morphometrics for biologists. Elsevier Academic Press, London, 443 pp. https://doi.org/10.1016/B978-0-12-778460-1.X5000-5